



# LUND UNIVERSITY

## Robotic Friction Stir Welding for Flexible Production

De Backer, Jeroen

2012

[Link to publication](#)

*Citation for published version (APA):*

De Backer, J. (2012). *Robotic Friction Stir Welding for Flexible Production*. [Licentiate Thesis, Innovation]. Lund University.

*Total number of authors:*

1

### General rights

Unless other specific re-use rights are stated the following general rights apply:

Copyright and moral rights for the publications made accessible in the public portal are retained by the authors and/or other copyright owners and it is a condition of accessing publications that users recognise and abide by the legal requirements associated with these rights.

- Users may download and print one copy of any publication from the public portal for the purpose of private study or research.
- You may not further distribute the material or use it for any profit-making activity or commercial gain
- You may freely distribute the URL identifying the publication in the public portal

Read more about Creative commons licenses: <https://creativecommons.org/licenses/>

### Take down policy

If you believe that this document breaches copyright please contact us providing details, and we will remove access to the work immediately and investigate your claim.

LUND UNIVERSITY

PO Box 117  
221 00 Lund  
+46 46-222 00 00



# **Robotic Friction Stir Welding for Flexible Production**

*Jeroen De Backer*

---

*Division of Machine Design • Department of Design Sciences  
Faculty of Engineering LTH • Lund University • 2012*

# **Robotic Friction Stir Welding for Flexible Production**

Copyright © 2012 Jeroen De Backer

Division of Machine Design, Department of Design Sciences  
Faculty of Engineering LTH, Lund University  
Box 118  
221 00 LUND

ISBN 978-91-7473-342-6

ISRN LUTMDN/TMKT-12/1029-SE

Printed and bound in Sweden by Media-Tryck, Lund



## Acknowledgments

My interest for this subject started in 2009 when I did my master thesis within the area of friction stir welding, thanks to a great teamwork with my classmate and friend Bert Verheyden. It took however a couple of good reasons to convince me to move to Sweden and start as PhD-student in a research project. Some reasons disappeared, even an iconic exclusive car company, Saab. But one reason became stronger along the way to this licentiate thesis: the firm belief that friction stir welding is a wonderful technology with a lot of potential in several industries, not the least within the automotive.

The close collaboration with industrial partners, Saab, Volvo and ESAB made this work extra interesting. I've been working with fantastic people like Mathias Fremäng, Mikael Soron and our project leader Tommy Christensen who supported me despite their sometimes crowded agenda. Your input is greatly appreciated!

It has been very pleasant working at University West, in one of Sweden's most modern research centres, the Production Technology Centre, with an excellent group of colleagues. Thanks all for the inspiring conversations during our many *fikas*.

I want to thank Anna-Karin Christiansson, not only for being a great project leader but also for the continuous support in my research and in learning Swedish.

Special thanks to my supervisors Gunnar Bolmsjö and Torbjörn Ilar and to Giorgos Nikoleris for taking over the role of main supervisor during the last part of this work.

Finally I want to say thanks to my parents, Willy and Viviane, and my sister Sanne for their support and for not getting annoyed when I didn't show up on any social media for a couple of days. I hope this thesis shows that I have been busy with other things...

Trollhättan, 12<sup>th</sup> of March 2012

Jeroen De Backer



## Populärvetenskaplig sammanfattning

Friction Stir Welding eller ”friktionsomrörningssvetsning” är en svetsprocess som kräver ett roterande verktyg som genom friktionsvärme får materialet att mjukna. Verktøget blandar runt det plastiska materialet mekaniskt och skapar en fog av hög kvalitet. Processen fungerar utan gas, utan rök, utan tillsatsmaterial och utan att smälta materialet. Alla dessa fördelar skapar stort industriellt intresse inom flera branscher. Idag används tekniken nästan uteslutande i styva maskiner som svetsar raka eller cirkulära fogar och framförallt för aluminium. Eftersom processen kräver stora krafter mellan material och verktyg är det svårt att implementera processen på en robot. En robot möjliggör svetsning av tredimensionella geometrier och ökar dessutom flexibiliteten. Flera forskargrupper runt i världen har tagit fram en fungerande FSW robot som kan svetsa tunn lättviksmaterial som aluminium med hög kvalitet. Användningen i industrin av FSW robotar är däremot obefintlig och det finns ett antal anledningar till det. Först är roboten vek vilket gör att verktyget kan missa svetsfogen i hårda material och svetsdefekter kan uppstå. En annan anledning är att det inte finns en användbar automatiserad processtyrning tillgänglig, mest för att FSW är en robust process och inte kräver en avancerad styrning vid svetsning av raka fogar.

De praktiska arbeten som redovisas i denna licentiatuppsats är huvudsakligen utförda i en robotiserad FSW-demonstrator på Högskolan Väst. FSW-roboten är en modifierad industrirobot som är försetts med spindel och kraftåterkoppling för att styra kraften som roboten applicerar på arbetsstycket.

Detta arbete har identifierat ett antal problem som behöver lösas för att få en robust robotiserad FSW process i en flexibel produktionsmiljö. I denna licentiatrapport beskrivs en lösning hur en typ av svetsdefekter kan förhindras genom en sensorbaserad bankompensering. Både en kamera- och lasersensor-baserad mätmetod presenteras. En annan bankompenseringsstrategi är beskriven, som använder kraftsensorn från befintlig kraftåterkoppling istället för att lägga till extra sensor. Denna strategi kan utvecklas till en komplett utböjningsmodell på roboten i hela arbetsområdet. Robotens begränsningar gällande svetsbarhet av hårda material har undersökts och med hjälp av parameteroptimering och förvärmning kan även hårda nickelbaserade legeringar svetsas med roboten.

### Nyckelord:

Friktionsomrörningssvetsning, automation, robotik, aluminium, fordonstillverkning



## **Abstract**

Friction Stir Welding (FSW) is a modern welding process that joins materials by frictional heat, generated by a rotating tool. Unlike other welding processes, the material never melts, which is beneficial for the weld properties. FSW is already widely adopted in several industries but the applications are limited to simple geometries like straight lines or circular welds, mostly in aluminium. The welding operation is performed by rigid FSW machines, which deliver excellent welds but puts limitations on the system in terms of flexibility and joint geometries. Therefore, several research groups are working on the implementation of the FSW process on industrial robots. A robot allows welding of three-dimensional geometries and increases the flexibility of the whole system. The high process forces required for FSW, in combination with the limited stiffness of the robot brings some extra complexity to the system. The limitations of the robot system are addressed in this licentiate thesis.

One part of the thesis studies the effect of robot deflections on the weld quality. A sensor-based solution is presented that measures the path deviation and compensates this deviation by modifying the robot trajectory. The tool deviation is reduced to an acceptable tolerance and root defects in the weld are hereby eliminated. The sensor-based method provided better process understanding, leading to a new strategy that uses existing force-feedback for path compensations of the tool. This method avoids extra sensors and makes the system less complex. Another part of this work focuses on the extra complexity to maintain a stable welding process on more advanced geometries. A model is presented that allows control of the heat input in the process by control of the downforce. Finally, the robot's limitations in terms of maximal hardness of the materials to be welded are investigated. Parameter tuning and implementation of preheating are proposed to allow robotic FSW of superalloys.

### **Keywords:**

Friction Stir Welding, Automation, Robotics, Aluminium, Lightweight design



## Appended publications

### Paper A

‘A Local Model for Online Path Corrections in Friction Stir Welding’ – Presented at the 8<sup>th</sup> Friction Stir Welding and Processing conference in Lille, France, February 2010 – *Authors:* Mikael Soron<sup>1</sup>, Jeroen De Backer<sup>2</sup>, Anna-Karin Christiansson<sup>2</sup>, Torbjörn Ilar<sup>2</sup>

### Paper B

‘Friction Stir Welding with Robot for Light Weight Vehicle Design’ – Key-note presentation at the FSW Symposium in Timmendorfer Strand, Germany, May 2010 – *Authors:* Jeroen De Backer<sup>2</sup>, Mikael Soron<sup>1</sup>, Torbjörn Ilar<sup>2</sup>, Anna-Karin Christiansson<sup>2</sup>

### Paper C

‘Surface Quality and Strength in Robotic Friction Stir Welding of Thin Automotive Aluminium Alloys’ – Presented at the Swedish Production Symposium in Lund, Sweden, May 2011 – *Authors:* Jeroen De Backer<sup>2</sup>, Anna-Karin Christiansson<sup>2</sup>

### Paper D

‘Investigation of Path Compensation Methods for Robotic Friction Stir Welding’ – Accepted in March 2012 for publication in *Industrial Robot, An International Journal* – *Authors:* Jeroen De Backer<sup>2</sup>, Anna-Karin Christiansson<sup>2</sup>, Jens Oqueka<sup>2</sup>, Gunnar Bolmsjö<sup>2</sup>

### Paper E

‘Influence of Roll Angle on Process Forces and Lap Joint Strength in Robotic Friction Stir Welding’ – Accepted for presentation at the 9<sup>th</sup> FSW Symposium in Huntsville, AL, USA, May 2012 – *Authors:* Jeroen De Backer<sup>2</sup>, Mikael Soron<sup>1</sup>, Lars Cederqvist<sup>3</sup>

### Paper F

‘Three-Dimensional Friction Stir Welding of Inconel 718 using the ESAB Rosio FSW-Robot’ – Accepted for presentation at the Trends in Welding Research Conference in Chicago, IL, USA, June 2012 – *Authors:* Jeroen De Backer<sup>2</sup>, Mikael Soron<sup>1</sup>

<sup>1</sup> ESAB Welding Equipment AB, <sup>2</sup> University West, <sup>3</sup> Svensk Kärnbränslehantering AB





## **Authors' contribution to the appended publications**

The issue of path deviations and a possible way of compensating was proposed in the PhD-thesis by Dr. Soron. The experiments in 'Paper A' are based on this idea. Jeroen De Backer performed the main part of the welding tests as well as data-analysis. The paper was written jointly by Mikael Soron and Jeroen De Backer. Anna-Karin Christiansson and Torbjörn Ilar reviewed the paper and have made minor changes.

'Paper B' continues with the idea of path deviations. Further analysis of previous data and concepts for online path deviation were developed by Jeroen De Backer. The first writing of the paper was done by Jeroen De Backer but all 3 co-authors have made substantial contributions.

The idea of investigating surface quality in 'Paper C' was initiated by the automotive project partners. This paper is written from an industrial perspective. Jeroen De Backer performed all experiments and the major part of the analysis and writing.

'Paper D' is a development of Papers A and B. Jeroen De Backer performed all welding experiments. Jens Oqueka developed the camera-measurement system and the image analysis. Jeroen De Backer wrote the major part of the paper and Gunnar Bolmsjö contributed in the introduction, the state-of-the-art description on robotics and the discussion section. Anna-Karin Christiansson reviewed the article.

The idea of investigating the side-tilt angle in 'Paper E' is suggested in the section future work in the PhD-thesis by Dr. Cederqvist. All authors contributed to the experimental design and the welding experiments. Jeroen De Backer performed the data analysis and wrote the main part of the paper. The other authors complemented with literature references, discussion and conclusions.

The industrial project partners made the selection of the superalloy to perform the tests in 'Paper F'. The experiments were performed by Jeroen De Backer and Mr. Säll at ESAB. Mikael Soron assisted in selection of tools and contributed with knowledge from earlier welding tests in high-strength alloys. Volvo Aero contributed with their experience of superalloys. Jeroen De Backer analysed the samples and data and wrote the paper.



# Table of Contents

<b>1 Introduction .....</b>	<b>1</b>
1.1 Background.....	1
1.1.1 <i>Welding</i> .....	2
1.1.2 <i>The friction stir welding process</i> .....	2
1.2 The StiRoLight research project.....	5
1.3 Research questions .....	5
1.4 Scientific framework and research method.....	6
1.5 Scope and delimitations .....	7
1.6 Outline .....	8
<b>2 State-of-the-art in Robotic FSW .....</b>	<b>9</b>
2.1 Friction stir welding .....	9
2.1.1 <i>Weldability of aluminium alloys</i> .....	9
2.1.2 <i>Classification of aluminium alloys</i> .....	10
2.1.3 <i>Competing welding processes</i> .....	10
2.1.4 <i>Material flow around a FSW tool</i> .....	11
2.1.5 <i>Metallurgy</i> .....	12
2.1.6 <i>From lightweight to high-temperature alloys</i> .....	13
2.1.7 <i>Tool materials</i> .....	14
2.1.8 <i>Tool geometries</i> .....	15
2.1.9 <i>Process variants</i> .....	16
2.2 Robotisation of the FSW process .....	17
2.3 Process control and automation .....	18
2.3.1 <i>Force control in FSW</i> .....	18
2.3.2 <i>Temperature control</i> .....	19
2.3.3 <i>Seam tracking for FSW</i> .....	19
2.3.4 <i>In-process quality control</i> .....	20
<b>3 Experiments &amp; System Development.....</b>	<b>21</b>
3.1 Experimental platform .....	21

3.1.1 The FSW Robot.....	21
3.1.2 Robot programming.....	21
3.1.3 Measurement system .....	22
3.2 FSW process analysis .....	24
3.3 FSW robot analysis .....	25
3.3.1 Plunge operation .....	26
3.3.2 Robot force control .....	26
<b>4 Summaries of the appended papers .....</b>	<b>29</b>
Paper A – A Local Model for Online Path Corrections in Friction Stir Welding .....	29
Paper B – Friction Stir Welding with Robot for Light Weight Vehicle Design.....	29
Paper C – Surface Quality and Strength in Robotic Friction Stir Welding of Thin Automotive Aluminium Alloys .....	30
Paper D – Investigation of Path Compensation Methods for Robotic Friction Stir Welding .....	30
Paper E - Influence of Side-Tilt Angle on Process Forces and Lap Joint Strength in Robotic Friction Stir Welding .....	31
Paper F - Three-Dimensional Friction Stir Welding of Inconel 718 using the ESAB Rosio FSW-Robot .....	31
<b>5 Conclusions .....</b>	<b>33</b>
<b>6 Discussion and Future Work.....</b>	<b>35</b>
6.1 Strategy for temperature control .....	35
6.2 Strategy for path compensation using force feedback .....	36
<b>References .....</b>	<b>39</b>
<b>Appendix A: IsMoving function for plunge depth detection .....</b>	<b>45</b>
<b>Appended Papers</b>	
Paper A: A Local Model for Online Path Corrections in Friction Stir Welding	
Paper B: Friction Stir Welding with Robot for Light Weight Vehicle Design	
Paper C: Surface Quality and Strength in Robotic Friction Stir Welding of Thin Automotive Aluminium Alloys	
Paper D: Investigation of Path Compensation Methods for Robotic Friction Stir Welding	
Paper E: Influence of Side-Tilt Angle on Process Forces and Lap Joint Strength in Robotic Friction Stir Welding	
Paper F: Three-Dimensional Friction Stir Welding of Inconel 718 using the ESAB Rosio FSW-Robot	

## List of abbreviations

<b>AWS</b>	American Welding Society
<b>EBW</b>	Electron Beam Welding
<b>FSW</b>	Friction Stir Welding
<b>GMAW</b>	Gas Metal Arc Welding
<b>GTAW</b>	Gas Tungsten Arc Welding
<b>HAZ</b>	Heat Affected Zone
<b>MIG</b>	Metal Inert Gas, subdivision of GMAW
<b>MAG</b>	Metal Active Gas, subdivision of GMAW
<b>StiRoLight</b>	Friction <b>Stir</b> Welding with <b>Robot</b> for <b>Light</b> weight Vehicle design
<b>TCP</b>	Tool Centre Point of a robot
<b>TIG</b>	Tungsten Inert Gas welding, same as GTAW
<b>TWI</b>	The Welding Institute (Cambridge, UK)



# 1 Introduction

*... The low mass 2020 car body-in-white would be constructed using a low energy joining process proven on high speed trains; this process is already used on some low volume automotive applications. This low energy, low heat, friction stir welding process would be used in combination with adhesive bonding, a technique already proven on Lotus production sports cars. In this instance, the robotically controlled welding and adhesive bonding process would be combined with programmable robotic fixturing, a versatile process which can be used to construct small and large vehicles using the same equipment ...*

*Lotus Engineering Inc., 2010*

## 1.1 Background

Joining materials is one of the vital processes in the manufacturing industries. There is an extremely wide variety of methods to join one piece of material with another. Four main categories that could be identified are mechanical fasteners, adhesive bonding, soldering-like-processes and welding. A general trend in the 21<sup>st</sup> century is the implementation of processes that are not only cost-efficient but also sustainable and energy-efficient.

Mechanical fasteners are a very competitive alternative for welding as they can be cheap, sufficiently strong and time-efficient. Typical mechanical fasteners in automotive industry are clinch joints, rivets, nuts and bolts. The use of adhesives is increasing significantly, mainly because more advanced chemical compositions have greatly improved the joining properties and because of the lack of alternatives to join dissimilar materials such as metals and plastics. Nowadays, adhesive joints can be equally strong as a comparable weld but are often more expensive. Adhesive joining often require some surface preparation to ensure a good bond, which also has an environmental impact (Sutherland et al., 2004).

Soldering and brazing are similar to welding but use a filler material with lower melting point than the actual work pieces. The difference between the two is the melting point of the material; soldering is performed at lower temperatures (e.g. with lead or zinc) and brazing at higher temperatures (e.g. with copper or nickel). Soldering is used a lot in electronics, to connect electronic components to each other through printed circuit boards.

### 1.1.1 Welding

Joining metals by welding has been under constant development for thousands of years (Balasubramaniam, 1998). Initially, forge welding was the only known welding process. Forge welding is performed by hammering two metal components while the material is red-glowing hot. The heat, combined with the mechanical energy will cause the material to bond, due to solid-state diffusion. During the industrial revolution, electric welding was developed and replaced basically all forge welding applications. Most adopted type of welding is Gas Metal Arc Welding, using a shielding gas and a continuously fed consumable which is melted by electric current between an electrode and the materials to be joined.

The American Welding Society (AWS) adopts a classification scheme with seven categories: arc welding, solid state welding, resistance welding, soldering, brazing, oxyfuel gas welding and other processes (Messler, 2004). Most welding processes can also be divided into two main categories, based on the welding temperature:

- **Solid-state welding:** materials plasticise but do not exceed the melting temperature, e.g. forge welding, friction welding, friction stir welding, explosion welding and diffusion bonding.
- **Liquid-phase welding:** solid materials are locally converted into a molten state. The joint is created as the material solidifies. These processes are often called fusion welding e.g. arc welding, laser welding and electron beam welding.

It was only around the beginning of the 19<sup>th</sup> century that electric fusion welding methods were developed and spread in the industry. At the beginning of the 20<sup>th</sup> century, the Swede Oscar Kjellberg invented the coated iron electrode, improving the weld quality significantly. His invention led to the foundation of ESAB ('Electric Welding Ltd. Company'). The idea of electric welding with coated electrodes is still widely adopted nowadays, together with other types of fusion welding processes.

Resistance welding processes such as spot welding were developed in the same period and are still widely adopted in the automotive industry. Many other processes have been invented throughout the 20<sup>th</sup> century and Friction Stir Welding is one of them. The FSW process is an evolution from the typical friction welding process, where materials, typically rods or tubes, are rotated against each other under pressure until the plasticised material creates a solid-state joint.

### 1.1.2 The friction stir welding process

Friction Stir Welding was invented at The Welding Institute in Cambridge, UK, in 1991 and the first patent for FSW in butt joint configuration was filed in 1991 by Wayne Thomas (Thomas et al., 1991). The FSW process is one of the latest innovations in the area of welding. It has several advantages compared to traditional fusion welding techniques and is mainly used for lightweight alloys such as aluminium and magnesium.



The process, shown in Figure 1 uses a rotating, non-consumable tool, consisting of a bigger circular area, the shoulder, with a smaller diameter pin sticking out, the probe. The process is typically described in four steps:

- The plunge operation: the rotating probe is slowly pressed down until the shoulder makes contact with the material.
- The dwelling period: the tool maintains its position, generating frictional heat until the desired temperature is reached.
- The actual welding operation: the rotating tool is moved along a joint line with a certain contact pressure between the tool and the material and a predefined traverse speed. This creates a solid state joint, i.e. without melting the material. The heat generation is mainly due to the frictional heat, generated between tool and material, and also by material deformation, similar to a hot-working<sup>1</sup> process. The probe on the tool stirs the plasticised material, creating a very fine micro-structure. To create more pressure and preventing void formation behind the probe, the tool is often tilted towards the trailing edge of the tool. This “tilt-angle” is typically between 1 and 3°.
- Finally when the joint is created, the tool is pulled up, leaving a small “key-hole” in the end.

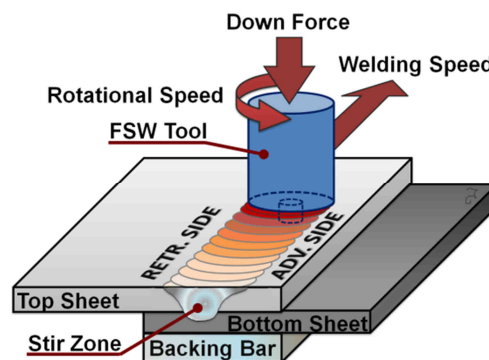


Figure 1: Principle of the friction stir welding process for overlap joint configuration

Table 1 compares FSW with GMAW and laser welding for common aluminium welding applications. A major advantage is that FSW is a solid-state joining process, which means the material stays always below the melting temperature. The main drawback of the process is the required contact force, which makes it more difficult to implement on robots and also requires a solid support, the so-called backing bar, on the backside of the weld.

<sup>1</sup> Hot-working refers to processes where metals are plastically deformed above their recrystallization temperature, e.g. by extrusion or hammering. This allows the material to recrystallize during deformation. The lower limit of the hot working temperature of a material is typically 0.6 times its melting temperature.

Another disadvantage is the “key-hole” in the end of the weld, which – depending on the application – has to be removed.

Table 1: Advantages (✓), intermediate (Δ) and disadvantages (✗) of different methods for welding light-weight alloys in general applications.

Advantages	GMAW	LASER	FSW
Absence of filler material	✗	Δ	✓
Absence of shielding gas	✗	✗	✓
Solid State Joining	✗	✗	✓
Absence of intensive light	✗	✗	✓
Absence of fumes	✗	✗	✓
Low temperature gradient	✗	✗	✓
Low distortion	✗	Δ	✓
Low energy consumption	✗	Δ	✓
Implementation on robots	✓	✓	✓
No contact forces	✓	✓	✗
Absence of solid backing bar	✓	✓	✗

Because FSW is a solid-state joining process without filler material, the composition of the welded material is not modified; there is only a recrystallization of the present material structure. The typical fine-grain microstructure in the weld nugget can be stronger than the base material. Research has proven that all common aluminium alloys can be joined by FSW and even combinations of different alloys as shown in Figure 2.

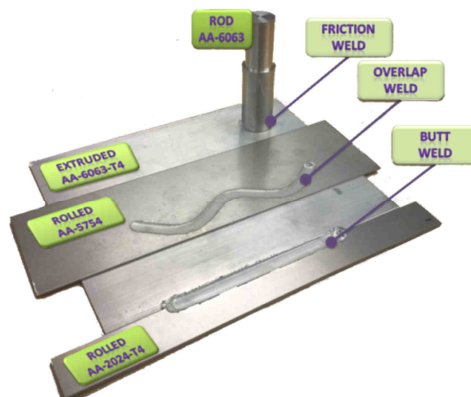


Figure 2: Friction Welding and FSW of a lap joint and a butt-joint, performed with a FSW-robot

## 1.2 The StiRoLight research project

The StiRoLight research project started in 2009 at University West in Sweden in cooperation with Swedish industrial partners SAAB Automobile, ESAB, Volvo and Innovatum. This 3-year research project was funded by the FFI program of the Swedish Governmental Agency for Innovation Systems, Vinnova. A FSW-robot cell was established at the Production Technology Centre in Trollhättan, Sweden (Figure 3). The project aimed to bring robotic FSW closer to industrial applications by eliminating constraints, related to the robotic implementation of the FSW process and by further control and automation of the process.

The objectives in this work were:

- Further development of the process for more complex geometries
- Develop design methodology to fully utilise FSW-joints for complex geometries
- Demonstration of robotised FSW-functionalities and limitations

Achieving these goals leads towards the introduction of robotic FSW in the Swedish vehicle industry, where the demands for alternatives to existing manufacturing solutions are strong.

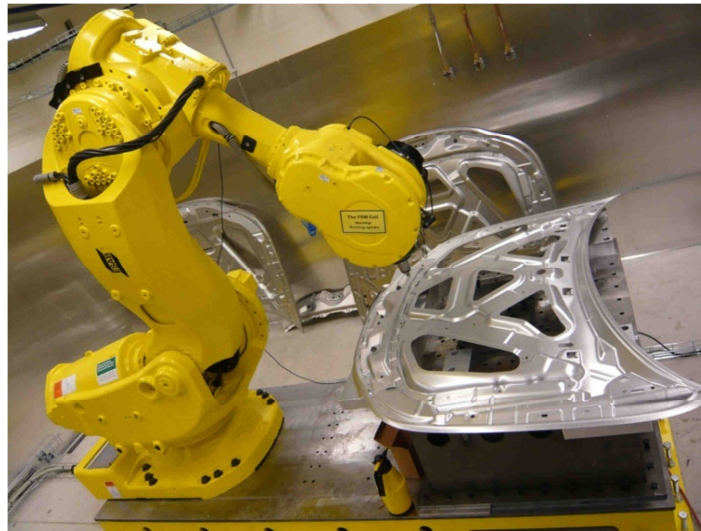


Figure 3: The ESAB Rosio™ FSW robot welding automotive body parts at the Production Technology Centre

## 1.3 Research questions

The implementation of FSW on robots has certain implications for the process. One obstacle is the required process force of several thousand Newtons, combined with the limited stiffness and path accuracy of serial kinematic robots. These types of robots are by

far the most used in the industry and therefore attractive to combine with FSW. However, minor deflections in the robot joints can result in significant deviations of the welding tool. This results in welding defects as the tool is missing the joint line. The research question in this licentiate thesis can thus be formulated as:

- *How can root defects, due to tool path deviations be avoided in FSW? And can the robot deflection be compensated without introducing extra sensors to the system?*

The use of a robot also allows welding of complex, three-dimensional joint geometries. Most work in literature is focussed on straight joint lines with little emphasis on the extra complications associated with 3D-joints. Control of the heat input in preheated areas of the material is one example of process control that is not required for most industrial FSW applications today. A relevant question regarding further development of a flexible automated FSW process is:

- *Which additional parameters have to be controlled to guarantee a robust FSW process for welding complex geometries in an automated production line?*

#### **1.4 Scientific framework and research method**

This research within the frame of the StiRoLight project is a typical example of how a modern research project could be used to deliver scientific results which are directly related to industrial applications. Process suppliers were required to do additional product development to meet specific demands of certain end-users. This development needed however a profound scientific base, for example understanding of how the process forces influence the robot dynamics. The university provided the scientific results which allowed process suppliers to further develop their system and adapt it to the end-users' needs.

The great benefit of this type of research is that industrial partners are in close cooperation with the university. Instead of pure scientific projects where the results could be applied in a next step, this is fitted into a technological project, where companies have clear aims and expectations from the start. It is then the task of the researcher and supervisors to find a good scientific base to start the research, without falling into technical solutions for a specific production problem. In this context, the government through Vinnova can be seen as an institution, judging whether the funding is used for innovative research that is generally applicable or just as an extra cash-input for the R&D department in one specific company. This approach corresponds well to the triple helix structure where it is stated that university, industry and government are in constant interaction in modern research as described in (Sismondo, 2007). The participating companies take benefit from the research first, but other interested parties can also access the scientific results through publications and conference presentations.

Nunamaker presented a framework for information systems which can be applied to the research described in this thesis (Nunamaker and Chen, 1990). The followed method is described by means of Figure 4. The main part of this thesis describes the improvement of robot performance for in-contact welding operation. The motivation for this study is based on the observations that the robot performance (i.e. path accuracy) is inadequate for welding certain materials. To obtain a good understanding of the effect of the process forces on the robot performance, an appropriate measurement method has to be developed (A). The system development is therefore included in this research. From the measurements, theories are built regarding the robot behaviour and compensation methods are developed (B). The control method has to be implemented in the system (C) and verified through experiments (D). The experiments are evaluated (E) which provides new knowledge about the requirements and how the compensation method could be implemented in a better way (F).

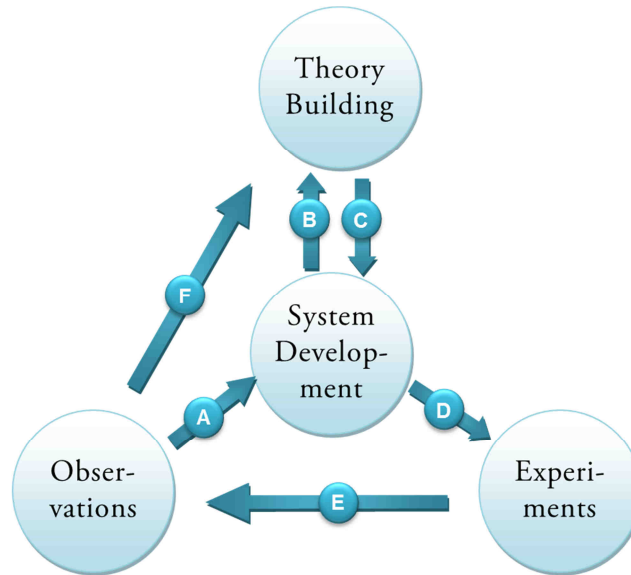


Figure 4: Scientific research method with included system development

### 1.5 Scope and delimitations

The study covers three research domains: Friction Stir Welding, Process Automation and Robotics. All these topics are woven together into this thesis. A part of the research in this thesis is conducted with the specific needs for the vehicle industry in mind. This is for example expressed in the automation strategy, where several sensors are first used for profound understanding of the process but at a later stage removed again to decrease complexity of the whole system. This study is focussed on automation of a robotic FSW process. The overall aim is that the operator does not need a profound knowledge of the robot, nor of the physical effects in the welding process to be able to use the FSW robot

system to perform a successful weld. Furthermore, automation can make the system more flexible. When a new product is introduced in a company, usually a number of pre-production parts are sacrificed to test and optimise the welding parameters. Process automation can decrease the number of pre-production parts, which can imply a significant cost reduction, especially for low-volume production.

The study does not cover any physical process modelling of the FSW process. The term ‘model’ will always refer to a control model from an automation perspective unless specified differently.

The researcher limited the welding tests to FSW of different aluminium alloys and combinations of these. Only one type of robot system was evaluated. Even though there is a wide range of material properties that could be evaluated (e.g. fatigue-life, corrosion resistance, hardness) the investigation of weld quality in this thesis is limited to microstructure analysis, tensile tests and visual inspection. The choice of welding tools is based on literature review or advice from other researchers; no specific tools are designed.

## 1.6 Outline

This thesis is written as an aggregation of different research questions within the area of Friction Stir Welding, robotics and automation.

Chapter 1 is an introduction to the thesis and describes the background for this research, as well as the followed research method.

Chapter 2 includes a frame of reference for the relevant research topics and describes the state-of-the-art in robotic FSW.

The complete platform in which this research is conducted in terms of hardware, robot and computer software, measurement systems, process analysis and system limitations is described in Chapter 3.

A brief summary of the appended papers is included in Chapter 4.

In Chapter 5, all the individual investigations are brought together into a general conclusion of the performed research. These results are further discussed in Chapter 6 where they are put into an industrial perspective. The chapter also provides some remaining research question for the future.

Finally, all the published research is appended to this thesis as Paper A to F.

## 2 State-of-the-art in Robotic FSW

### 2.1 Friction stir welding

After 20 years of development, the number of tool geometries, materials, joint geometries, patents and industrial applications of FSW has increased tremendously; the scientific database “ScienceDirect” indicates an exponential increase from less than 10 publications before 1997 to about 150 publications in 2004 and 470 publications in 2011. The United States is by far the biggest source of papers, with a total of over 750, followed by about 500 papers from China<sup>2</sup>.

Fusion welding processes had several difficulties to join aluminium alloys due to oxides, reflectivity, low-melting alloying elements etc. FSW could reduce a number of these drawbacks associated with fusion welding and got great attention from the aluminium industry. Originally aluminium and later also magnesium were described as the application domain of FSW. Recently a lot of development efforts are now put into materials with a high melting point such as low carbon steel and nickel-based alloys.

#### 2.1.1 Weldability of aluminium alloys

Aluminium alloys have some very interesting properties that make them attractive in many industrial applications. Aluminium alloys have a low density, very good corrosion resistance and provide a good strength and toughness. Fusion welding of aluminium is generally assumed to be more difficult than welding steel. The strong oxide layer is hard to break with for example an arc welding beam. The high thermal conductivity of aluminium makes it more difficult to concentrate the heat and requires thus a higher heat input. The high expansion factor makes it sensitive for distortions and the shrinkage of aluminium alloys is the double of ferrous alloys (Davis, 1993). These properties make the welded aluminium alloy, depending on the alloying elements, very sensitive to weld cracking. The strongest heat-treatable aluminium alloys are often considered as “unweldable” with classic fusion welding techniques. AA 7075-T6 and AA 2024-T3 for example are amongst the strongest aluminium alloys which make them of big interest for aerospace applications. However, these alloys are almost impossible to weld without defects for two main reasons: the presence of alloying elements with a low melting point (such as bismuth or lead) and hot-cracking. This phenomenon is influenced by mechanical,

---

<sup>2</sup> Values are based on the analytics tools from [www.scopus.com](http://www.scopus.com) with keyword search “friction stir welding”.

thermal and metallurgical factors and causes cracks due to solidification shrinkage (ESAB Welding and Cutting, 2012, Martukanitz, 1990). Aluminium alloys are also more sensitive to hot-cracking than ferrous alloys. Therefore, very few applications are known where these high-strength aluminium alloys are welded. Instead, riveting is often used as joining process.

### *2.1.2 Classification of aluminium alloys*

Aluminium is typically divided into categories, based on their alloying elements (Davis, 1993). The most commonly used standard classifies the alloys with 4 digits where the first digit specifies the main alloying element. The alloying elements are also determining whether the alloy is heat-treatable<sup>3</sup> or not. If the alloy is heat treated, another letter and/or number are added e.g. “-T6” for artificial aging and “-H32” for strain-hardening.

1xxx is the most “pure” aluminium and has relatively low strength. 3xxx has a limited amount of manganese. 5xxx contains a significant amount of magnesium, which gives strongest non-heat-treatable aluminium alloys. In the heat-treatable series, 6xxx is the most commonly used alloy series, e.g. AA 6016-T4 in automotive body parts. This alloy contains magnesium and silicon. The strongest alloys are 2xxx with copper and 7xxx with magnesium and zinc as major alloying elements. Several new alloys are presented as the 8xxx series, with lithium as alloying element. These alloys are characterised by a low-density and improved elasticity modulus and are expected to be used in the aerospace industry (Lavernia and Grant, 1987).

### *2.1.3 Competing welding processes*

Next to the widely used GMAW and resistance spot welding, several new methods have been presented in the 20<sup>th</sup> century which were proven to be very successful in their specific domain of applications. Some examples are listed here:

- In the 1950’s plasma arc welding was invented. The process is similar to TIG welding but it uses ionized gas, plasma, which reaches much higher temperatures, around 20’000°C. Plasma welding uses a non-consumable tungsten electrode and the plasma beam is forced through a fine-bore copper nozzle.
- Ultrasonic welding: The process was invented in the 1960’s in the USA, within the aerospace industry. High-frequency ultrasonic acoustic vibrations are sent through work pieces that are clamped against each other, creating a solid-state weld (Balamuth et al., 1962).
- Laser beam welding uses an intense focussed light beam to heat and weld the materials. The thin beam gives smaller heat-affected zones than most arc welds.

---

<sup>3</sup> Heat treatment involves the heating and cooling of materials to modify the physical (and sometimes chemical) properties such as the hardness of a material.



Laser beam welding can be used both with and without filler material. A variant is “remote laser welding”, where the optics are located at a relatively long distance – about 1m – from the workpiece. Very precisely controlled mirrors and lenses can quickly refocus the laser beam, with extremely small time losses in between 2 welds. (Mangiarino et al., 2004)

- Electron beam welding was also invented in the 1950’s and is a fusion welding process in which a beam of high-velocity electrons is sent through the metals. The kinetic energy in the beam will be transformed into heat inside the material. EBW can weld very thick materials but has the disadvantage of requiring a vacuum atmosphere. (Schultz, 2002)
- The ‘friction welding’ process generates heat through mechanical friction between a moving workpiece and a stationary component. This can be both rotational (e.g. gas tube welding) and linear movement. Friction welding generates high-quality solid-state joints. The major difference between FSW and regular friction welding is the use of a non-consumable tool in FSW.

In the automotive industry today, more and more hybrid designs are adopted, i.e. different material combinations such as aluminium, plastics, steel and high-strength steel. This requires new joining methods. In the near future, remote laser welding, adhesive joining, FSW, friction welding, nailing-like and riveting-like technologies can be expected to be the main technologies for lightweight and hybrid material joining.

#### *2.1.4 Material flow around a FSW tool*

In order to predict weld properties, an accurate physical process model is required. These properties can be either measured during the process (e.g. force and temperature) or when the welding process is completed (e.g. residual stresses and deformation). Several approaches have been presented throughout the years. In this section, the extrusion model by Arbegast is chosen to provide a basic understanding of the material flow in FSW (Arbegast, 2008). The model allows describing the conditions under which volumetric defects will, or will not, occur during FSW.

The material flow can be seen as an extrusion of material from the front to the back of the tool, through two thin zones at the side of the tool. As the tool rotates and the material sticks to the tool, more material will be extruded through the retreating side than through the advancing side (zone II and zone I respectively in Figure 5b). This causes a different extrusion pressure and accordingly an asymmetry in the side-forces on both sides of the tool. The extruded material will consolidate behind the tool (i.e. the trailing edge of the tool) and flow from retreating side to advancing side (as indicated by the arrow from II to I in Figure 5c).

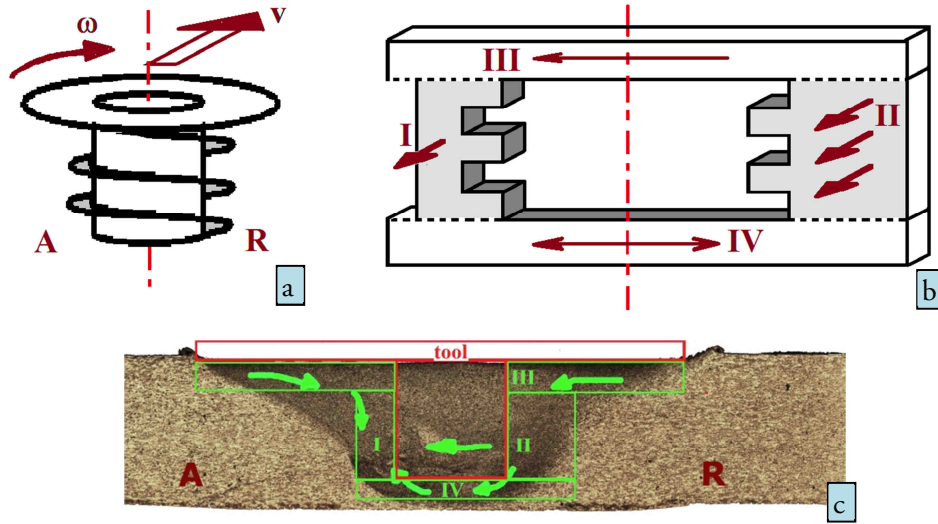


Figure 5: A threaded tool with indicated rotation and travel direction (a) with the four corresponding extrusion zones around the tool (b) and the material consolidation behind the tool pin (c) according to the extrusion model by Arbegast. The arrows indicate the flow of material.

A typical problem with the physical models is that they make assumptions that influence the accuracy of the model significantly. One of these assumptions is the friction between tool and material. This can be either sliding conditions (Chao et al., 2003), where the speed of the material around the tool is equal to zero (dynamic friction coefficient) or sticking conditions, where the material just around the tool has the same speed as the tool surface (static friction coefficient). Combinations of both are presented, introducing a “slip rate” as distribution key for sticking and sliding conditions (Schmidt et al., 2004). There is however no practical method presented to identify this slip rate.

### 2.1.5 Metallurgy

The main difference between FSW and fusion welding is the absence of a fusion zone, where the material has been melted. This zone contains usually filler material with different material properties than the base material. The four different zones that can be identified in FSW are indicated in Figure 6. Typical features are:

1. Weld Nugget: also called “Stir zone”, is a fully recrystallized material zone that has been exposed to severe mechanical deformation, resulting in a fine microstructure.
2. Thermo-mechanically affected zone: The material has not been stirred but is exposed to a high temperature gradient and strong mechanical deformation.

3. Heat affected zone: The material has not been deformed but went through a thermal cycle, affecting the microstructure.
4. Parent material: This material has not been affected by the welding process.
5. Toe-flash: Often material is extruded at the sides of the weld, leaving a trace of material at the side. This can be significantly decreased with scrolled shoulder tools.
6. Wormhole-defect: also called “Cavity” is common on the advancing side of the weld and is caused by a lack of consolidation at the trailing edge of the tool. The result is a tunnel inside the weld that is invisible from the outside.
7. Root defect: Tool misalignment or a too short tool pin causes a lack of consolidation at the bottom of the material in butt joints.

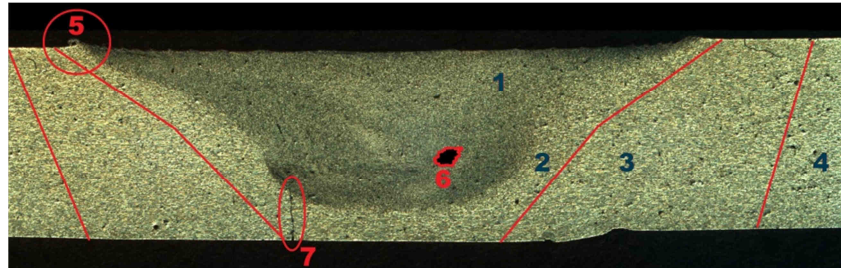


Figure 6: Microstructure of a FSW butt joint in cross-section with characteristic zones and defects.

#### 2.1.6 From lightweight to high-temperature alloys

The first investigations of FSW were performed on aluminium alloys (Thomas et al., 1991). In section 2.1.1 is described how several aluminium alloys are difficult to join with fusion welding. FSW of AA-2024 alloy is however no problem and can reach a joint efficiency<sup>4</sup> of above 80%. Often hardness measurements are performed to get a first indication of the mechanical properties. FSW shows typically a W-shaped hardness curve, with the lowest hardness in the HAZ. Several aluminium alloys such as AA-2024 will naturally age: the mechanical properties are expected to improve and stabilize after a week, as demonstrated in (Mishra and Mahoney, 2008).

Because of the excellent joint properties, also other materials became of interest for this process. Several combinations of aluminium with other alloys using FSW have been presented such as lap joints of aluminium to copper alloys (Abdollah-Zadeh et al., 2008) and aluminium to magnesium alloys (Somasekharan and Murr, 2004). Often intermetallic compounds are reported, which can initiate cracks.

---

<sup>4</sup> Joint efficiency is defined as the ratio of the strength of the weld to the strength of the parent material

The investigation of high-temperature alloys such as stainless steel and nickel alloys was a logical step forward. One of the first reports is a feasibility study by Thomas et al. from 1999. The fact that the stir zone in FSW can be stronger than the base material and the defect-free character of the weld is definitely an important advantage and will support the industrialization of FSW of steel for certain niche branches. However, there are a lot of application domains where classic welding techniques are much cheaper so FSW is not worth to be considered as an alternative (Thomas et al., 1999). Successful tests demonstrated that steel has to reach a temperature of over 800°C to make the material sufficiently soft and has to stay below 1200°C (Bhadeshia and DebRoy, 2009).

#### *2.1.7 Tool materials*

Traditional FSW tools for aluminium are usually made out of hardened tool steel, sometimes with coating. For welding aluminium, there is little tool wear and welding seams of several kilometres can be performed with one single tool. For welding high-temperature alloys, the demands on the tool properties are much higher. The tool needs to remain strong and hard at high temperatures but may not break during plunging. There are only a limited amount of materials that fulfil these requirements.

The first refractory metal<sup>5</sup> tools used tungsten (Lienert et al., 2003). These tools have the required strength but are extremely brittle. Therefore a rigid machine, a pre-drilled hole and preheated pin is required to perform a successful weld operation, i.e. without breaking the tool. More recently, the expensive tungsten-rhenium alloy is used which has an increased fracture resistance. These tools wear relatively fast, leaving a trace of tungsten in the stir zone. The effect of these tool particles on material properties is not well documented but due to the small quantity, it is expected to be little.

The other type of high-strength tools are made of so-called superabrasive material. These materials are formed under extreme pressure and temperature and can be classified as ceramics. These materials are extremely strong at high temperatures but accordingly very brittle. The most common superabrasive material for friction stir welding tools is polycrystalline boron nitride (PCBN). These tools were first reported in 1998 (Sorensen and Nelson, 2007). PCBN was already used in the early 80's for metal cutting tools, due to its superior performance compared to tungsten based tools. The high production output and long tool life to reduce machine downtime was already reported at that time (Obeloer, 1983).

Recent advances in superabrasive materials are for example PCBN-Q70 from MegaStir™. As reported by Sorensen, the tool wear is investigated during FSW of structural steel with a Q70 tool. There is no noticeable tool wear after 18 meters of welding. A full scale demonstrator welded butt joints of over 60 meters with one single PCBN tool.

---

<sup>5</sup> Refractory metals are a class of metals that are extraordinarily resistant to heat and wear. Conventionally, the group includes five elements: niobium, molybdenum, tantalum, tungsten and rhenium.

In an attempt to reduce tool wear, a plunge hole can be pre-drilled and the material can be preheated, for example by induction heating (Mishra and Ma, 2005) or by laser (Fujii et al., 2008). This is reported to decrease tool forces and increase tool lifetime.

Recently, other research groups experimented with new tool materials. Miyazawa reported good initial results with iridium-based FSW-tools (Miyazawa et al., 2011). SLV in Germany conducted promising tests with tantalum-based tools. The weld quality was comparable to the welds with PCBN tools (Boywitt, 2011).

It is expected that eventually one of these alloys will show to have the best lifetime/cost ratio and will be used in industrial applications.

### 2.1.8 Tool geometries

The original FSW tools had a concave shoulder and a cylindrical pin. An impressive amount of tool geometries have been developed since then, Typical features that are added for improved material flow are scrolls on the shoulder and threads on the pin. The shoulder can be convex, concave or hybrids in between. Sometimes very complex tools were presented in recent years such as the MX Triflute™ by TWI with a frustum-shaped pin and both clock- and counter-clockwise threads, as shown in Figure 7c (Thomas et al., 2003). Recent development in FSW with steel and other hard materials faced problems with the lack of material flow. Adding features like a scrolled shoulder (Figure 7b and Figure 7c) and a threaded pin (Figure 7a) contributes to a better material flow. The tool features can be seen as a way to compensate the lack of friction between the tool material and the welded material. This can allow higher welding speeds. The scrolled convex shoulder has another imported advantage: the material is mechanically pushed towards the centre of the tool, giving an excellent looking weld without any flash.

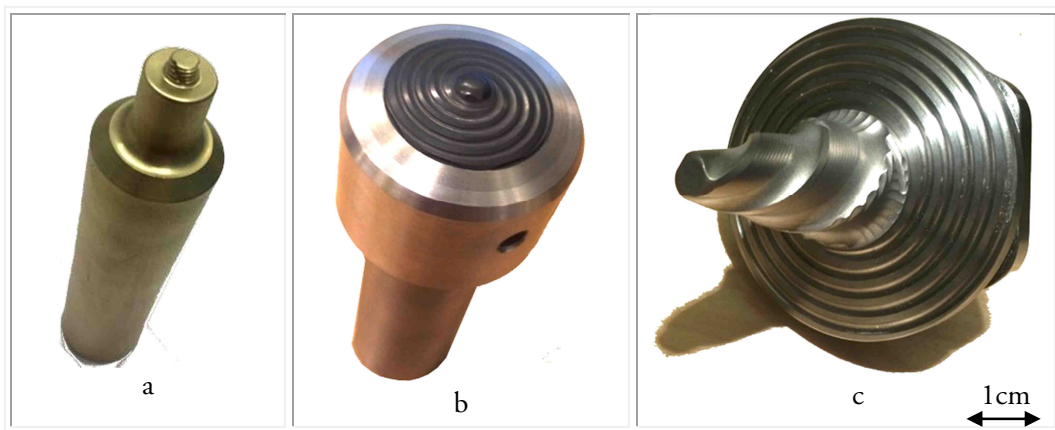


Figure 7: Three different FSW tool designs: steel tool for thin aluminium overlap joints (a), PCBN tool for high-temperature alloys with convex scrolled shoulder (b) and tungsten tool for thick copper with MX Triflute™ pin geometry (c)

### 2.1.9 Process variants

Next to the “classic” FSW process, several process variants have been presented throughout the years. Some of these are listed here.

- Stationary Shoulder Friction Stir Welding – SSFSW: The tool consists of 2 separated cylinders: the shoulder and the pin. Only the pin is rotating while the shoulder provides the required pressure. This gives a lower energy input and makes it possible to weld corner joints (Martin et al., 2011).
- Friction Stir Spot Welding – FSSW: This process is simpler than FSW as the forward movement is absent; the tool only plunges and retracts, creating a ring-shaped joint. FSSW is already adopted in the automotive industry (Aluminum Now Magazine, 2003)
- Friction Spot Welding – FSpW: The process, developed at HZG in Germany is a development from FSSW. It introduces a tool with 3 separately moving cylinders. The material is extruded between the inner and outer ring. During retraction, the material is pushed back, filling the typical keyholes. The absence of this hole results in a much stronger joint than FSSW. (Rosendo et al., 2011)
- Friction Surfacing is a form of metal deposition. The process can be seen as a combination of FSW and friction welding. A consumable rotating tool in the same material as the workpiece is pressed along a path on that workpiece. A trace of consumable material with a limited thickness is left on the surface. When the path is repeated several times, a layer-structure is built on the workpiece. (Thomas, 1992)
- Friction Riveting: A small cylindrical component such as nuts, bolts or screws is rotated and pressed against a surface. Applications are demonstrated where steel bolts are joined with polymer plates. (Amancio-Filho and dos Santos, 2009)
- Shoulder-less FSW : The tool is cone-shaped and allows continuous variation of penetration depth. The results with these tools are satisfying, though the obtained results in terms of ultimate tensile strength are worse than with the standard tools (Lammlein et al., 2009).
- Hybrid Friction-Diffusion Bonding (HFDB): This FSW process variant for joining thin sheets (up to 1 mm) in overlap configuration is similar to FSW but characterised by the absence of a pin on the tool. A cylindrical non-consumable tool is rotated against the surface. Diffusion bonding between the two plates provides a high-quality joint (Roos, 2010).

## 2.2 Robotisation of the FSW process

It was not until the Friction Stir Welding Symposium in Gothenburg, Sweden in 2000 that the first robotic FSW application was demonstrated. Two research groups presented successful welding in aluminium, one group using a serial kinematics robot (Smith, 2000), the other using a parallel kinematics robot (Von Strombeck et al., 2000). The work by C. Smith was initiated in 1997 with internal feasibility studies at Tower Automotive (Smith, 1997) and could be seen as the first investigation of robotic FSW. In the first welding trials an ABB IRB-6400 robot was used, combined with a 220 W electric spindle motor.

The serial kinematics design is the most common for industrial robots. It is widely adopted in the automotive industry and has been tested in the area of FSW by several research groups in the past (Smith et al., 2003, Soron, 2007, Voellner et al., 2006). Alternative systems have been demonstrated, using parallel kinematic robots (Von Strombeck et al., 2000). Such robot systems have a much better stiffness but lack the large workspace that serial kinematics robots offer and are far more expensive. A serial kinematics robot has great advantages but the limited stiffness has always been an issue. A robot consists of many components with certain flexibility. These inaccuracies are mainly caused in the joint by torsional flexibility in the gears, bearing deformation and shaft windup (Spong and Vidyasagar, 1989). A common way to overcome the deflection problems during in-contact welding operation is implementation of force control. The contact forces are measured and handled by a force controller. This will modify the desired TCP position according to a chosen force-handling strategy. In addition to position corrections, also robot damping can be controlled by implementing a control relation between robot-speeds (i.e. time derivatives of the poses) and measured forces. This can add to the robot's stability during in-contact operations.

In a study on three-dimensional FSW (Zäh and Voellner, 2010), design rules were given to obtain good welding quality on highly curved surfaces. A good weld was only obtained if the force in the curves was reduced and if the trailing edge (i.e. the backside) of the tool remained in contact with the material. This resulted in a tilt angle of over 18°. The diameter of the tools was limited by the bending radius of the work piece. Furthermore, the tool deviations in welding direction were reported up to 5 mm.

Cook studied the process forces in FSW on a typical position-controlled FSW machine. It was demonstrated that a stepwise increase of the welding depth did not cause an increased axial force. Instead the axial force reached the same steady-state value and increased production of flash on the sides of the weld was observed (Cook et al., 2004). Another conclusion in the study is the significant reduction of axial force when the spindle speed is increased. This was a result of the increased heat input, which causes the material to soften more. Thus, within a certain parameter range, the reaction forces can be reduced through proper setting of the process parameters including tool design to make it possible to apply robots for FSW.

In an attempt to decrease the load on the robots, several alternatives to the conventional FSW approach have been presented where the load is carried by the tool or by a device, mounted on the robot instead of by the robot itself. One successful attempt is the bobbin tool, where no downforce from the robot is required. Instead, the process forces will be produced between the two tool shoulders which are mechanically locked to each other (Thomas et al., 2009). Another process variant is friction stir spot welding (FSSW) with a so-called C-frame. This is a big C-shaped metal block, mounted on the robot, in which a rotation tool is mounted. The tool can be pressed down with an electric or hydraulic actuator. The downforce is generated by this actuator and not by the robot. The robot can be seen as a device that carries and moves the FSW equipment. Several types of FSSW have been presented. The most revolutionary FSSW variant is probably Friction Spot Welding, invented at HZG in Germany and now commercially available from the company Harms & Wende (Schilling and Dos Santos, 2000).

## **2.3 Process control and automation**

It is a necessity to understand the physical effects that arise in the process in order to develop a robust control strategy. Modelling of the process is an important part of process understanding. Various process models are presented (see section 2.1.4) and verification shows how well the presented model (and used physical laws) correspond to the actual process (Schmidt and Hattel, 2005). But even the most detailed model will never be able to compensate for unexpected disturbances in the process. Examples are insufficient clamping, oxides, varying plate thickness, tool wear, oil stains, etc. All these factors will influence the process temperature and the material flow and thus the quality of the obtained weld. Only closed-loop process control is able to detect these variations and avoid a reduced weld quality.

Even though there is a lot of on-going research within FSW, the number of publications on process automation and closed-loop control is still relatively small. The main reason for this is the fact that FSW is a very robust process and therefore it does not require closed-loop control for the applications in the industry today. However, to make the process more flexible, i.e. different components and different materials, there is a clear need for further process automation. Using robots adds some extra complexity to the welding operation because of its limited stiffness.

### *2.3.1 Force control in FSW*

Apart from FSW, several other industrial applications using robot force control are reported. In 1986, a force control method was presented for deburring (De Schutter, 1986) but the lack of robustness at higher speeds made the system not useful for industrial applications.



The required force for deburring is rather low, making it difficult to split signal from noise in the force signal. A good working filtering algorithm is therefore required (Willersrud et al., 1995). Thomessen presented a system that allows automatically programming a path for deburring and grinding of contours with a set force of around 40 N. The controller could handle speeds up to 100 mm/s and even path discontinuities were traced. The system replaced a manual jog-and-teach-approach, which reduced the programming time by 80% (Thomessen and Lien, 2000). Lee and Asada presented a model for force-guided assembly task with a robot (Lee and Asada, 1999). Also more and more milling applications investigate robots because of their flexibility. Federspil reported an experimental study on robotic milling of oak wood and human temporal bone specimen, used for implants. The study shows the first development of a functional robotic milling procedure for otological and otoneurosurgery<sup>6</sup> with force-based speed control (Federspil et al., 2003).

### *2.3.2 Temperature control*

At the Swedish Nuclear Fuel and Waste Management Company (SKB) a temperature controller was developed to provide a reliable method to seal 50 mm thick copper canisters with nuclear waste. A cascade controller has been presented, using both power feedback from the spindle motor and temperature feedback from the tool (Cederqvist et al., 2012).

Fehrenbacher presented a temperature control for FSW of thin aluminium. Weld temperatures in the range from 555°C to 575°C were commanded to an integral compensator, which regulated the spindle speed between 850 rpm and 1250 rpm to adjust the heat generation and achieve the desired weld temperatures in 3.18 mm thick 6061-T6 aluminium alloy. Thermocouples were inserted in the tool shoulder. The process is modelled as a first order transfer function plus time delay, with speed (rpm) as control variable and temperature (°C) as output variable. A typical PID-type controller is suggested, with only integral action (Fehrenbacher et al., 2011).

### *2.3.3 Seam tracking for FSW*

There exists a need for path compensation, due to robot deflections as indicated in section 2.2. There are however other reasons that can cause misalignment between tool and workpiece. Incorrect programming or difference between virtual and real environment in case of offline programming is a typical issue for robot applications and also exists for robotic FSW. For manual programming of the welding path, the effect of misalignment depends a lot on the application. Lap joints, for example are not sensitive to path deviation for obvious reasons. Alignment is more important for butt joints, where the tolerance is limited to about half of the pin diameter (Takahara et al., 2007). In the case of T-

---

<sup>6</sup> Otology is a branch of biomedicine which studies anatomy and physiology of the ear. Otoneurosurgery is the surgical specialty that deals with the hearing part of the nervous system.

joints, detection of the joint is difficult as it is invisible from the top side. Furthermore the combination of a force-controlled operation with open-air clamping of thin-walled T-joints can cause the tool to sink into the material as there is insufficient support (Fleming et al., 2009). Fleming presented a strategy for seam tracking in T-joints. Combining the information from both axial and traverse force measurements could predict the absolute position offset. A general regression neural network was trained as offset controller during welding. The paper states that their model could also be used for lap joints and for implementation on robotic friction stir welding applications; however the method is based on force-measurements during position-controlled welding and as such not suitable for serial kinematics robots, due to their force-controlled motion.

#### *2.3.4 In-process quality control*

The ability to detect defects during welding is of great interest for industrial applications. This would either allow the operator to abort the process without wasting more tools and material or it would enable an online controller to change the welding parameters and still produce a good quality weld. A very interesting investigation at Wichita State University demonstrated the ability to detect the formation of defects, before the actual defect is visible in the microstructure. The system is based on frequency analysis of force measurements and used a trained neural network to determine whether a defect was present or not. Low frequency oscillations were an indication of wormhole formation and could be identified in the frequency spectrum.

This new NDE-method is evaluated and proven to be faster in defect detection than two of the most reliable techniques in the industry today: Ultrasonic Phased Array and X-ray (Gimenez-Britos et al., 2010).

## 3 Experiments & System Development

In this section, the platform is described in which the research is conducted. The process and the robot system is analysed and controllable welding parameters are described. Furthermore the problems related to robot deflections are described.

### 3.1 Experimental platform

The main part of the experiments was carried out at the Production Technology Centre in Trollhättan, one of Sweden's most modern production research centres. It is equipped with a complete robotic FSW facility and a materials lab is available for analysis of welding experiments.

#### 3.1.1 The FSW Robot

The welding lab is equipped with the ESAB Rosio™ friction stir welding robot. This robot is a heavily modified ABB IRB-7600 robot with ABB IRC5 control system. The last robot axis is completely removed and replaced by the FSW equipment. The control system is adapted to a 5-axis controller and a force sensor for direct force control is implemented. The robot comes with several instructions for programming FSW of simple geometries.

The spindle motor is mounted on the 5<sup>th</sup> robot link and connected through a gearbox to the spindle, mounted on the 6<sup>th</sup> robot link. The motor has a maximum speed of 4500 rpm and a stall torque of 45 Nm. The gearbox ratio is 2:3, resulting in maximum rotational speed at the tool of 6000 rpm and a torque of 30 Nm. This enables both welding with high traverse speed (high rpm requirement) and welding of up to 7 mm thick material (high torque requirement). The robot is capable of moving at speeds up to 8 m/min but welding is only verified up to 3 m/min.

#### 3.1.2 Robot programming

A virtual FSW robot model is created in RobotStudio, the offline programming software from ABB. This software is chosen because it is user-friendly and it works well together with the IRC5 robot control system. It does not provide all the features as other commercially available robot simulation software (such as for example Process Simulate) but has enough functionalities for this application. An Ethernet connection between the

control system of the robot and computer with RobotStudio guarantees a stable communication.

The robot system comes with several software features for programming simple geometries such as squares, lines and circles. These functions only require some teach-points to define that geometry (e.g. four corner points to define a square path). The welding path with desired tilt-angle is calculated from those points. The robot did not include a function that can use offline-programmed robot paths for FSW. For implementation of a FSW-robot in flexible production, the robot should be programmed offline. To facilitate the programming, a function for offline programming of FSW joints is developed and programmed in the RAPID language, the default programming language for ABB control systems. With the new function, the force-controlled robot is able to use the offline programmed paths for 3D FSW operations.

For the project demonstrators, CAD parts from industrial project partners are exported as VRML2-format files, which are easily imported into RobotStudio. When all the relevant parts from the robot cell are added in the virtual environment, the position of the welding locations has to be calibrated. The offline model has to correspond to the real world in a very precise way. Therefore, points on the fixtures are taught-in carefully and sent to the virtual environment. The corresponding points on the CAD parts are then mapped with these real-world coordinates (see Figure 8).

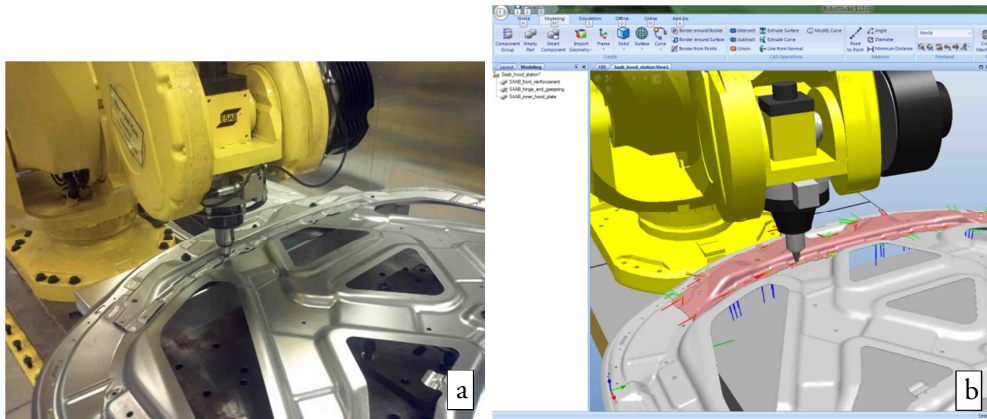


Figure 8: The real welding environment (a) and the corresponding offline robot studio model (b)

### 3.1.3 Measurement system

As part of the experimental platform, a measurement system was installed in the robot cell, consisting of a measurement PC and a National Instruments data acquisition system with different measurement modules such as thermocouples and analogue input (voltage and current). The measurement system is connected to the PC through USB.

For analysis of robot path accuracy, a laser distance sensor from Micro Epsilon, type optNCDT1302-200 is mounted on the robot. This sensor can measure distances with high accuracy ( $40\text{ }\mu\text{m}$ ) within a range of 200 to 260 mm from the sensor at speeds up to 750 Hz. A vision-based approach for deviation measurements is tested using a monochromatic camera from Allied Vision, type Prosilica EC650. This camera is connected through FireWire to the measurement PC. The data stream is opened in a LabVIEW program and passed on to MATLAB for image analysis. This is further described in Paper D.

For measurement and understanding of thermal effects on complex geometries, a thermal camera was used and compared to thermocouple measurements. Recently there are very compact IR-cameras available on the market that can be mounted on the robot. Experiments in this thesis are conducted with an Optris PI-160 thermal camera. The outer dimensions are  $45\times 45\times 50\text{ mm}$ . The camera is able to measure temperatures up to  $900^{\circ}\text{C}$  at frequencies up to 120 Hz with a resolution of  $160\times 120$  pixels. The system has USB connection and comes with the necessary software, making its installation as easy as the installation of a webcam. For analysis of the force data, two different methods were used. The first method is reading the force sensor data in the RAPID program and logging the data in a text file at a sample rate of 3 Hz. The cycle speed of the RAPID program in the IRC5 robot control system restricts the sampling rate to a maximum of about 5 Hz. The second and faster method uses ABB TestSignalViewer software. It is a tool provided by the robot manufacturer for diagnostics of the system. This can read out for example electric current data, joint angle data and position- and force data at the TCP. The software reads the force data from the robot via an Ethernet connection and can read force data at 200 Hz.

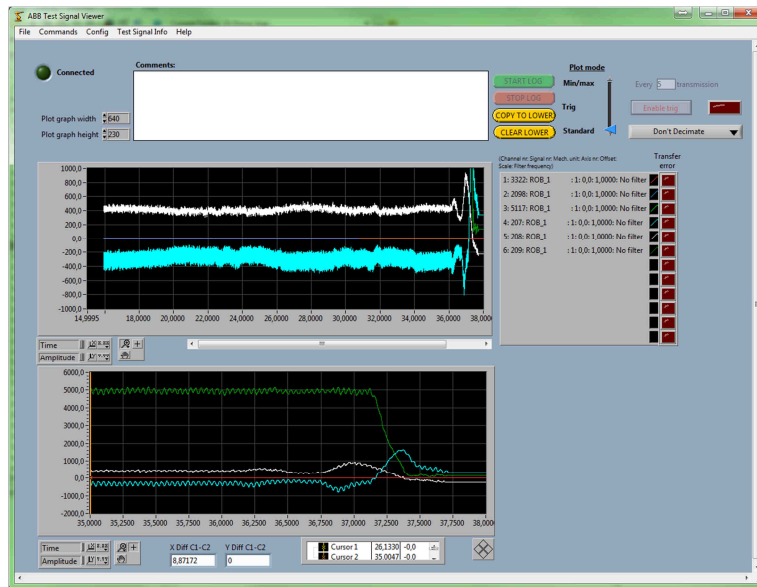


Figure 9: Force measurement during FSW using TestSignalViewer

### 3.2 FSW process analysis

In order to control the process, a profound understanding of the effect of parameter changes on the process is required. Rotational speed is usually used for control of the heat input, because it gives the fastest process response. The unique feature with the robotic FSW system is however the embedded force control, which makes it possible to use the downforce as control signal for temperature control.

The spindle speed is an important process parameter and is the main contributor to the material flow and total heat input. The travel speed also affects the heat input and can be used for benchmarking FSW against other welding process. The maximal welding speed is related to the friction coefficient between the tool and the material. At lower speeds, the spindle speed / travel speed ratio, sometimes called “pitch” is introduced. At a constant pitch, the material flow is similar and a comparable weld quality can be achieved. However, as the pitch increases, the limited friction will cause a reduced material flow and finally, the tool will only slide through the material and there is no proper material flow anymore, resulting in welding defects.

Especially for robotic FSW, understanding of the process forces is important as it affects the stability and accuracy of the system. The forces acting on the tool are:

- *Downforce*: The downforce is one of the main process parameters and affects the friction between the tool and the plates. This friction is the main contributor to the heat generation in the process.
- *Traverse force*: This force is a result of the materials resistance to the tool movement along the joint line. This force will be influenced by the welding parameters and the type of welded material.
- *Side-force*: This force is perpendicular to the traverse force. It is caused by the asymmetric character of the welding process. The force is directed towards the advancing side of the weld. These forces are applied to the welding tool, causing the robot to deflect from the joint line.

Several other controllable and uncontrollable variables are relevant to investigate:

- *Torque*: The torque is a result of the friction between the tool and the work piece and corresponds to the heat input into the system. Higher contact forces and a larger contact area result in a higher torque.
- *Tilt angle*: By tilting the tool backwards, there will be more pressure on the material behind the pin, improving consolidation of the material and decreasing the risk of defects.

- *Side-tilt angle*: The tool is tilted into the advancing side or retreating side. The effect of this parameter is not well known. This angle is further discussed in Paper E.
- Material properties, including thickness, hardness, alloying elements, natural aging.
- Fixture properties, including backing bar material, cooling and heat dissipation.
- Tool properties including material type, geometry, friction coefficient, wear resistance.

Most of these variables are defined by the application (e.g. material and fixturing) or are not possible to modify during the process (e.g. tool properties). There are however a set of parameters that can be used for control of the process. Rotational speed and downforce are the most suitable for this.

### 3.3 FSW robot analysis

There is a substantial difference between robots operating in the free space and robots performing in-contact operations where external forces are involved. The control of the latter is usually more complex and requires in some cases both motion control and force control. Although the mathematics for robot systems are complex and computationally intensive, the control scheme for a motion-controlled robot can be written as a simple closed-loop system, shown in Figure 10.

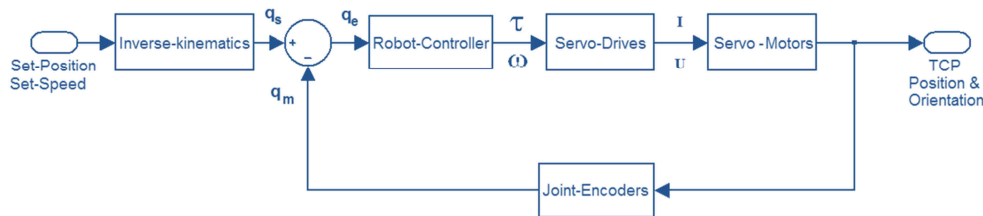


Figure 10: Basic motion control scheme for robots

The research described in this thesis relies on the existing force controller from the robot manufacturer where both kinematic and dynamic control is included in a complete force control strategy. This is used for controlling the axial load of the tool on the workpiece during FSW. The FSW process puts high requirements on a robot system in terms of force, stability, path accuracy and temperature. Both stability and accuracy can be significantly improved by implementing force control. The used system uses direct force control in the z-direction to maintain a constant downforce and guarantee a stable heat gen-

eration between tool and material. This strategy increases the welding performance greatly and guarantees a stable welding process.

### *3.3.1 Plunge operation*

One issue is the transition from position to force control. If the reference-force for welding is set before the tool is in contact with the material, the tool will be smashed into the material, due to fairly low damping and a high set force. In (Sorono, 2007) the start position of the weld has to be taught precisely at about 0.1 mm above the surface. From there, the force control is enabled and the robot starts measuring how deep the tool is plunging into the material. Due to deflections in the robot structure during the plunging phase, and subsequent welding, the programmed depths must be larger than the actual plunge depth. Finding the plunge depth parameter is a trial-and-error approach that is increased until the plunge depth is considered 'deep enough'. When the robot system measures that the programmed plunge depth is reached, the transition is made from downwards to forward movement along the joint line.

For the research described in this thesis, a new strategy is developed for the plunge operation. Instead of teaching a point very close to the surface, a low force is set at about 10 mm from the surface. The rotating spindle will touch the surface but will not plunge into the material. The TCP speed will become close to zero. This drop in speed is detected by the system and from there the plunge force is set. As soon as the pin has penetrated through the material, the shoulder will touch the plate and again a drop in TCP speed can be detected. This approach eliminates the plunge depth parameter entirely and adds to the flexibility of the system. The RAPID code is attached in Appendix A.

Besides the downforce, also the side-force has to be considered for robotic FSW. The asymmetric character of the welding process generates a force on the tool towards the advancing side, which causes the robot to deviate from its programmed path. This can result in welding defects. The control strategy for compensation of path deviations can be significantly reduced. Dynamic problems can be ignored for three reasons: The path offset is relatively constant along the welding path, the forces are high so signal-noise issues are irrelevant and FSW can be considered a slow process with a constant welding speed. A strongly reduced direct force control is suggested here, based on a torque/deflection model. The model is only implemented in side-force direction to compensate for path deviations.

### *3.3.2 Robot force control*

In recent literature (Siciliano and Villani, 1999), force control is often divided in two categories: direct and indirect. Indirect force control is based on modification of the motion control loop and does not have a closed-loop force control. Direct force control is based on a closed-loop force controller and allows the user to set the force to a desired value.



A friction stir welding robot with direct force control is adopted for all conducted research in this thesis. The whole force control is based on force sensor measurements with an ATI Omega 190 force-torque sensor. This sensor can measure forces in axial direction of 18 kN and 7.2 kN in xy-direction. The maximal torque is 1400 Nm around all axes.

The axial force is used for direct force control using ABB's force controller in the IRC5 control system.

To compensate for path deviations, a solution is presented in Paper D using the laser sensor and camera, described in section 3.1.3. Both methods allow absolute deviation measurements. The correction value is sent from the measurement PC to a register inside the robot controller. A function is available in the system that allows defining an offset from a programmed path. This function suits well for path compensation of FSW. The additional control loop for path compensation is indicated in green in Figure 11.

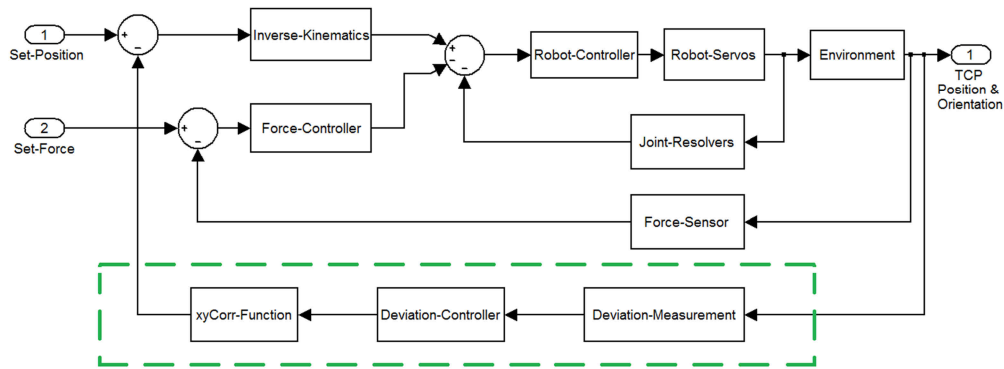


Figure 11: Force control strategy for FSW robots with sensor-based path compensation



## 4 Summaries of the appended papers

### Paper A – A Local Model for Online Path Corrections in Friction Stir Welding

The paper is a first step towards path compensation of robotic FSW. It is observed in welding tests that the robot tends to deflect, due to the high process forces, which results in path deviations and welding defects. First a set of aluminium alloys is welded with different parameters. With calibrated microscopic images, the deviation from the joint line is measured. Possible relationships between measured process parameters and deviations are investigated. The side-force was shown to have the best correlation with the path deviations, though with highly scattered measurements. A linear approximation model is presented that predicts the deviation of the tool, based on force measurements during the start of the process. This deviation is given as input to an existing path offset function in the robot control system. The model is verified with welding tests in hard aluminium alloys and proven to be sufficient to compensate the robot path in a limited workspace to a deflection within the tolerances for good weld quality.

The paper was presented at the Friction Stir Welding and Processing conference in Lille, France, February 2010.

### Paper B – Friction Stir Welding with Robot for Light Weight Vehicle Design

This paper presents the StiRoLight research project and the milestones that should be reached in order to implement FSW in the automotive production line. Furthermore, the state-of-the-art in robotic FSW and challenges associated with the use of robots were discussed. The results from Paper A are further analysed and related to different welding directions. The scattered measurements could be related to the welding direction and instead different models, depending on the welding direction are proposed. A part of the paper describes temperature measurements during FSW of preheated material. This preheating is not caused by external heat sources but by previous FSW, close to the new weld. Thermocouples were inserted between the plates, giving accurate measurements of the temperature around the pin. Also a thermal camera was used to relate the thermocouple measurements to the temperatures at the edge of the tool. The effect of preheated material on the maximum welding temperature was hereby demonstrated as well as the need for temperature control on complex joint geometries in FSW.

The paper was presented at the 8<sup>th</sup> International FSW Symposium in Timmendorfer Strand, Germany, May 2010.

#### Paper C – Surface Quality and Strength in Robotic Friction Stir Welding of Thin Automotive Aluminium Alloys

The paper investigates weld quality and visual quality of automotive aluminium alloys from an industrial perspective. One part of the study showed the robustness of the welding process; by changing process parameters, the variations in tensile strength were shown to be limited. The identified process window can be used as the range in which process parameters can be controlled at a later stage. A second part of the paper attempts to classify the visual quality of the weld in a quantitative manner. This is done by roughness and waviness measurements. Especially for outer body panels in automotive applications, this visual quality is very important. Some criteria to approve a body panel with FSW are suggested. It was shown that with the present fixturing and tools, the surface quality is insufficient for use on class-A surfaces i.e. the outer body parts of the car. Finally, the paper suggests a method for the operator to detect welding defects and predict if a weld is sufficiently strong by “human-eye inspection”. This is important for a production line, where not each sample can be analysed by destructive testing.

The paper was presented at the Swedish Production Symposium in Lund, Sweden, May 2010.

#### Paper D – Investigation of Path Compensation Methods for Robotic Friction Stir Welding

This journal paper is a conclusion of all work done on path compensation since the start of the project in 2009. The paper shows the evolution from a model for local workspace, based on microscopic analysis, to a sensor-based path compensation method in a global workspace. Two methods using camera and laser-distance sensor are implemented and compared and both methods could measure the deviation of the tool from the joint line accurately. The paper gives better insight in the FSW process forces on robots. The novelty in the paper is the study of lateral process forces and relating it to path deviations, which is not of interest for most FSW research as the typical machines are very stiff and don't deflect. Furthermore it presents a model for implementation in the used robot system to compensate deviations in FSW in the complete robot workspace, similar to seam-tracking systems known in other welding processes.

The paper is accepted in March 2012 for publication in *Industrial Robot – An International Journal*.

Paper E - Influence of Side-Tilt Angle on Process Forces and Lap Joint Strength in Robotic Friction Stir Welding

This article investigates the side-tilt angle in FSW. This is a so-far unstudied parameter, mainly because it requires 5 degrees of freedom to tilt the tool in both travel direction and sideward. Having the FSW robot system available, it is possible to tilt the tool in the plane perpendicular to the welding direction, applying more pressure on either advancing or retreating side of the weld. Based on the hypothesis that more force on one side will decrease the asymmetry in the welding process, several samples in the strong AA7075-T6 alloy were welded with different side-tilt angles. The effect is studied by microstructure investigation and tensile tests. There is a slight increase of strength when the tool is tilted towards the advancing side. Furthermore, the forces on the tool are measured for different side-tilt angles.

The paper is accepted for presentation at the 9<sup>th</sup> International FSW Symposium in Huntsville, AL, USA

Paper F - Three-Dimensional Friction Stir Welding of Inconel 718 using the ESAB Rosio FSW-Robot

The paper is one of the few publications that describe three-dimensional FSW of high-temperature superalloys. FSW of non-linear geometries require a 5-axis machine which is more expensive than a robot. Implementing the process on a serial-kinematics robot system puts however heavy demands on the robot in terms of force, torque and temperature. The nickel-based superalloy Inconel 718 was selected for investigation and welded with a ceramic PCBN tool. The major part of the paper focuses on parameter optimisation to allow a decrease of the process forces. By implementing preheating and increasing the rotational speed of the tool, the forces could be reduced to 12 kN, which is within the force capabilities of the ESAB Rosio FSW robot. The importance of a hardened backing bar is shown to obtain defect-free welds. The torque of the spindle motor was proven to be insufficient and was solved by implementing a lower gear ratio in the system that increased the maximal torque to 100 Nm. A successful weld operation could be performed on the robot system but initial tests did not provide an acceptable joint quality. Higher preheating temperatures are suggested to increase the quality of future welds.

The paper is accepted for presentation at the Trends in Welding Research conference in Chicago, IL, USA.



## 5 Conclusions

This licentiate thesis is a first step towards the implementation of robotic friction stir welding in a flexible automated production line. A few key-points that require further automation are highlighted, in order to let the FSW robot perform good welds in an automated production line. One of these points is the need for compensation of robot deflections. The observations in early welding tests clearly demonstrated the need for path compensation to guarantee a defect-free weld. Decreasing the tool deviations could improve the weld quality. This is the main conclusion in Paper A. An initial strategy for path compensation in a limited workspace, the “local workspace model” is presented. To allow one robot to perform welds in a bigger working envelope, a new method is developed in Paper B, using a camera- and a laser-distance-sensor-based measurement system to detect path deviations in the whole robot workspace. The performance of this system is discussed in Paper D. The main drawback is however the need of extra sensors. The main advantage with the used robot system is compactness, due to the removal of the 6<sup>th</sup> robot axis. The described sensor-based compensation method, however, requires re-introduction of a 6<sup>th</sup> axis for aligning the sensors with the welding path. A new strategy is therefore discussed in In Paper D. The new approach avoids additional sensors and allows path compensations for the whole workspace, based on the already existing force sensor.

The effect of the limited robot stiffness on the robustness of the welding process is addressed in Paper C. Also the sensitivity for material thickness variations in lap joints is investigated and some practical rules are presented as well as restrictions to the applications of FSW where the visual quality of the weld is important.

One of the aims of this research was to find out the limitations of the robot system. Paper F describes FSW of superalloys where the robot system is pushed to its limits. This provided knowledge of the maximal applicable forces of the system, the maximal torque and the maximal temperature. The possibility to use a robot for FSW of high-strength alloys is demonstrated.

Finally to allow successful welds on complex geometries, the effect of angular tool deviations had to be investigated. Paper E shows the effect of different tool orientations on the welding quality and demonstrates that small variations in side-tilt angle don't have a significant influence on the strength of the weld.





## 6 Discussion and Future Work

The research results in this thesis have addressed the raised research questions in section 1.3. The path deviations could be reduced to a deviation within the tolerance window of the process, avoiding the typical wormhole defects. Along with the development of a sensor-based compensation method, a better insight into the process and how this affects the robot's behaviour is provided. This allows the development of improved compensation methods in the future, based on the present force sensor. The additional process automation as referred to in the second research question is addressed by identifying the problem of overheating and the presentation of a temperature control strategy.

The limitations of the robot are addressed in terms of maximum payload in the robot's workspace. The capacity of the robot is far above the values specified by the robot manufacturer on certain locations in the workspace. This implies that alloys with high melting point such as the nickel alloy 718 could be joined by the FSW robot. This is further discussed in Paper F. These tests on a classical FSW machine show that the maximal payload is indeed within the robot's force capabilities. Another limitation is the maximal deliverable torque from the electric spindle motor. This is overcome by changing the gear configuration to a higher ratio, providing a higher torque and by using preheated material for FSW.

### 6.1 Strategy for temperature control

In the temperature experiments, described in Paper B it is observed that parameter changes are required to maintain a stable welding process on complex welding joints. The main reason is that previous welding locations pre-heat the following locations and therefore the maximum temperature of the weld increases. In the worst case, the material reaches temperatures close to the melting point, softens too much and the tool sinks through the material. A possible solution is the implementation of a temperature controller that decreases the applied downforce of the robot. This will both reduce the heat generation and the contact pressure, preventing the tool from sinking through the softened material. The suggested approach is indicated in red in Figure 12.

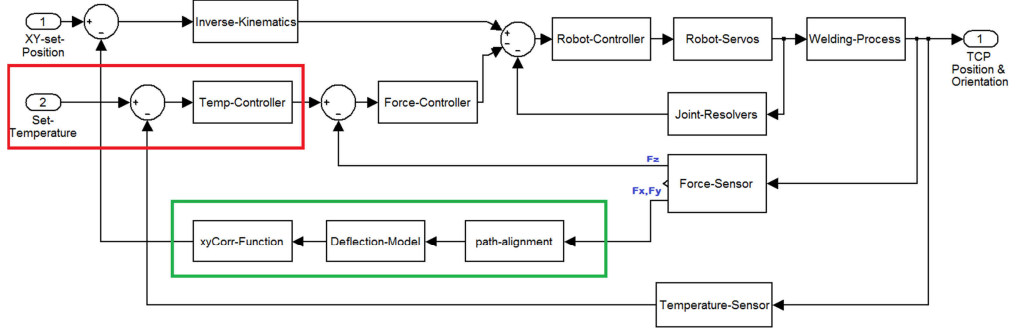


Figure 12: Design of two additional controllers for robotic FSW

## 6.2 Strategy for path compensation using force feedback

Based on the research on path deviations and robot deflection, a new approach is presented to predict the robot behaviour and compensate for deviations within the tolerance window for successful defect-free welding. This method assumes a linear relationship between the joint torque and the joint deflection. For each of the robot joint, a spring-constant can be identified. An easy way of finding this spring constant is by applying a force on the tool at strategically chosen robot configurations. This method is explained for identification of the spring constant at the first robot axis.

For the robot configuration in Figure 13, the force on the robot tool is applied in  $y$ -direction and the 4<sup>th</sup> robot axis intersects the TCP. For this specific location, only one rotational axis – the 1<sup>st</sup> robot axis – is deflecting, according to the assumption above. This gives a torque ( $M$ ) on the first robot axis, equal to the applied force ( $F$ ) times the distance from the first axis ( $x$ ). The angular deviation ( $\alpha$ ) of the robot axis is approximated as the linear deviation ( $d$ ) at the tool times the distance from the first axis ( $x$ ).

The spring constant for axis one ( $k_1$ ) is thus the angular deviation per torque unit ( $\alpha/M$ ).

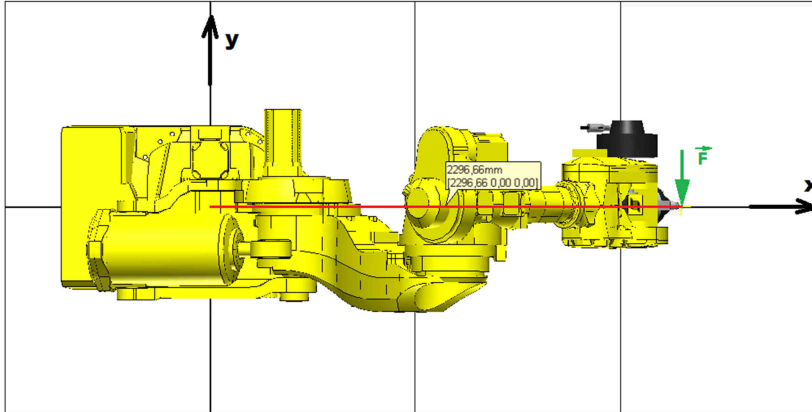


Figure 13: Robot configuration for identifying the spring constant at the first robot axis

By repeating these steps in different robot configurations, the spring constants can be identified for each axis and a complete deflection model for the robot can be composed.

The in-process measured side-forces are recalculated to the torques on each robot axis and the model will be able to predict the corresponding tool deviation from the joint line. The implementation of this additional controller is indicated in green in Figure 12. Initial studies show that this approach is feasible and therefore an interesting subject for further research.



## References

- ABDOLLAH-ZADEH, A., SAEID, T. & SAZGARI, B. 2008. Microstructural and mechanical properties of friction stir welded aluminum/copper lap joints. *Journal of Alloys and Compounds*, 460, 535-538.
- ALUMINUM NOW MAGAZINE. 2003. *Mazda the First to Use Friction Stir Welding for Aluminum Body Assembly* [Online]. Available: [http://www.aluminum.org/Content\\_bk100511/ContentFolders/AluminumNowMagazine/MayJune2003/Mazda\\_the\\_First\\_to\\_1.htm](http://www.aluminum.org/Content_bk100511/ContentFolders/AluminumNowMagazine/MayJune2003/Mazda_the_First_to_1.htm) [Accessed 2012-03-21 2012].
- AMANCIO-FILHO, S. T. & DOS SANTOS, J. F. 2009. Joining of polymers and polymer-metal hybrid structures: Recent developments and trends. *Polymer Engineering & Science*, 49, 1461-1476.
- ARBEGAST, W. J. 2008. A flow-partitioned deformation zone model for defect formation during friction stir welding. *Scripta Materialia*, 58, 372-376.
- BALAMUTH, L., KURIS, A. & KLEESATTEL, C. 1962. *Ultrasonic Welding*. USA patent application. 11 Sep 1962.
- BALASUBRAMANIAM, R. 1998. The decorative bell capital of the Delhi iron pillar. *JOM Journal of the Minerals, Metals and Materials Society*, 50, 40-47.
- BHADESHIA, H. K. D. H. & DEBROY, T. 2009. Critical assessment: friction stir welding of steels. *Science and Technology of Welding & Joining*, 14, 193-196.
- BOYWITT, R. 2011. Entwicklung und Erprobung von neuen Werkzeugmaterialien für das Rührreibschweißen von Stahl. Große Schweißtechnische Tagung 2011, 2011 Hamburg. DVS, 166-170.
- CEDERQVIST, L., GARPINGER, O., HÄGGLUND, T. & ROBERTSSON, A. 2012. Cascade control of the friction stir welding process to seal canisters for spent nuclear fuel. *Control Engineering Practice*, 20, 35-48.
- CHAO, Y. J., QI, X. & TANG, W. 2003. Heat Transfer in Friction Stir Welding - Experimental and Numerical Studies. *Journal of Manufacturing Science and Engineering*, 125, 138-145.
- COOK, G. E., CRAWFORD, R., CLARK, D. E. & STRAUSS, A. M. 2004. Robotic friction stir welding. *The Industrial Robot*, 31, 55-55-63.
- DAVIS, J. R. 1993. *Aluminum and aluminum alloys*, Materials Park, OH, ASM International.
- DE SCHUTTER, J. 1986. Compliant robot motion: task formulation and control. *Production Engineering, Machine Design and Automation (PMA) Section*.

- ESAB WELDING & CUTTING, U. S. 2012. *What are unweldable aluminum alloys?* [Online]. Available: <http://www.esabna.com/us/en/education/knowledge/qa/What-are-unweldable-aluminum-alloys.cfm> [Accessed 2012-03-14 2012].
- FEDERSPIL, P. A., GEISTHOFF, U. W., HENRICH, D. & PLINKERT, P. K. 2003. Development of the First Force-Controlled Robot for Otoneurosurgery. *The Laryngoscope*, 113, 465-471.
- FEHRENBACHER, A., DUFFIE, N. A., FERRIER, N. J., PFEFFERKORN, F. E. & ZINN, M. R. 2011. Toward automation of friction stir welding through temperature measurement and closed-loop control. *Journal of Manufacturing Science and Engineering, Transactions of the ASME*, 133.
- FLEMING, P. A., LAMMLEIN, D. H., WILKES, D. M., COOK, G. E., STRAUSS, A. M., DELAPP, D. R. & HARTMAN, D. A. 2009. Misalignment detection and enabling of seam tracking for friction stir welding. *Science and Technology of Welding & Joining*, 14, 93-96.
- FUJII, H., TATSUNO, T., TSUMURA, T., TANAKA, M. & NAKATA, K. 2008. Hybrid Friction Stir Welding of Carbon Steel. *Materials Science Forum* 580 - 582, 393-396.
- GIMENEZ-BRITOS, P., WIDENER, C., BOLDSAIKHAN, E. & BURFORD, D. PROBABILITY OF DETECTION ANALYSIS OF NDT METHODS FOR FRICTION STIR WELDED PANELS. In: TWI, ed. 8th International Friction Stir Welding Symposium, 2010 Timmendorfer strand, Germany. TWI.
- LAMMLEIN, D. H., DELAPP, D. R., FLEMING, P. A., STRAUSS, A. M. & COOK, G. E. 2009. *The application of shoulderless conical tools in friction stir welding: An experimental and theoretical study*, Kidlington, ROYAUME-UNI, Elsevier.
- LAVERNIA, E. J. & GRANT, N. J. 1987. Aluminium-lithium alloys. *Journal of Materials Science*, 22, 1521-1529.
- LEE, S. & ASADA, H. H. 1999. A perturbation/correlation method for force guided robot assembly. *Robotics and Automation, IEEE Transactions on*, 15, 764-773.
- LIENERT, T. J., STELLWAG, W. L., GRIMMETT, B. B. & WARKE, R. W. 2003. Friction stir welding studies on mild steel. *Welding Journal*, 82.
- LOTUS ENGINEERING INC. 2010. *An Assessment of Mass Reduction Opportunities for a 2017 – 2020 Model Year Vehicle Program* [Online]. Available: [http://www.theicct.org/sites/default/files/publications/Mass\\_reduction\\_final\\_2010.pdf](http://www.theicct.org/sites/default/files/publications/Mass_reduction_final_2010.pdf) [Accessed 2012-03-09 2012].
- MANGIARINO, C., CARBONATO, G., GATTIGLIO, M. & MENIN, R. 2004. *System and method for remote laser welding*. USA patent application.
- MARTIN, J. P., STANHOPE, C. & GASCOYNE, S. 2011. Novel Techniques for Corner Joints Using Friction Stir Welding. *Friction Stir Welding and Processing VI*. John Wiley & Sons, Inc.
- MARTUKANITZ, R. P. 1990. Selection and weldability of heat-treatable aluminum alloys. *ASM Handbook - Welding, Brazing and Soldering*, 6, 528-536.

- MESSLER, R. W. 2004. *Principles of welding processes, physics, chemistry, and metallurgy* [Online]. Weinheim: Wiley-VCH. Available: <http://public.eblib.com/EBLPublic/PublicView.do?ptiID=482178>.
- MISHRA, R. S. & MA, Z. Y. 2005. Friction stir welding and processing. *Materials Science and Engineering: R: Reports*, 50, 1-78.
- MISHRA, R. S. & MAHONEY, M. W. 2008. *Friction stir welding and processing*, Materials Park, Ohio, ASM International.
- MIYAZAWA, T., IWAMOTO, Y., MARUKO, T. & FUJII, H. 2011. Development of Ir based tool for friction stir welding of high temperature materials. *Science and Technology of Welding & Joining*, 16, 188-192.
- NUNAMAKER, J. F., JR. & CHEN, M. Systems development in information systems research. System Sciences, 1990., Proceedings of the Twenty-Third Annual Hawaii International Conference on, 2-5 Jan 1990 1990. 631-640 vol.3.
- OBELOER, M. 1983. Machining of Hard Ferrous Materials and Gray Cast Iron With Polycrystalline CBN Cutting Tools *Advances in Hard Metal Production*, 1.
- ROOS, A. 2010. *Grundlegende Untersuchung über ein neues Schweißverfahren namens HFDB (Hybrid Friction Diffusion Bonding)*.
- ROSENDO, T., PARRA, B., TIER, M. A. D., DA SILVA, A. A. M., DOS SANTOS, J. F., STROHAECKER, T. R. & ALCÂNTARA, N. G. 2011. Mechanical and microstructural investigation of friction spot welded AA6181-T4 aluminium alloy. *Materials and Design*, 32, 1094-1100.
- SCHILLING, C. & DOS SANTOS, J. 2000. *Method and device for linking at least two adjoining work pieces by friction welding*.
- SCHMIDT, H. & HATTEL, J. 2005. Modelling heat flow around tool probe in friction stir welding. *Science and Technology of Welding & Joining*, 10, 176-186.
- SCHMIDT, H., HATTEL, J. & WERT, J. 2004. An analytical model for the heat generation in friction stir welding. *Modelling and Simulation in Materials Science and Engineering*, 12, 143-157.
- SCHULTZ, H. 2002. *Electron beam welding*, Cambridge, Abington.
- SICILIANO, B. & VILLANI, L. 1999. *Robot force control*, Boston, Mass. [u.a.], Kluwer Academic Publ.
- SISMONDO, S. 2007. *An introduction to science and technology studies*, Malden, Mass. [u.a.], Blackwell Publ.
- SMITH, C. 2000. Friction Stir Welding using a Standard Industrial Robot. *2nd International Friction Stir Welding Symposium*. Gothenburg, Sweden: TWI.
- SMITH, C., HINRICHS, J. & CRUSAN, W. 2003. Robotic Friction Stir Welding: The State-of-the-Art. *4th International Friction Stir Welding Symposium, Salt Lake City, UT, May 2003*.
- SMITH, C. B. 1997. Robotic Friction Stir Welding: Phase I Initial Feasibility Study. Tower Automotive

- SOMASEKHARAN, A. C. & MURR, L. E. 2004. Microstructures in friction-stir welded dissimilar magnesium alloys and magnesium alloys to 6061-T6 aluminum alloy. *Materials Characterization*, 52, 49-64.
- SORENSEN, C. D. & NELSON, T. W. 2007. Friction Stir Welding of Ferrous and Nickel Alloys. In: MISHRA, R. S. & MAHONEY, M. W. (eds.) *Friction Stir Welding and Processing*. ASM International, Materials Park, OH, USA.
- SORON, M. 2007. *Robot System for Flexible 3D Friction Stir Welding*. PhD, Örebro University.
- SPONG, M. W. & VIDYASAGAR, M. 1989. *Robot dynamics and control*, Wiley.
- SUTHERLAND, J., GUNTER, K., ALLEN, D., BAUER, D., BRAS, B., GUTOWSKI, T., MURPHY, C., PIWONKA, T., SHENG, P., THURSTON, D. & WOLFF, E. 2004. A global perspective on the environmental challenges facing the automotive industry: state-of-the-art and directions for the future. *International Journal of Vehicle Design*, 35, 86-110.
- TAKAHARA, H., MOTOYAMA, Y., TSUJIKAWA, M., OKI, S., CHUNG, S. W. & HIGASHI, K. 2007. Allowance of Deviation and Gap in Butt Joint on Friction Stir Welding. *Advanced Materials Reserch*, 15-17, 375-380.
- THOMAS, W. M., NICHOLAS, E. D., NEEDHAM, J. C., MURCH, M. G., TEMPLE-SMITH, P. & DAWES, C. J. 1991. *Friction stir butt welding*.
- THOMAS, W. M., STAINES, D. G., NORRIS, I. M. & DE FRIAS, R. 2003. Friction stir welding tools and developments. *Welding in the World*, 47, 8.
- THOMAS, W. M., THREADGILL, P. L. & NICHOLAS, E. D. 1999. Feasibility of friction stir welding steel. *Science and Technology of Welding & Joining*, 4, 365-372.
- THOMAS, W. M., WIESNER, C. S., MARKS, D. J. & STAINES, D. G. 2009. Conventional and bobbin friction stir welding of 12% chromium alloy steel using composite refractory tool materials. *Science and Technology of Welding & Joining*, 14, 247-253.
- THOMAS, W. M. G., NICHOLAS, EDWARD DAVID (GB), NEEDHAM, JAMES CHRISTOPHER (GB), SEARLE, JOHN GILBERT (GB). 1992. *Friction surfacing*. EP0474455.
- THOMESSEN, T. & LIEN, T. K. 2000. Robot control system for safe and rapid programming of grinding applications. *The Industrial Robot*, 27, 437-444.
- WILLERSRUD, A., GODTLIEBSEN, F. & THOMESSEN, T. 1995. *Automatic programming of grinding robot restoration of contours*, Oslo, NORVEGE, Research Council of Norway.
- VOELLNER, G., ZÄH, M. F., KELLENBERGER, O., LOHWASSER, D. & SILVANUS, J. 2006. 3-Dimensional Friction Stir Welding using a modified high payload robot. *6th International Friction Stir Welding Symposium, Saint Sauveur, Canada*.



- VON STROMBECK, A., SCHILLING, C. & DOS SANTOS, J. F. Robotic friction stir welding - tool technology and applications. 2nd International Friction Stir Welding Symposium, 2000 Gothenburg, Sweden. TWI.
- ZÄH, M. & VOELLNER, G. 2010. Three-dimensional friction stir welding using a high payload industrial robot. *Production Engineering*, 4, 127-133.



## Appendix A: IsMoving function for plunge depth detection

```
FUNC bool IsMoving(pos startpos, PERS Tooldata toolx, PERS Wobjdata wobjx)

VAR iodev shouldercontact;

Var clock timer1;
Var pos previouspos;
Var pos presentpos;
Var num dist;
Var num speed;

speed:=1000;
startpos:= CPos(\Tool:=toolx \WObj:=wobjx);
presentpos:= startpos;
dist:= Distance(startpos,presentpos);
waittime 1;
while speed>1 do
    previouspos := presentpos;
    waittime 0.2;
    presentpos := CPos(\Tool:=toolx \WObj:=wobjx);
    dist:= Distance(previouspos,presentpos);
    speed:=dist/0.2;
    if clkRead(timer1)>5 then
        speed:=0;
    endif
endwhile

while speed>0.4 do
    previouspos := presentpos;
    waittime 0.2;
    presentpos := CPos(\Tool:=toolx \WObj:=wobjx);
    dist:= Distance(previouspos,presentpos);
    speed:=dist/0.2;
endwhile
RETURN FALSE;
ENDFUNC
```

The function reads the position of the tool every 200 ms and compares this to the previous position. When the shoulder is in contact with the material, the speed will instantly decrease and the function will return a Boolean “false” value.



## **Appended Papers**



**Paper A**

**A local model for online path corrections  
in Friction Stir Welding**

Soron, Mikael

De Backer, Jeroen

Christiansson, Anna-Karin

Ilar, Torbjörn

*Friction Stir Welding and Processing Conference*  
Lille, France, 28<sup>th</sup> to 29<sup>th</sup> of January, 2010

## Abstract

Friction stir welding (FSW) has always been associated with high forces and rigid machines. Today's trends towards joining of more complex structures in e.g. the automotive and aerospace industry, the applications require machinery with increased dexterity and flexibility, which cannot be achieved with the traditional FSW systems. But the introduction of more flexible machines, with more complex workspace capacity, will lead to undesired tool path deviations and in worst case a weld seam with inferior quality. In this study an industrial robot system is used to emphasise the need to compensate for the deviations caused by the high lateral forces resulting from the FSW process. A local model to compensate for such deviations is implemented, evaluated and compared to uncompensated welds in terms of quality and reliability.

## 1 Introduction

Friction Stir Welding (FSW) was invented at TWI (The Welding Institute, Cambridge), UK, in 1991 (patent filed in 1992 [1]). The FSW process, which is one of the latest innovations in the area of welding, has several advantages compared to traditional fusion welding techniques. First, it enables welding of materials often considered unweldable, like the 2xxx and 7xxx aluminium series, but also joining material such as magnesium [2], copper [3], which are all material characterized by a low melting temperature. Also, joining of dissimilar material, such as aluminium to copper [4] or aluminium to steel [5] has been performed in laboratory setups. Secondly, problems often associated with welding of aluminium, such as shrinkage, porosity and distortions are eliminated to a great extent by the FSW process [6]. This is due, mainly to the following facts:

- The welding process takes place in solid state around 80-90% of the melting temperature of the material.
- The filler material (wire) used in traditional methods is absent.

Today, FSW is mainly used in the aircraft, aerospace, automotive and electrical industries, and is considered a valuable technique for butt and lap joint welding of aluminium alloys with a range in plate thickness from 0.8 to 75 mm, and with a welding speed up to 600 cm/min.

The drawbacks that have been associated with FSW, mainly the high forces and torques needed to generate heat, did originally require heavy duty machinery. But the lack of flexibility in these systems limited the process to straight or circumferential welding, with



hardly any possibility for rapid changes in the applications without re-designing the complete system.

During recent years, a new generation of high payload industrial robots have reached the market. These robots, having a payload capability over 500 kg, have the following benefits compared to the traditional FSW machinery:

- A 3-dimensional workspace.
- Advanced motion programming interface.
- Relative low cost.

The different types of robots, which have shown promising result in FSW, are either of serial [7] or parallel [8] design. The most common industrial robot, the serial design, normally gains in workspace and lower cost, while the parallel design gains in stiffness but has a complex Cartesian workspace [9].

## 2 Background

During the FSW process there are several forces acting on the welding tool. The most obvious, and most recognised is the down force, which is subject to the tool being pressed towards the work object. Secondly there is the traverse force, which is the result of the tool being moved forward along the joint line. The third force, which is the topic of this study, is the force perpendicular to the traverse force acting to “push” the tool off the predefined path or joint line. The magnitude of this lateral force is expected to be the result of the tool’s rotational speed, the friction between the tool’s shoulder and the work object, and the resulting material flow.

As all machines suffer from compliance, it is rather the magnitude of the lateral force that defines whether or not such force may be neglected. There may very well exist a need to correct the drift to withhold a high quality weld, if the application requires it, e.g. in thick material applications, or if the system performing the weld is not rigid enough. The lack of rigidity will be emphasised for all systems with high dexterity since the revolute joints that are needed to apply rotational alignments are more exposed compare to machines with prismatic joints.

Along with the more and more complex applications in FSW, where the joint line is no longer straight, 5- or 6-axes machines are necessary to carry out the operation, in which at least two axes are revolute. The standard industrial robot is based on only revolute joint, normally six, and is therefore a system of less rigidity compared to a gantry type solution. The system utilized in this study is the ESAB Rosio<sup>TM</sup> (Figure 1), which is a modified 5-axes industrial robot, see [10,11]. Being based on an ABB IRB7600 robot

with 500 kg payload it has the capacity of welding aluminium plates up to 7 mm thick. The control system allows the robot to apply its motion in a force controlled mode to ensure proper contact condition between the tool and the work piece, even when the robot complies. The forces are also measured in 3 degrees of freedom during the welding sequence for further off-line analysis.

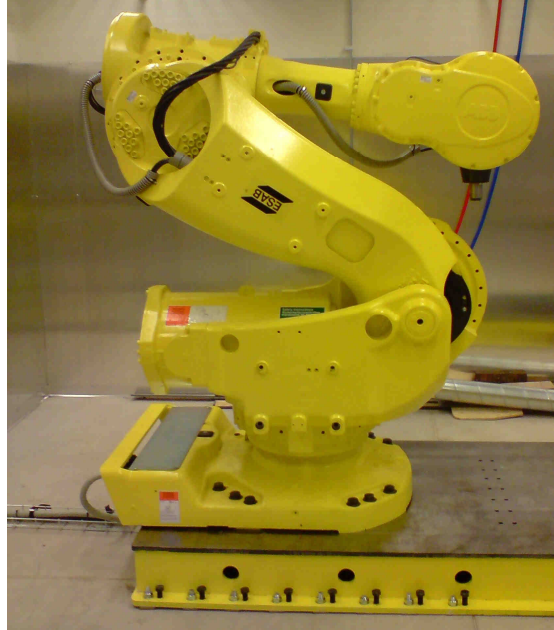


Figure 1: ESAB Rosio™ Friction Stir Welding Robot.

### 3 Measuring the Deviation

To model the extent of the deviation from the actual path and the desired joint line a set of experiments were conducted. A total of more than 50 test welds were performed on various materials under different conditions. The materials, the tool rpm and the traverse speed are summarized in Table 1.

**Table 1:** The materials used with speed and spindle settings for the deviation tests.

Material	Rpm (range)	Speed (range)
AA2024-T3	700-1200	2-15 mm/s
AA5754	1000-1500	5-15 mm/s
AA6063-T6	2500	8-10 mm/s
AA7075	800-1250	5-12 mm/s

All materials had a thickness ranging from 2.0 to 3.2 mm for which the tools used had the geometries displayed in Table 2.

**Table 2:** Pin tool geometries used during the tests.

Pin length	Pin diameter	Shoulder diameter
1.8 mm	3 mm	10 mm
2.8 mm	4 mm	10 mm
3.0 mm	5 mm	14 mm

The welds were conducted in two different setups in the work space. The first, with a motion travelling in the positive x-direction (away from the robot) of the robot's coordinate system, was placed in front of the robot at a mid-range position. The second setup, in which the motions were applied in both the positive and the negative y-direction, was placed close to the first. This means that all the welds were applied within a confined volume, hence there will be a local Cartesian model as output of this study.

The measurement of the deviation is performed off-line by use of microscope, see Figure 2. Deviations were measured both slightly after the starting point of the weld, as well as slightly prior to the end key-hole. An average value was then entered to represent the deviation of that weld. To summarize the test welds, the measured data was inserted in a plot (Figure 3) to be further analyzed.

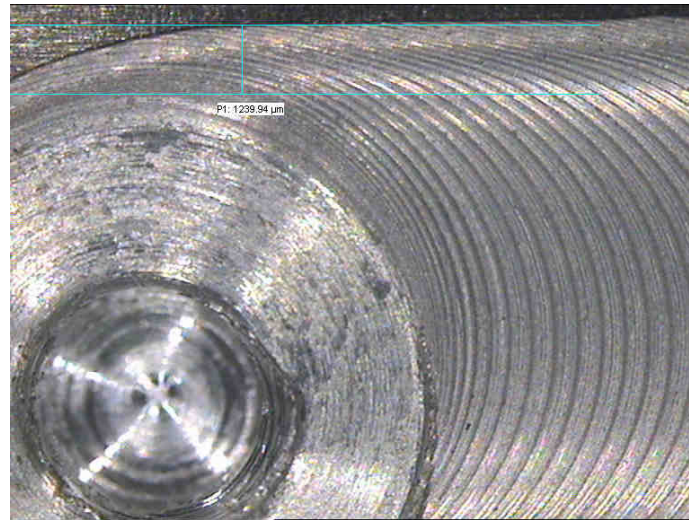


Figure 2: Microscope deviation measurement at the end key-hole.

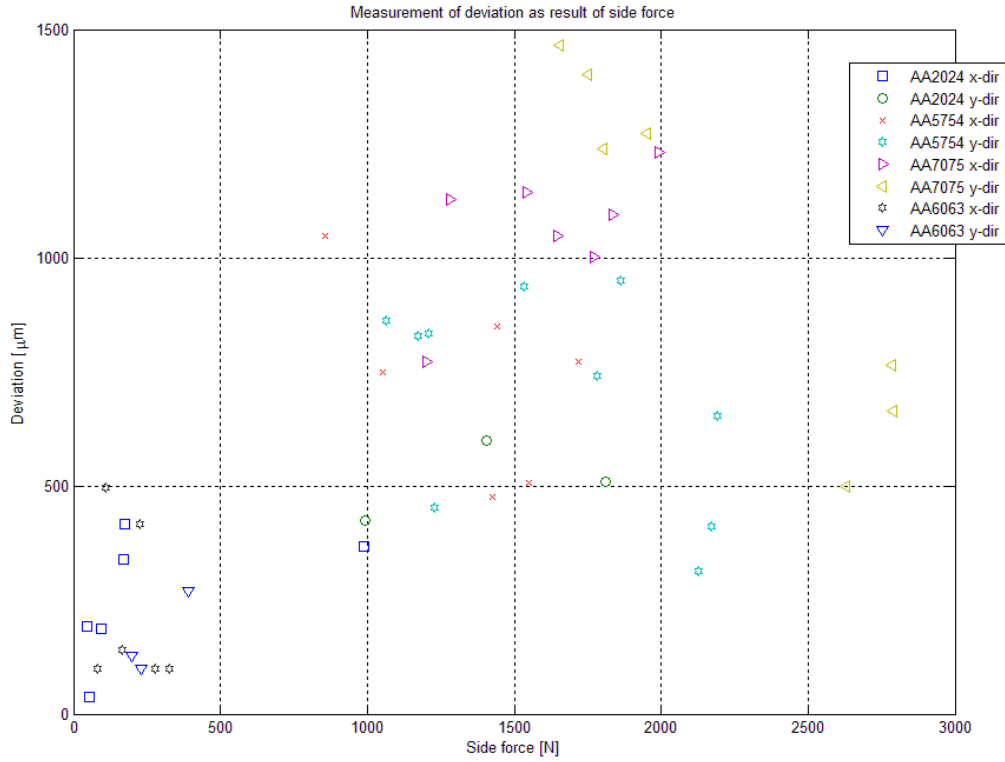


Figure 3: The complete plot over all test welds displaying the measured deviation to corresponding side force.

## 4 Model and Implementation Strategy

Apart from the magnitude of the side force, there may be other factors contributing to the deviation from the desired path. When reviewing Figure 3, where all data is included, one may draw the conclusion that the data is too scattered to imply a correlated relationship.

But the deviation, measured in Cartesian space, is a subject to where in the working envelope of the robot the weld is being performed. In this study, two different setups were used. One in which a weld was performed in front of the robot with a motion moving in the x-direction of the robot's base coordinate system. Such weld implies a deviation related mainly to the first axis of the robot. The second weld, performed at a different location travelling in the y-direction of the robot's base coordinate system, would have a resulting deviation mainly caused by axes 2 and 3.

Therefore two models are estimated and introduced based on least square estimation of a first degree polynomials (for all data in Figure 3 for x- and y-directions respectively:

$$\begin{aligned} d_x(f) &= 0.47f + 172 \\ d_y(f) &= 0.18f + 417 \end{aligned} \quad (1)$$

in which the deviation  $d$  in  $\mu\text{m}$  is given as a function of the side force  $f$  further displayed in Figure 4.

The implementation of the models on the control system is based on the strategy of measuring the side forces during the start-up phase of the weld, for which the estimated correction is applied based on the given model. This as the actual deviation (and side force) vary to a minimum during the weld itself, hence only one correction needed throughout the weld.

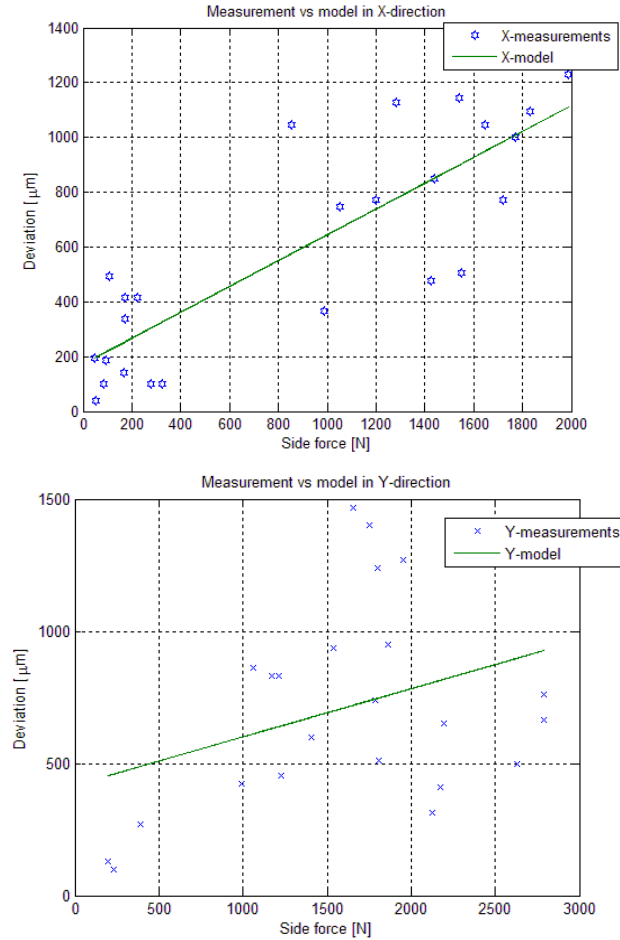


Figure 4: Models and deviation measurements for x- and y-direction of travel.

## 5 Verifying the Model and Accuracy

The models were verified by correcting the robot path for a set of welds. The corrections are based on the linear models in (1) and the measured side force  $f$  until steady state is reached. The side force is increasing during the first 5-6 seconds. These are then compared to uncorrected weld. The initial study suggested a greater inaccuracy for the y-direction model, see right plot in Figure 4, hence spread of collected data, which is why it was used for the verification.

The material selected was AA7075 since it is one of the most difficult aluminium to FS weld due to that it is a strong and tough material which would most likely require means to correct path deviations. A number of welds are performed, denoted Weld #1 etc in Figure 5.

The first uncorrected weld gave a result very similar to the ones from the initial study, i.e. a clear deviation from the joint line with an approximate offset similar to the collected data in the initial study as shown in Figure 4. The compensated welds, on the other hand, resulted in much less deviation, difficult to detect without microscope. An average value for the correction was estimated for each sample and a correction of the robot path was applied. After having filled the buffer no more correction was applied, hence the correction reached a maximum level (steady state), see Figure 5, in which correction build-up is visualized during the first six seconds of welding.

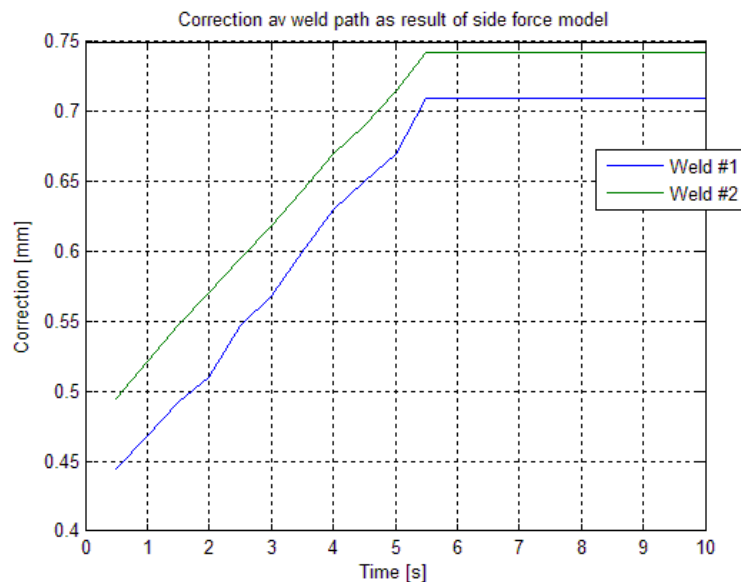


Figure 5: Corrections applied during the initial phase of the welding.

## 6 Conclusions

In this study an attempt is made to model the machines', or in this case robot's, deviations as a result of the process side force and the direction of travel. This study has provided results to support the necessity to apply such a correction since deviations up to 1.5mm may occur during un-compensated welding and thereby lead to inferior quality. The study has also supported the need for more than one single model, as the direction of travel affects the deviation.

The evaluation of the models was provided by first applying an uncompensated weld, than one compensated on AA7075 welding in the y-direction. It was clear that the uncompensated weld had a clear deviation in terms of the welding path. The compensation of approximately 0.7mm corresponds well with the estimation.

As future work one may include a larger work space area as first step, blending of models to handle changes in travel direction and finally a joint space model, covering all directions and locations within the robot's reach. The latter is however difficult to obtain, the prior is easier to put in practice, since it only involves an expansion of the experiment.

## 7 Acknowledgements

The authors would like to acknowledge the financial support from Vinnova and the StiRoLight project group members, SAAB Automobile, ESAB, and Volvo. Their financial and technical support is highly appreciated.

## 8 References

- [1] W. M. Thomas, E. D. Nicholas, J. C. Needham, M. G. Church, P. Templesmith, and C. J. Dawes, 1991. International Patent Application no. PCT/GB92/02203 and GB Patent Application no. 9125978.9.

- [2] S. A. Lockyer and M. J. Russel. Mechanical properties of friction stir welds in Magnesium alloys. In *International conference on Magnesium alloys and their applications*, Munich, Germany, 2000.
- [3] C. G. Andersson, R. E. Andrews, B. G. I. Dance, M. J. Russel, E. J. Olden, and R. M. Sanderson. A comparison of Copper fabrication by the electron beam and friction stir processes. In *2<sup>nd</sup> International Symposium on Friction Stir Welding*, Gothenburg, Sweden, 2000.
- [4] L. Karlsson, H. Larsson, E. L. Bergqvist, and S. Stoltz. Friction stir welding of dissimilar al-alloys. In *2<sup>nd</sup> Friction Stir Welding International Symposium*, Gothenburg, Sweden, 2000.
- [5] W. H. Jiang and R. Kovacevic. Feasibility study of friction stir welding of 6061-T6 aluminium alloy with AISI 1018 steel. In *Proceedings of the Institution of Mechanical Engineers*, pages 1321-1331, 2004.
- [6] Y. J. Chao, X. Qi, and W. Tang. Heat transfer in friction stir welding – experimental and numerical studies. *Manufacturing Science and Engineering*, 125:138-145, 2003.
- [7] C. B. Smith. Robotic friction stir welding using a standard industrial robot. In *2<sup>nd</sup> International Friction Stir Welding Symposium*, Gothenburg, Sweden 2002.
- [8] A. V. Strombeck, C. Shilling, and J. D. Santos. Robotic friction stir welding – tool technology and applications. In *2<sup>nd</sup> International Friction Stir Welding Symposium*, Gothenburg, Sweden 2002.
- [9] P. Wenger and D. Chablat. Design of a three-axis isotropic parallel manipulator for machining applications: The orthoglide. In *Proceedings of the workshop on fundamental issues and future directions for parallel mechanisms and manipulators*, pages 16-24, 2002.
- [10] M. Soron. Towards multidimensionality and flexibility in FSW using an industrial robot system. *Welding in the World*, 2008. 52(9-10): p. 54-59.
- [11] M. Soron and I. Kalaykov. A robot prototype for friction stir welding. In *Proceedings of IEEE Conference on Robotics, Automation and Mechatronics*. Bangkok 2006.



## **Paper B**

# **Friction Stir Welding with Robot for Light Weight Vehicle Design**

De Backer, Jeroen

Soron, Mikael

Ilar, Torbjörn

Christiansson, Anna-Karin

*8<sup>th</sup> Friction Stir Welding Symposium*

Timmendorfer Strand, Germany, 18<sup>th</sup> to 20<sup>th</sup> of May 2010.

## Abstract

Reducing weight is one of the enablers to design more environmentally friendly vehicles. Friction Stir Welding (FSW) supports low weight design through its capability to join different combinations of lightweight materials, e.g. different aluminium alloys, but also through its possibilities in producing continuous joints. But until recently FSW has meant expensive equipment capable of producing joints only in two dimensions or on simple geometries such as cylinders. The introduction of robotic FSW will most likely change this, making the process feasible also for flexible mass production of objects based on more complex geometries.

This paper presents the scope of a recently started project for robotised FSW for joining of lightweight materials emphasising on the vehicle industry, an industry with a long-time experience of robotic welding. The system used for this project is an ESAB Rosio<sup>TM</sup> based on an ABB IRB7600.

The project at hand aims to investigate new possibilities and how new ideas can be introduced. The first task involves investigation of force feedback for maintaining the desired contact force. Another important aspect in robotised FSW investigated in this project is the compliance of the robot, which may result in deviations from the pre-programmed path as a result of the high process forces experienced during the welding operation. Models will be developed to correct for this compliance in different welding directions in order to apply the seam where it is intended and consequently get more reliable results.

The system platform utilized in this project is generic in the meaning that more sensors can be integrated for monitoring and on-line control, e.g. different temperatures can be used to modify the rotational speed and/or down force and/or travelling speed.

Project results will be given in the full paper, including the first investigation of path deviation as a result of process parameters, robot compliance and especially path direction showing the deviation during the retraction of the pin. Moreover, the results influence on the specific case of FSW in light weight vehicle design will be discussed.

## 1 Introduction

Even though Friction Stir Welding (FSW) is more and more considered as a 'state of the art' welding technique, the utilization of this process with an industrial robot is still in a developing state. The first FSW applications were in fact using milling machines with

some minor modifications, where the rotating FSW tool replaced the ordinary milling tool and performed the weld. These machines were an obvious choice because of the stiffness and the relative high deliverable down force, and of course the availability.

Today's industrial applications for FSW are mainly based on the same milling principle. They are often for mass-production, where inflexible machinery is used to perform friction stir welds on non-complex joints. However, to enable FSW growth to become an overall industrial success, the limitations of the dedicated machines must be overcome.

By using an industrial robot one can make the process more flexible, faster and cheaper. A robot that facilitates a three-dimensional workspace, allows FSW to compete with other 3D welding processes for aluminium, such as gas metal arc welding (GMAW). Another advantage enabled by the robot is the ability to switch between applications, materials and geometries, without any hardware modification. Industrial robots also have the advantage of well-developed human-machine interfaces (HMI) as well as a widespread use and knowledge in the industry of traditional robotic welding. Finally, as the FSW robot application may be modelled and simulated off-line, including the welding path, the operational time may be maximized and significantly decrease the production cost.

The StiRoLight<sup>1</sup> research project started in 2009 at University West in Trollhättan, Sweden in cooperation with Swedish industrial partners SAAB Automobile, ESAB and Volvo. The selection of system fell on an industrial robot with serial kinematic design. This type of robot design is the most common industrial robot and has been adopted in the area of FSW by several research groups in the past. In (Smith 2000) an ABB IRB-6400 robot was used and showed promising results, but the limited robot payload capacity of 150 kg was a severe drawback. In Smith et al., that robot was replaced by a newer and stronger ABB robot, the IRB-7600. This provided an increased stiffness and more than three times in payload capacity, and accordingly provided better welding results (Smith, Hinrichs et al.)

The same type of robot system was utilized by Soron et al. in (Soron and Kalaykov 2006). But by modifying the system to integrate the welding equipment, greater stiffness and increased capacity was enabled. This system also introduced the use of force feedback to handle the robot compliance on contact with the material during the process, which is an important feature to ensure good quality welding.

Along with the development and usage of industrial robots in heavy duty applications, robot manufacturers have followed the trends. Applications such as milling, grinding and drilling with robots are typical examples where stiffness and payload come in play. This evolution is of course beneficial for FSW, as it depends on high-volume applications to provide the means in terms of equipment.

The StiRoLight project is based on a strategic platform, consisting of "Work Packages" as shown in Figure 1. The overall project is reviewed by the steering group, consisting of industrial partners and the university (WP5). General knowledge about the FSW process

---

<sup>1</sup> StiRoLight – Friction **Stir** Welding with **Robot** for **Light** Weight Vehicle Design.

is built up (WP1), simultaneous with the construction of the FSW cell at Innovatum Technology Park and an experimental platform (WP3), suited for the needs of the participating companies: Saab Automobile AB, Volvo Aero Corporation and ESAB AB (WP2). These three work packages determine the basic process window which will lead to well-defined research topics and challenges for Robotic Friction Stir Welding (WP4).

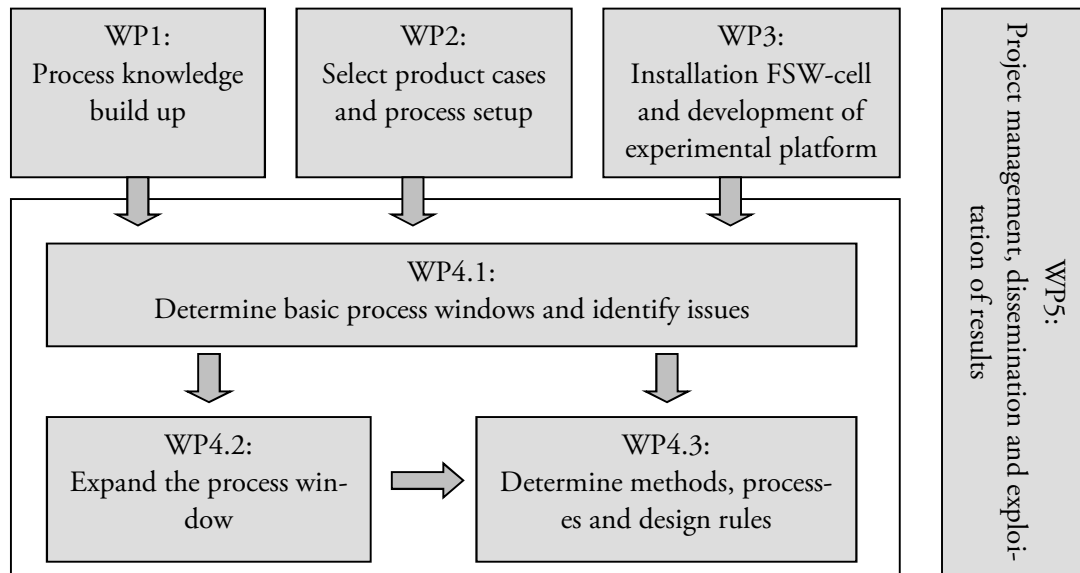


Figure 1: StiRoLight project construction

## 2 Project Aims and Deliverables

Friction Stir Welding is an outstanding technique for joining lightweight materials. This project aims to bring robotic FSW closer to industrial applications by eliminating constraints, related to the robotic implementation of the FSW process. The scientific goals in this work are:

- Further development of the process for more complex geometries
- Develop design methodology to fully utilise FSW-joints for complex geometries
- Demonstration of robotised FSW-functionalities and limitations

Achieving these goals should lead to the introduction of robotic FSW in the Swedish vehicle industry, where the demands for alternative to existing solutions are great.

The research will be concentrated on questions regarding the novel methodology for robotic FSW, including sensor integration and investigation of force feedback vs. the classic position control in robot systems. It will also address the issues associated with the

robot's compliance and how to fully utilize the advantages of FSW in terms of light weight design and curved joints, including tooling issues like shape and orientation.

To define the aims regarding the participating companies' desires of materials and joint types, workshops were set up. For automotive applications, it was decided that the focus in terms of materials will lay on the 5xxx and 6xxx series, typically AA5083, AA5754, AA6016, AA6063. All those materials have shown excellent FS weldability in previous studies. In terms of joint type the interest was mainly in lap joints to replace joining methods such as riveting and clinching. But there is also an interest for joining tailor blanks, which on a complex structure, e.g. car door, will require a full utilization of the robot's 3D capacity.

The companies involved in this research project also share an interest in high-strength aluminium, e.g. Al 7020, for use in both automotive and aerospace structures. These alloys have always meant difficulties in welding and are therefore often disqualified and replaced by other materials like stainless steel or super alloys such as Inconel 718.

However, initial studies have shown that high-quality welds of these high strength aluminium alloys can be obtained with the FSW robot system. The increased hardness of these materials is a limitation for the welding possibilities. They require more force, which limits the maximal thickness of the work pieces. Up to 5mm in alloys such as AA7075 and AA2050, have been achieved, but then in beneficial setup. The StiRoLight project will evaluate how changes, due to motion and configuration affect the ability to weld a component in terms of force capacity, compliance and drift.

This study will give a better view on the limitations of the robot system, especially when so-called high-temperature materials, e.g. inconel or titanium are to be joined by FSW. As there exist tool solutions today to support these operations, e.g. with PCBN tools, it will in principle only be the process carrier (i.e. the robot) that limits the weldability. The robot's limited force capability and stability as well as lack of proper temperature monitoring may hinder progress in this area, but introducing hybrid techniques e.g. with pre-heating by laser, may make it feasible to perform FSW of high-temperature alloys with this robot system.

### **3 Experimental Set-up**

For this project the group decided to utilize the ESAB Rosio™ (Figure 2). The system, which is based on the IRB7600 robot from ABB, has a maximum force capacity of 1.3kN. As the system consists of an integrated welding head, stability is increased and the workspace of the original system is maintained.

This 'built-in' approach is different from other research groups, (Voellner, Zäh et al.) and (Smith, Hinrichs et al.), where robotic FSW is performed by mounting the dedicated equipment, which consist of a milling spindle, directly on the robot 6<sup>th</sup> axis. This normally leads to a large distance between the relatively weak 5<sup>th</sup> axis and the welding tool, which affects the capability of the system as well as the stability.

The welding spindle has a capacity of 4500 rpm and 30Nm, which enables both welding with high traverse speed (high rpm requirement) and welding of up to 7mm thick material (high torque requirement).

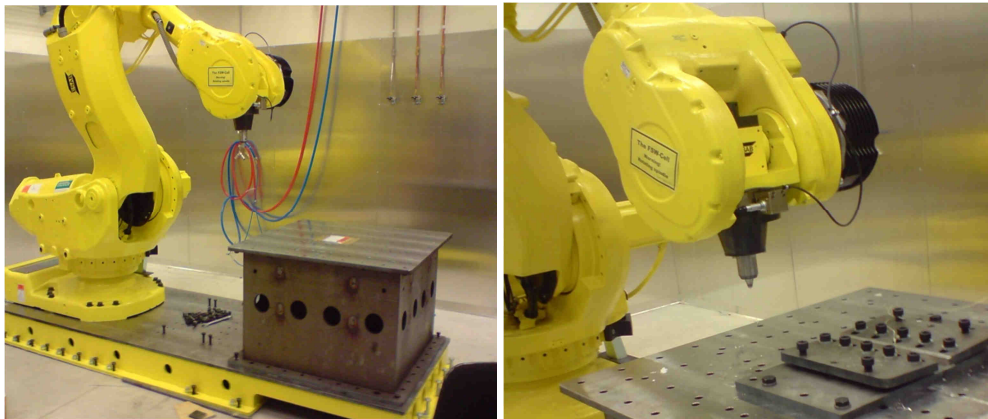


Figure 2: StiRoLight FSW robot cell

Due to the complexity of the configuration, robots cannot guarantee the same stiffness as the dedicated FSW machines. The actual position of the welding tool always deviates during the welding as a result of the high forces acting on the system. Lack of stiffness and back-lash causes erroneous encoder readings which are then fed back to the control system. As the contact force is the highest, the z-position will suffer most, but also side and traverse forces contribute to the inaccuracy.

To compensate for this error the system is equipped with a force sensor. The z-position relating to the contact is over-ridden by a force feedback control. Instead of achieving a desired z-position, the system strives towards a desired contact force. By the use of a high accuracy force sensor and an embedded control solution, the contact force is controlled accurately.

So far, only the z-force value was used to control the process. As the sensor can read the forces on all axes (x, y and z), there are means available to compensate deviations caused by the side force as well. These compensations are irrelevant during welding of thin and/or soft material but are necessary for butt-joint welding of high-strength aluminium alloys.

## 4 Initial Work

With the completely installed FSW robot cell at the Production Technology Centre in Trollhättan, high quality welds in different types of aluminium have been performed. Furthermore, an experimental platform is set up, where all relevant data are measured and logged into a database. These data contain of course the welding parameters, including downforce, and all the values of the force sensor.

It is generally known that FSW by using a robot has a number of advantages when it comes to flexibility due to its 6 degrees of freedom. However, all these joints have a servomotor, gearbox and transmission axes, which all contribute with some compliance, leading to deflections. While moving in the free air, these deflections are negligibly small as pre-known loads and mass can be accounted for, but when the tool comes in contact with the work piece, all these joints cause a limited deviation between the p redefined robot path and the actual followed path. This leads to deviations, away from the joint line, what results in bad weld quality.

The investigation and modelling of forces in FSW in other research is mostly used to get an understanding of the required downforce and torque (Zimmer, Langlois et al.) while the other force values in x and y direction (reference frame in Figure 4) are investigated to predict the weld quality (Balasubramanian, Gattu et al. 2009). For the robot system, it is of interest to link these force values to the path deviation issue.

To get a better understanding of the robot behaviour during welding, test part in aluminium are linearly welded in butt-configuration with a very wide range of parameters and material properties. All these welds were done with a steel tool with threaded pin.

Table 1: Welding parameters for different aluminium alloys

Material type (3mm sheet)	Rot speed (rpm)	Speed (mm/s)	Desired Force [N]
AA2024-T3	700 > 1200	2 > 15	6500 > 7500
AA5754	1000 > 1500	5 > 10	5500
AA6063-T6	2500	8 > 10	3000 > 5000
AA7075	800 > 1250	5 > 12	8000 > 9000

The forces are measured in a reference frame, attached to the work piece: the downforce (z-direction), the side force (y-direction) and the force in traverse direction (x-direction). All these values are logged at a sample interval of 1Hz and afterwards compared with the corresponding path deviations. In the first experiments, path deviations were measured by microscopic investigation of plunging and retraction locations as described in next paragraph. In later experiments, a less time consuming and more accurate approach is developed where a camera is mounted on the robot (Figure 3). During linear butt welding, the camera will detect the joint line and accordingly give an absolute value of deviation.

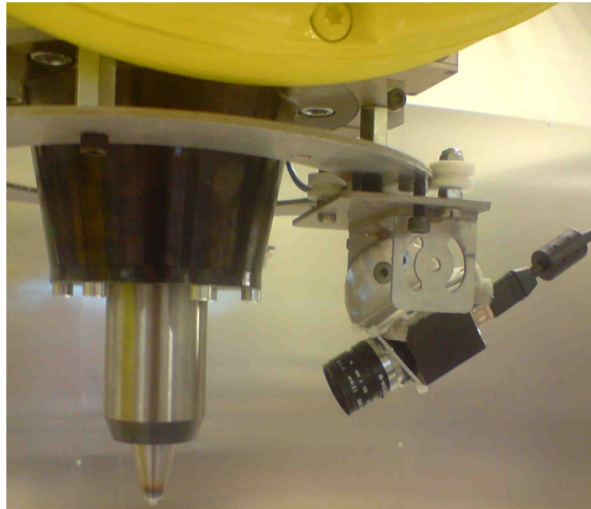


Figure 3: Robot head with camera for path deviation detection

## 5 Results

Both the start and end point were investigated and it was demonstrated that the path deviations are up to 2 mm in linear butt welds of aluminium AA-7075 (measured in y-direction in Figure 4). There are some hypotheses of what might cause these deviations but more research on this specific topic is required, in order to get a better understanding of the robot behaviour.

In prior research within the StiRoLight project, (Soron, De Backer et al. 2010) it was demonstrated that the robot path can be corrected by measuring the side forces during welding (y-direction in Figure 4) and predicting the deviations with a model on the robot control system. The deviations, while welding in the x-direction of the robot's base coordinate system spanned from nearly negligible in AA-6082 (3mm thickness) up to 1.5mm in AA-7075 (3mm thickness) as displayed in Figure 5.



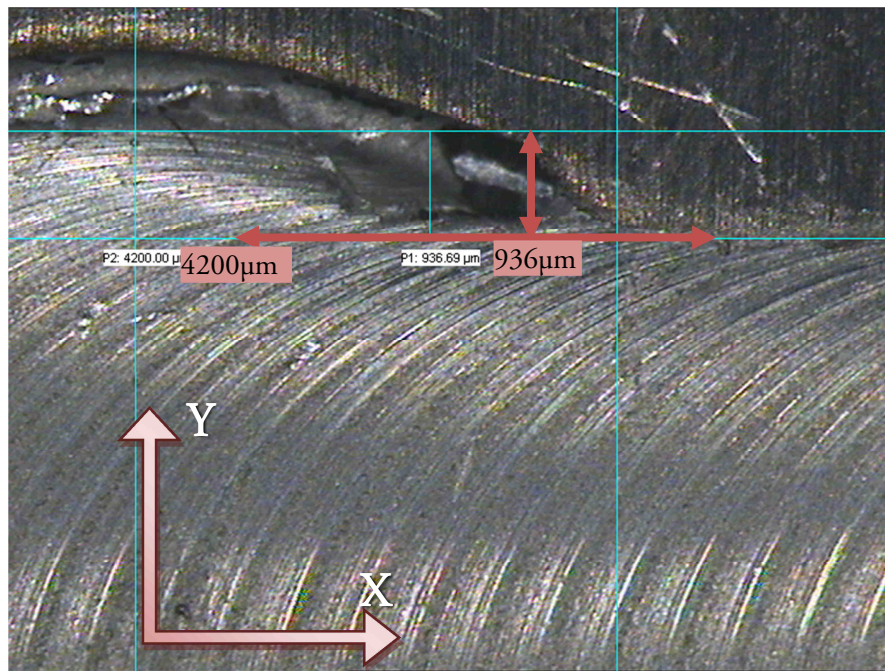


Figure 4: Path deviation measurement in AA-7075

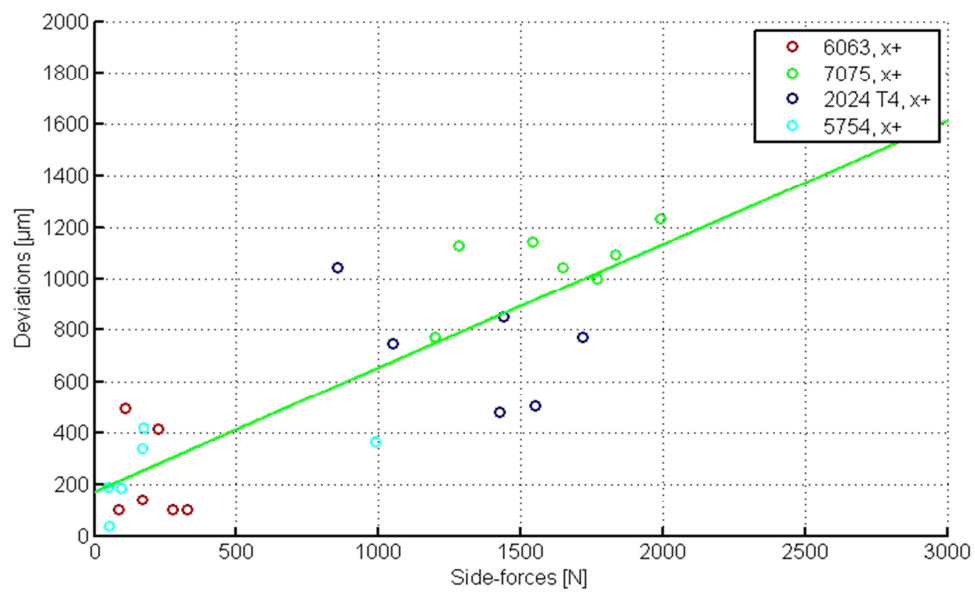


Figure 5: Side force versus path deviation while welding in x+ direction

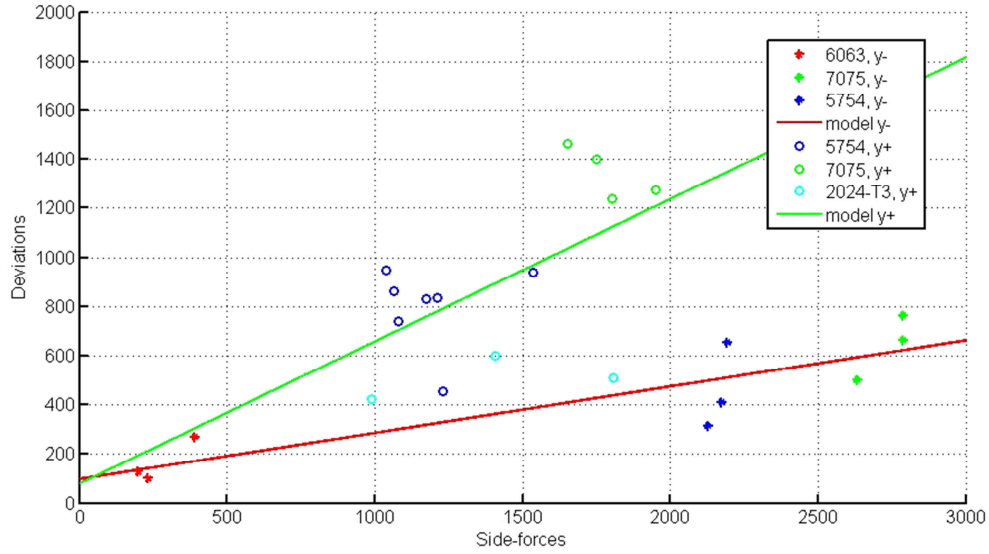


Figure 6: Side forces versus path deviation while welding in y direction

Another important conclusion was the traverse direction dependence of the path deviations. It was demonstrated that welding in x+ direction generated more deviations than welding in y- direction, referring to the robot base frame. For welds applied in different directions and/or locations in the workspace this can be explained by the fact that different welding directions require a different joint space setup to apply the motion. But as also welds performed on the same path, yet in an opposite direction (y- and y+) results in significant differences (Figure 6), more research in this area will be required to fully understand the compliance behaviour of the robot system, where a final solution would embed a deviation model for the complete joint space. From the measured values in y- and y+ direction, 2 different compensation models are created by fitting a first order equation to the measured points. These models are plotted in Figure 6 as a green (y-) line and red (y+) line.

Hence the interesting results from previous test, more experiments in this topic will be carried out. For these experiments, the camera will be used to make similar models as above. First test demonstrate that the deviation can be determined, even in soft aluminium alloys (6xxx). In Figure 7, it is shown that, on the moment that the shoulder comes in contact with the work piece, the tool is deviating slightly from the joint line. This goes from 114 pixels (when only the pin is in contact) to 126 pixels (when the traverse motion starts).

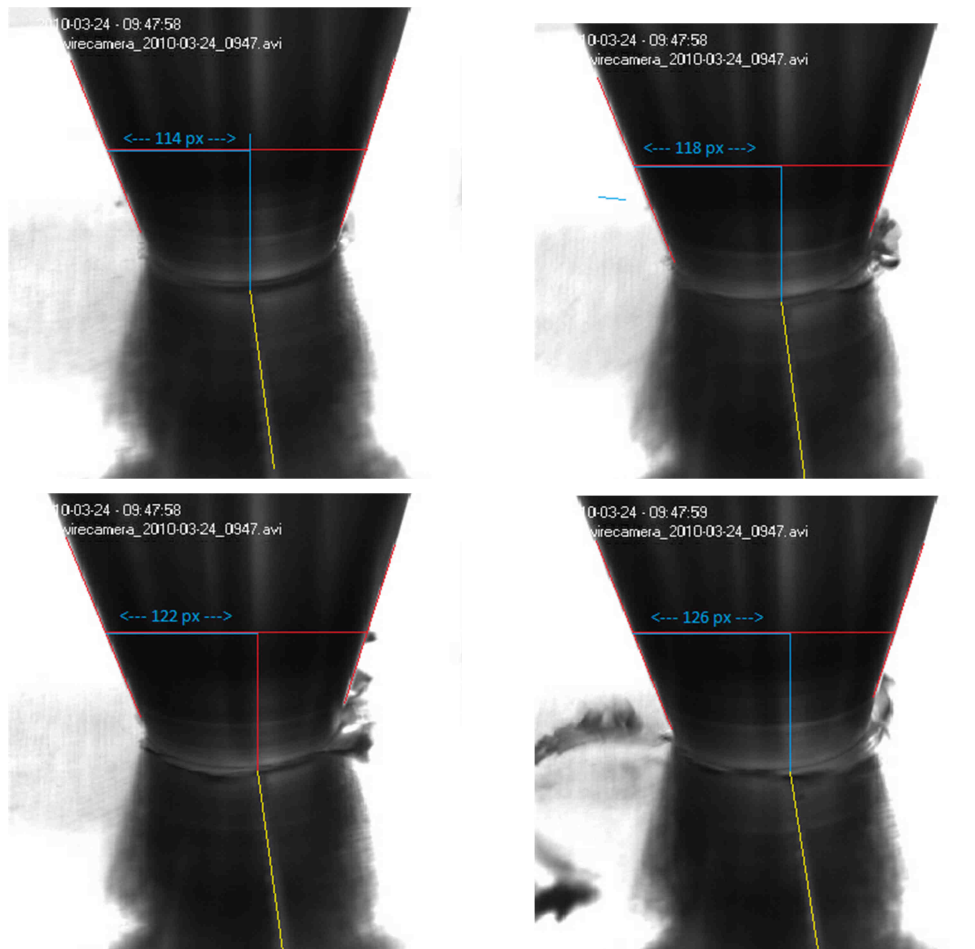


Figure 7: Deviation measurement by camera

Apart from the path deviations, there are more issues related to robotic FSW. Most FSW applications weld a linear track with approximately the same ‘ambient’ temperature (i.e. the temperature of the work piece before welding). However, when the robot would weld more complex curves, the work piece temperature will depend on pre-heating effects from previously welded locations. When the tool enters an area on a higher temperature, e.g. because the area was welded before, the material will overheat, becoming too soft and cause the tool to sink into the weld.

In a first attempt to measure the temperature, two parallel linear welds are performed directly after each other. The distance between these two welds is 20mm. Thermocouples are welded on the sheet, approximately 4,5mm from the welding line. This location represents the edge of the shoulder. Each weld had 2 thermocouples on resp. 50 and 150mm from the start point.

It is shown in Figure 8 that the first weld influences the temperature of the second weld. The maximum temperature in the second weld is influenced by the ‘pre-heating effect’ of the first weld. If the tool returns into a heated zone shortly after the first weld, overheat-

ing will inevitably occur. A temperature compensation model can be a requirement to guarantee a good quality for more complex welding paths. This model allows modifying the heat input by changing FSW parameters (e.g. rotational speed). The approach of decreasing rotational speed to generate a lower heat input has been adopted in (Cederqvist 2008).

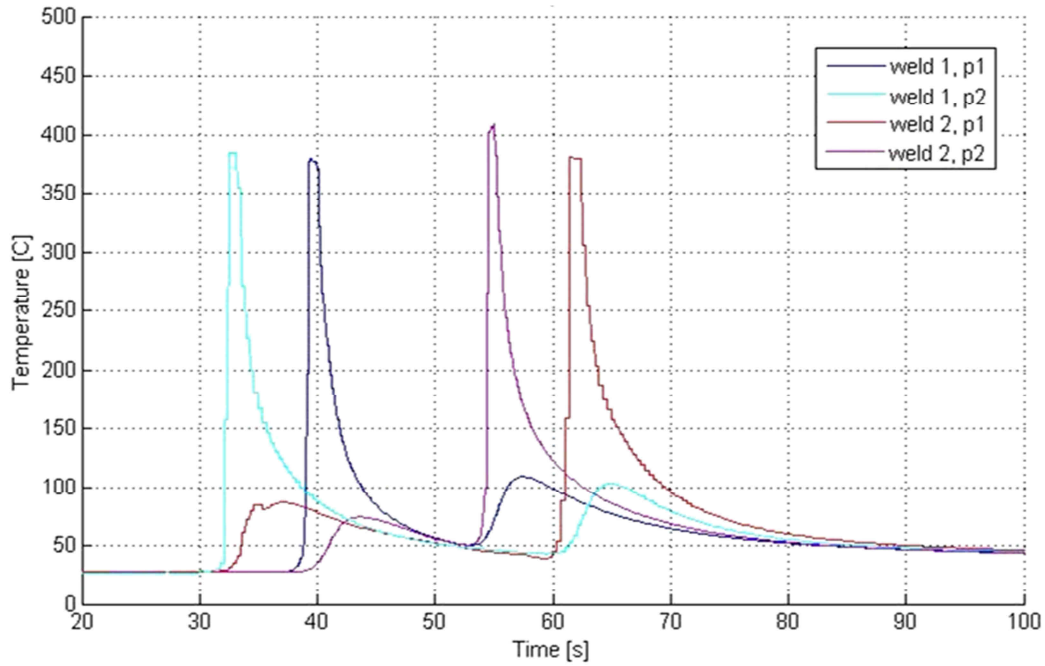


Figure 8: Thermocouple measurements of 2 parallel FSW lines

## 6 Discussion and Conclusions

While regression analysis was performed on the scattered plot, showed in Figure 5 and Figure 6, it was noted that there was a positive correlation, though with a rather extensive standard deviation. One possible cause of this spread can be the lack of a proper method to measure path deviations. The microscopic measurements on the start and stop location (Figure 4) might be inappropriate because of the robot's oscillatory behaviour in these 'transient' positions. The first results with the camera suggest a better precision. By calibrating the camera for this specific application, pixel measurements will be transformed in a real physical distance, i.e. the path deviation. Furthermore, this camera system gives is a less time consuming method because the variation in deviation along the

welding line is measured and logged during welding. Later on, a better correlation model can be made for a larger working area and the measurements can be used for online compensation.

In butt welded configuration, path deviations are of course detrimental as they shift the weld zone away from the joint line and accordingly provide an unsatisfactory root closure. This issue seems to be less relevant during lap configurations, as the joint quality will not be affected by the positional error. But it is of course important to fully understand the behaviour of the robot system, regardless of joint configuration, as high positional accuracy is normally required for all systems performing FSW.

The thermal measurements suggest that complex welding paths might require a control model for the heat input to avoid overheating. In future experiments on thermal behaviour, it will be important to know to which extend the preheating effect from previous welds affect the quality of other welding points. There will be more tests with combination of thermocouples and thermal camera.

Overall, the performance of this robot system is very satisfying for the tests. The implementation of the FSW spindle in the robot is seen as a big benefit, due to the compact and robust construction. There are a lot of possibilities to use this robot system for more advanced welding paths and faster welding speed. The welding speed is especially in automotive applications the main interest.

## **7 Acknowledgements**

The authors would like to acknowledge the financial support from Vinnova and the StiRoLight project group members, SAAB Automobile, ESAB, and Volvo. Their financial and technical support is highly appreciated.

## **8 References**

Balasubramanian, N., Gattu, B. and Mishra, R.S. (2009), "Process forces during friction stir welding of aluminium alloys", *Science and Technology of Welding & Joining*, 14, 141-145.

Cederqvist, L. (2008), "Adaptive control of novel welding process to seal canisters containing Sweden's nuclear waste using PID algorithms", *18th international conference FAIM 2008, Skövde, Sweden*.

Smith, C. (2000), "Friction Stir Welding using a Standard Industrial Robot", *2nd International Friction Stir Welding Symposium, Gothenburg, Sweden*.

Smith, C., Hinrichs, J. and Crusan, W. (2003), "Robotic Friction Stir Welding: The State-of-the-Art", *4th International Friction Stir Welding Symposium, Salt Lake City, UT, May 2003*.

Soron, M., De Backer, J., Christiansson, A.-K. and Ilar, T. (2010), "A local model for online path corrections in Friction Stir Welding", *Friction Stir Welding and Processing Conference 2010 - Lille, France*.

Soron, M. and Kalaykov, I. (2006). "A Robot Prototype for Friction Stir Welding", *IEEE Conference on Robotics, Automation and Mechatronics, 2006*

Voellner, G., Zäh, M.F., Kellenberger, O., Lohwasser, D. and Silvanus, J. (2006), "3-Dimensional Friction Stir Welding using a modified high payload robot", *6th International Friction Stir Welding Symposium, Saint Sauveur, Canada*.

Zimmer, S., Langlois, L., Laye, J. and Bigot, R. "Experimental investigation of the influence of the FSW plunge processing parameters on the maximum generated force and torque", *The International Journal of Advanced Manufacturing Technology*, 47(1), 201-215.

## Paper C

C

# **Surface Quality and Strength in Robotic Friction Stir Welding of Thin Automotive Aluminium Alloys**

De Backer, Jeroen

Christiansson, Anna-Karin

*4<sup>th</sup> Swedish Production Symposium*  
Lund, Sweden, 3<sup>rd</sup> to 5<sup>th</sup> of May 2011

## Abstract

Friction Stir Welding (FSW) is a sustainable method for joining materials without any consumables and without melting the materials. It uses a rotating tool that creates frictional heat and mixes the materials mechanically together. Robotic application of FSW allows three-dimensional welding of light-weight metals in e.g. the automotive industry. The StiRoLight project is driven by Saab Automobile AB and performed at University West for investigations of robotic FSW on three-dimensional welding seams. It aims to introduce FSW in the automotive production line. This paper describes the effect of penetration depth of the FSW tool during force controlled robotic welding of thin ( $< 2$  mm) aluminium in overlap configuration. The influence of pin length on strength of welded aluminium sheets is investigated using tensile and peel tests. The main limiting factor for penetration depth is the surface quality on the backside of the weld, which often is important in automotive applications. Further, the roughness of the plates on the backside is measured and related to pin length and backing bar properties. This paper shows a relation between penetration depth and tensile strength, and suggests an optimal pin length to guarantee a good weld quality while maintaining an acceptable surface quality. The influence of sheet thickness tolerance is also discussed. Knowledge is fed back to designers and manufacturing engineers to facilitate for use in production with guaranteed product quality.

**Keywords:** Robot, Friction Stir Welding, Surface Quality, Automotive, Aluminium

## 1 Introduction

After 20 years of technological development, Friction Stir Welding (FSW) research has become an important alternative to the classic fusion welding processes [14]. A welding process without consumables, without shielding gas and with a very low energy consumption were important properties that caught the attention in several areas such as marine, aerospace, railway and automotive industry [8].

The FSW principle, as demonstrated in Figure 1, generates heat by friction between the work piece and the shoulder of a rotating tool. The softened material is mechanically blended with the tool pin at about 85 % of the melting temperature, creating a welding joint with excellent properties. The on-going research covers a very wide field of topics. On the modelling side, researchers try to predict the behaviour of the process to get a better understanding of the material flow, heat transfer, internal stresses etc. in order to predict defects and quality [10]. Recently, a lot of interest is paid to the high-strength



alloys which are now possible to join by FSW with an excellent joint quality. Developments in PCBN and Tungsten-rhenium based tools make FSW of e.g. steel more and more economically feasible [11]. Next to the 'basic' FSW principle, numerous process variants are invented to get better results in each specific application. One example is laser-assisted FSW where the forces on the tool are significantly reduced by preheating the material [6]. Another example is Refill Friction Stir Spot Welding where the classical "keyhole" is filled during retraction, providing a much stronger spot weld [9].

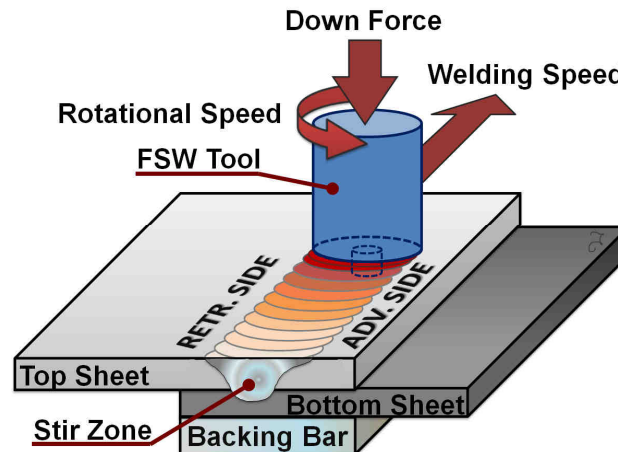


**Figure 1: The FSW process**

Worldwide, different industries picked up the FSW technology for joining lightweight materials. In general welding applications, the optimal weld is the one that has the highest tensile strength, the best fatigue properties and a negligible distortion at a low cost. The choice for FSW will thus be based on these factors. Hydro Aluminium in Norway was one of the pioneers in FSW of aluminium. This company reports a reduction of 15% man-hour per ton rate. Boeing reported a cost reduction of 60% in the production of Delta rocket fuel tanks. Often, the cost benefits are not directly related to the actual welding cost reduction (e.g. by absence of filler material) but indirect costs (e.g. limited defect reparation). A case-study from the shipyard industry [3] shows that the low distortion in FSW allows prefabrication of stiffened boat panels instead of manually ARC-welding them on the shipyard. This reduces the required man-hour, the production time and defect rate, resulting in a significant cost reduction.

For the application of FSW in the automotive industry, a few other important factors should be taken into consideration. FSW as a part of the automotive production line should compete with other welding methods (e.g. spot and laser welding) and with mechanical joining methods (e.g. clinching and riveting) in terms of speed, cost and strength. In addition to this, certain applications require an extremely fine surface finish of the backside of the weld on the so-called class A surfaces. These are body parts that are visible from the outside of the vehicle. It is not allowed to have any kind of deformation, roughness or colour changes on these parts after the body-in-white vehicle has passed the paint shop. In this paper, the importance of a good surface quality is highlighted and related to welding depth and backing bar quality.

Another aspect of this paper is an investigation of the plunge depth in thin aluminium sheets to allow different thicknesses being welded with the same FSW tool. This can result in a single-tool station, which gives a considerable time reduction.

## 2 Industrial Application

The StiRoLight research project at University West in Trollhättan, Sweden started in spring 2009 and aims to introduce robotic friction stir welding in the Swedish vehicle industry. The main industrial partners are Saab Automobile AB, Volvo AB and ESAB AB. Both Saab and Volvo are aiming with this project to investigate at different departments, from design to production, how FSW could replace existing joining methods. In the automotive industry, the most common joining method is resistance spot welding. Because of the significant weight reduction by using aluminium, the use of these alloys are increasing. Spot welding has, however, not the same robustness for aluminium as for steel and therefore other and less efficient or more expensive methods are used. Clinching has the advantage of being fast, cheap and easy to implement. Rivets are used on locations where clinch joints lack the required strength. The joint quality of a rivet is significantly better than clinch joints but the higher price per rivet implies a significant extra cost for serial produced vehicles [15].

In an investigation by Cederqvist [2], a joint between 2xxx and 7xxx aluminium alloys were welded in lap joint configuration with thicknesses between 3 and 6 mm. Due to the asymmetry of the weld, the failure load will always be located in the advancing side of the weld. Therefore double pass welds were performed. This approach provides a symmetric and stronger weld but the time-critical factor in automotive applications will most likely exclude the option to perform double-pass welding. Instead single-pass welding with a strategic location of the advancing side will be preferred. To overcome the asymmetry in the weld, a new method is developed at TWI where the rotation direction of the tool is switched after one or more revolutions. This technique gives a good symmetric weld but makes the required equipment more complex [13].

### 3 Experimental Set-up

All the tests in this paper were performed with the ESAB Rosio FSW robot. This robot is a serial kinematics robot with up to 12 kN payload and 40 Nm torque [12]. It consists of a modified ABB-IRB7600 robot where the last robot axis is replaced by a welding spindle. Replacing the axis by the spindle provides a compact design with decreased robot compliance. Furthermore, the robot is equipped with an ATI Force and Torque sensor and the vertical direction of the welding operation is force-controlled by a closed-loop strategy. Force-control is enabled in these tests to get a good robotic welding operation. The FSW robot, shown in Figure 2 is owned by the StiRoLight research project and located at the Production Technology Centre, part of Innovatum Technology Park in Trollhättan, Sweden. The tool used for all these tests has a threaded cylindrical pin of 4 mm and a scrolled shoulder of 10mm.

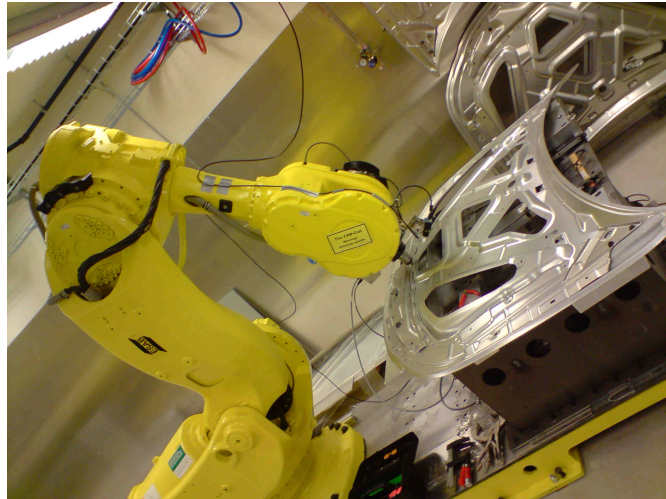


**Figure 2: FSW robot cell at the Production Technology Centre**

Special attention is paid to industrial applications at Saab Automobile and the requirements for friction stir welding in the automotive industry are taken into consideration. This implies that for visual and reachability issues, a set-up was chosen where thicker (up to 2 mm) 5000-series material is used as top sheet material and a thinner 6000-series material as bottom sheet material. Tensile and shear tests are done according to company standards on a Zwick Z100 testing machine. The specimen dimensions are described in Figure 3.

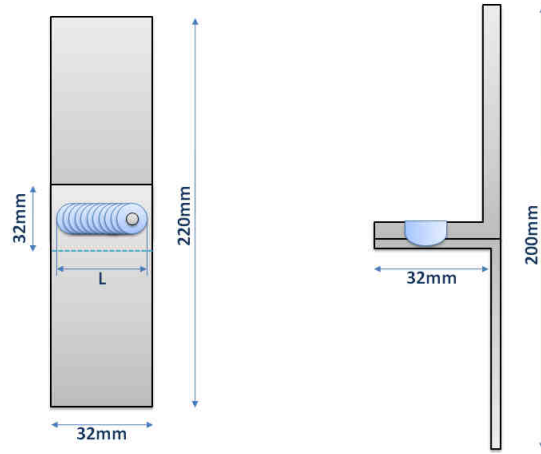


**Figure 3: Illustration of the specimen dimensions for (a) tensile tests and (b) shear tests**

In the first part of this study, the optimal parameters are determined by performing tensile test on several welded pieces, each with its own parameter set-up. The materials used in these tests are AA 6016-T4, AA 5182 and AA 5754. The tests consist of both tensile tests and peel tests. To determine the optimal parameters, a variety of parameters were used for welding AA-5182 (1.5 mm) to AA-6016 T4 (1.0 mm). All tests were performed at relatively high welding speed (2 m/min). Based on tensile test results, a set of parameters was selected for all further tests. Table 1 shows the different configurations.

The second part of the study makes use of the previously defined optimal parameters to weld parts with different welding lengths (L), in order to demonstrate the effect of start and stop holes and relation between welding length and welding strength. It should be mentioned that tests with a very short welding length of 1 and 2 mm is performed in the same way as the welds with a longer distance where both the tool design and the dwelling time are optimised for continuous lap joins. The shown results for 1 and 2 mm welds can thus not be considered as friction stir spot welding. The FSW data are compared to clinch joining and rivet joining data which were obtained from earlier tests at the industrial partners. The thicknesses of those riveted and clinched test parts differed up to 0.2 mm from the samples in this paper and results should thus be interpreted as an indication of achievable strength, rather than an exact value.

The third part of the results describes the effect of variable pin lengths and plate thicknesses on the tensile strength. This will provide a better insight in the sensitivity for penetration depth in friction stir welding. For each parameter set-up, there were 2 welds performed in opposite direction. In this paper, the results are related to penetration depth into the bottom sheet.

In the final part, special attention is paid to the influence of the backing bar roughness on the surface quality of the welded parts. Different penetration depths and different backing bar roughnesses are evaluated. The roughness is measured with a Mahr M2 perthometer. The width of the profile for roughness measurement is 5.6 mm and the

width of the profile for waviness measurement is 17.5 mm. More advance methods are demonstrated to investigate surface finish in friction stir welds, for example a laser-processed FSW seam is investigated with 3D laser scan images [7] on the top side of the weld. The texture on the welded side is not of interest within the context of this paper.

## 4 Experimental Results

### 4.1 Parameter Sensitivity

From an industrial point of view, the welds must be controlled on quality by either visual inspection (macroscopic defects) or non-destructive testing (microscopic defects). A quick visual control from the operator on macro defects is obviously cheaper and faster than the more advanced non-destructive testing methods. The parameter tests show that the process is rather insensitive to parameter variations with this specific material and tool as shown in Figure 4. The maximal strength was obtained in trial #6 with 4345 N.

**Table 1:** Parameter sensitivity test

Trial	Plunging parameters			Welding parameters			Tensile Strength [N]
	$F_p$ [N]	d [mm]	$\omega_p$ [/min]	$F_w$ [N]	$\omega_w$ [/min]	tilt [°]	
1	3000	3.0	2500	3000	2500	0.5	3522
2	"	3.2	"	"	"	"	3873
3	"	3.5	"	"	"	"	3809
4	5000	"	"	3500	"	"	3608
5	"	"	"	4500	"	"	3705
6	4500	"	"	3500	"	0	4219
7	"	"	"	"	"	2	4118
8	"	"	"	"	"	1	3859
9	"	"	"	"	3500	"	<b>4345</b>
10	"	"	"	2000	"	"	2669
11	"	"	"	2500	"	"	4200
12	"	"	"	4500	1500	"	3945
13	"	"	2000	"	2000	"	3809
14	"	"	"	"	"	"	4025

Only one sample (trial #10) had bad tensile properties and this could be predicted by the visual investigation: an open void, in literature also referred to as “lack of fill”, was visible at the advancing side of the welding line [1]. During the start of trial #1, a short “lack of fill” defect was visible and this is translated into a weaker weld at 3522N. This defect is attributed to insufficient plunging: the forward movement started before the shoulder was in contact with the plates. Especially during robotic FSW operations, the process is sensitive to the programmed penetration depth, due to the robot deflections [4]. All the other samples reached 85 % of the maximal welding strength.

The welds in these tests suggest that a visually defect-free weld always reaches 85 % of the maximum tensile strength. It should however be noted that peel and fatigue properties might be more sensitive to invisible defects. The effect of defects on fatigue properties is well documented for butt-joints. A work by Dickerson and Przydatek describes no change in fatigue properties for root flaws in butt joints [5].

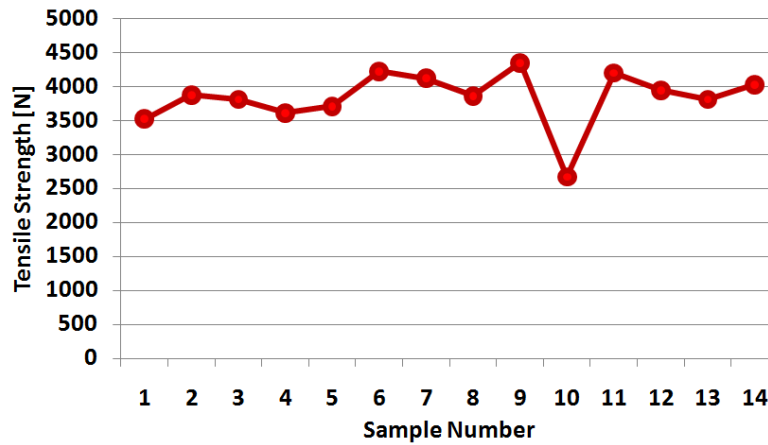
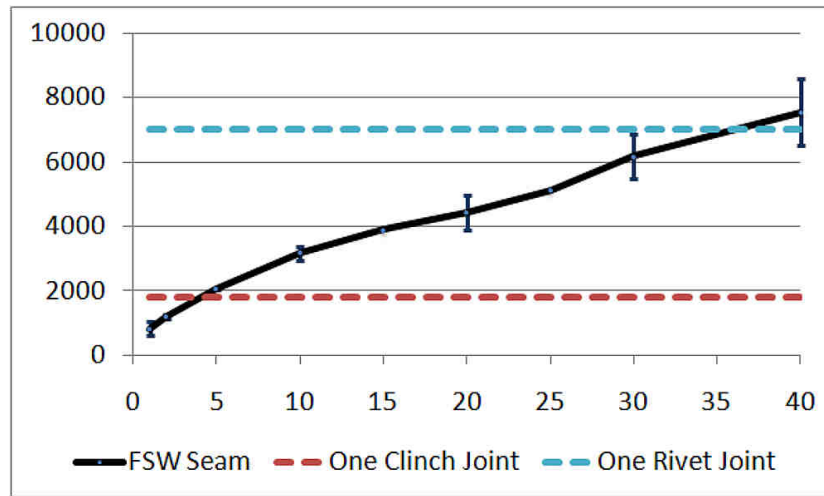


Figure 4: Tensile strength of specimen for the parameter setup in table 1.

## 4.2 Welding Length Dependence

In a different set-up, welds are performed at 2 different rotational speeds, 1500 and 2500 rpm. Tensile strength was measured for different welding lengths as demonstrated in Figure 5. The hotter weld at 2500 rpm (Series 1 and 2) was stronger than the cold weld at 1500 rpm (Series 3). Two short welds were performed with 1 and 2 mm movement, providing about 1 kN of strength. These short welds were comparable to the test results of clinch joints. The stronger rivets have a strength, similar to a 30 mm weld, around 7000 N. In a steady state situation, the strength increases approximately linear with 180 N/mm for the 2500 rpm weld. It is of particular interest for the industrial partners to get the strength per mm since this value can be set as a parameter in advanced simulation models of the full scale product, which allows detecting insufficient strength of certain welded parts in an early stage. The figure also demonstrates the benefits of a continuous joint over single-point connections.



**Figure 5: Tensile strength for different welding lengths**

#### 4.3 Penetration Depth Dependence

The influence of variable sheet thickness on strength is described in this paragraph. Figure 1 illustrates the process where the advancing side of the weld is near the top sheet edge. This situation is indicated with a “+” in Table 2. When the pin was only plunged in the top material and relatively far away from the bottom sheet ( $\geq 0.3$  mm), there was no joint (Sample 9 and 10 in Table 2). There was a small deformation noticeable in the bottom sheet but the oxide layer was not broken. When the pin was at the interface of the two sheets, a joint was created with good tensile properties (Sample 3 and 4). There was no important difference visible between the weld that touched the bottom sheet (0 mm penetration) and the weld that plunged slightly (0.05 mm) into the bottom sheet (Sample 5 and 6). The weld that plunged deeper into the bottom sheet (0.4 mm) was not stronger than the welds with less penetration. For samples 13 and 14, the oxides were removed and the plates were welded directly afterwards. The weld quality was not affected by this extra operation.

The maximal strength is obtained in sample 3 where the pin has the same length as the top sheet thickness. In another scientific work by Yadava [16], similar results are reported.

**Table 2:** Penetration depth and strength in 6xxx (6S) and 5xxx (5S) series

Sample	Top sheet	Bottom sheet	Direction	Pin length [mm]	Penetration [mm]	Strength [N]
1	6S 0.8	6S 0.8	+	1.2	0,4	3943
2			-	1.2		3968
3	6S 1.2	6S 0.8	+	1.2	0	4894
4			-	1.2		4882
5	6S 1.15	6S 0.8	+	1.2	0,05	4795
6			-	1.2		4842

7	6S 0.8	6S 1.5	+	1.2	0,4	4207
8			-	1.2		4852
9	6S 1.5	6S 0.8	+	1.2	-0,3	0
10			-	1.2		0
11	6S 1.5	6S 0.8	+	2.0	0,5	4903
12			-	2.0		4779
13	6S 1.5	6S 0.8	+	2.0	0,5	4815
14			-	2.0		4808
15	5S 2.0	6S 1.2	+	2.0	0	6869
16			-	2.0		5599
17	5S 2.0	6S 1.2	+	2.0	0	5101
18			-	2.0		5188

#### 4.4 Surface Finish

The perthometer measurements are performed on 4 welded plates and compared to the roughness of the corresponding points on the backing bar as described in Table 3. All the tests for the roughness measurements are carried out with 2mm 5000-series aluminium as top material and 1.2 mm 6000-series aluminium with 0.765 micrometer roughness as bottom material. All the tests had the same parameter setup, with a downforce during welding of 4700N.

Weld 1 had an unpolished steel backing bar. Weld 2 had a polished steel backing bar (polished to 0.2 micrometer), Weld 3 had an unpolished aluminium backing bar and weld 4 had a polished aluminium backing bar (polished to about 0.1 micrometer). The produced roughness profile is demonstrated in Figure 6. It is observed that the average roughness under the weld was smaller than on the rest of the sheet i.e. the welded zone is smoother than the base material. Only in the transition zone, a deformation of the sheet is visible of  $6.19 \mu m$ . One sample was sprayed with black paint to simulate the visual quality of the backside after the welded car body part went through the paint shop. There was no difference in surface finish noticeable between the base material and the welded part by human-eye inspection. Only the deformation in the transition zone, indicated in Figure 6, was clearly visible on the sprayed material. This transition can be described as "waviness" and is a cause of the forces applied by the FSW tool on the sheets.



**Table 3:** Roughness measurements on backing bar and work piece

Test	Sample	Measurement	Backing Bar	Weld
WELD 1 : Unpolished steel	A	Ra	1.620	1.303
		Rmax	12.9	17.7
	B	Ra	1.715	1.170
		Rmax	15.5	14.7
	C	Ra	1.775	1.370
		Rmax	16.9	16.6
WELD 2: Polished steel	A	Ra	0.206	0.172
		Rmax	0.167	2.85
	B	Ra	0.183	0.198
		Rmax	-	-
	C	Ra	0.218	0.203
		Rmax	-	-
WELD 3: Unpolished alum.	A	Ra	0.214	0.352
		Rmax	1.87	3.02
	B	Ra	0.210	0.266
		Rmax	1.93	2.22
	C	Ra	0.221	0.299
		Rmax	1.98	2.15
WELD 4: Polished alum.	A	Ra	0.110	0.106
		Rmax	1.36	-
	B	Ra	0.098	0.122
		Rmax	-	1.48
	C	Ra	0.095	0.147
		Rmax	1.65	- 1.51

The average roughness (Ra) measurements demonstrate a relation between the roughness of the backing bar and the roughness of the backside of the weld. The welded area can obtain a smoother surface than the base material, due to the high pressure on the plates during FSW. Surface roughness on the backside of the weld can be modified to a desired value by processing the backing bar to the same value.

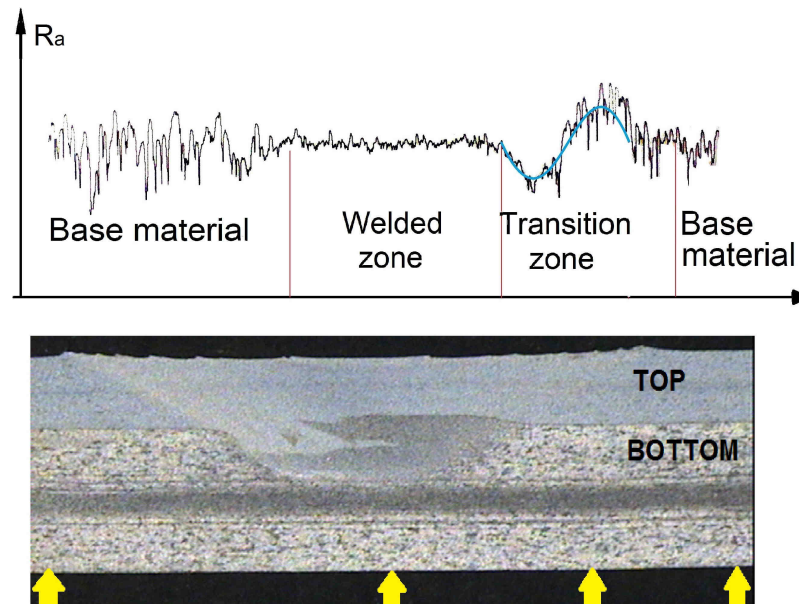


Figure 6: Roughness profile from the Mahr Perthometer

## 5 Discussion and Future Work

This paper provides an insight in the requirements for friction stir welds as part of the automotive production line. The paper demonstrates that plates with different thicknesses can be welded with one single tool, without a great variation in tensile properties. This allows more flexibility in production since the strength is not very sensitive to small plate thickness variations. Furthermore cost and process time can be reduced as there is no automated tool-change mechanism required. Large ( $\geq 20\%$ ) variations in process parameters did not result in great changes of the tensile properties. All welds without visual defects have a tensile strength of more than 85% of the maximal obtained strength in the same material. It is obvious that with a shorter pin, the amount of stirred material is reduced. If the stirred zone does not enter the bottom plate, no joint is created. Welds performed with a pin length, equal to the top sheet thickness had the best tensile properties.

The strength versus length measurements show a certain non-linearity. This might be explained by non-perpendicular testing: When the welding line is not fully perpendicular to the tensile direction, a peel effect will initiate from the side of the plate, causing an erroneous measurement of the strength. Another possible cause could be plain-strain -

plain-stress effects where the edges of the weld are more ductile than the centre. This effect is subject to further investigation.

This paper demonstrated the need for a backing bar with polished surface in order to get a good surface quality on the backside of the weld. The roughness of the backside of the weld is directly related to the roughness of the backing bar. It is shown that successful lap welds in aluminium at a welding speed of 2m/min can be performed with steel and aluminium backing bar. Aluminium fixtures have considerably lower manufacturing costs than steel and can therefore be a good alternative in low-volume production. The surface properties on the backside of the welded plates is a footprint of the backing bar and can be modified by choosing the right backing bar properties. Waviness was visible after spraying the plate with black paint. This waviness is not tolerated on class-A surfaces and possible solutions to decrease the plate deformation should therefore be investigated. Increasing the shoulder diameter or decreasing pin diameter could be a solution to get a better distribution of the pressure on the plate.

## 6 References

- [1] W. J. Arbegast. A flow-partitioned deformation zone model for defect formation during friction stir welding. *Scripta Materialia*, 58(5):372–376, 2008.
- [2] L. Cederqvist and A. P. Reynolds. Factors affecting the properties of friction stir welded aluminum lap joints. *The Welding Journal Research Supplement*, 80(12):281–287, 2001.
- [3] Kevin J. Colligan. Friction stir welding for ship construction, Concurrent Technologies Corporation, 2004.
- [4] Jeroen De Backer, Mikael Soron, Torbjörn Ilar, and Anna-Karin Christiansson. Friction stir welding with robot for light weight vehicle design. In *8th International Friction Stir Welding Symposium*. TWI, 2010.
- [5] T. L. Dickerson and J. Przydatek. Fatigue of friction stir welds in aluminium alloys that contain root flaws. *International Journal of Fatigue*, 25(12):1399–1409, 2003.
- [6] Hidetoshi Fujii, Takahiro Tatsuno, Takuya Tsumura, Manabu Tanaka, and Kazuhiro Nakata. Hybrid friction stir welding of carbon steel. *Materials Science Forum*, 580 - 582(Advanced Welding and Micro Joining / Packaging for the 21st Century):393–396, 2008.

- [7] Omar Hatamleh, James Smith, Donald Cohen, and Robert Bradley. Surface roughness and friction coefficient in peened friction stir welded 2195 aluminum alloy. *Applied Surface Science*, 255(16):7414–7426, 2009.
- [8] Stephan W. Kallee. Industrial applications of Friction Stir Welding, volume 1, pages 118–163. Woodhead Publishing ltd., Cambridge, UK, 2010.
- [9] T. Rosendo, B. Parra, M. A. D. Tier, A. A. M. da Silva, J. F. dos Santos, T. R. Strohaecker and N. G. Alcântara. Mechanical and microstructural investigation of friction spot welded aa6181-t4 aluminium alloy. *Materials and Design*, 32(3):1094–1100, 2011.
- [10] H. B. Schmidt and J. H. Hattel. Thermal modelling of friction stir welding. *Scripta Materialia*, 58(5):332–337, 2008.
- [11] Carl D. Sorensen and T. W. Nelson. *Friction Stir Welding of Ferrous and Nickel Alloys*, pages 111–121. ASM International, Materials Park, OH, USA, 2007.
- [12] M. Soron and I. Kalaykov. A robot prototype for friction stir welding. In *Robotics, Automation and Mechatronics, 2006 IEEE Conference on*, pages 1 –5, 2006.
- [13] W. M. Thomas, I. M. Norris, I. J. Smith, and D.G. Staines. Reversal stir welding-re-stir<sup>TM</sup>-feasibility study. *4th International Friction Stir Welding Symposium, Park City, Utah, USA, 14-16 May 2003*.
- [14] W.M. Thomas, E.D. Nicholas, J.C. Needham, M.G. Murch, P. Temple-Smith, and C.J. Dawes. Friction stir butt welding, 1991.
- [15] Juha Varis. Economics of clinched joint compared to riveted joint and example of applying calculations to a volume product. *Journal of Materials Processing Technology*, 172(1):130–138, 2006.
- [16] M. K. Yadava, R. S. Mishra, Y. L. Chen, B. Carlson, and G. J. Grant. Study of friction stir joining of thin aluminium sheets in lap joint configuration. *Science and Technology of Welding and Joining*, 15

## Paper D

# Investigation of Path Compensation Methods for Robotic Friction Stir Welding

D

De Backer, Jeroen

Christiansson, Anna-Karin

Oqueka, Jens

Bolmsjö, Gunnar

*Industrial Robot: An International Journal*

Emerald Group Publishing Limited

Accepted 2<sup>nd</sup> of March 2012.

## Abstract

Friction Stir Welding (FSW) is a novel method for joining materials without using consumables and without melting the materials. It uses a rotating tool that generates heat by the friction between the tool and the material, and mixes the materials mechanically together. Robotic FSW allows welding of light-weight materials in all orientations which is of great interest for the automotive industry. FSW is an in-contact welding operation with substantial reaction forces and the materials under study are aluminium alloys with possible weight savings and reduced fuel consumption of a car. In this perspective, robotic FSW is of great interest in automotive industry as a complement to other joining methods. To successfully introduce robotic FSW in industry it is important to understand the forces generated in the process and how these affect the accuracy of the robot.

This study focuses on the robot deflections during FSW, by relating process forces to the deviations from the programmed robot path and to the strength of the obtained joint. A robot adapted for the FSW process has been used in the experimental study. Two sensor-based methods are implemented to determine path deviations during test runs and the resulting welds were examined with respect to tensile strength and path deviation.

It can be concluded that deflections must be compensated for in high strength alloys. Several strategies can be applied including online sensing or compensation of the deflection in the robot program. The welding process was proven to be insensitive for small deviations and the presented path compensation methods are sufficient to obtain a strong and defect-free welding joint.

This paper demonstrates the effect of FSW process forces on the robot, which is not found in literature. This is expected to contribute to the use of robots for FSW. The experiments were performed in a demonstrator facility which clearly showed the possibility to apply robotic FSW as a flexible industrial manufacturing process.

**Keywords:** Industrial Robotics, Friction Stir Welding, Path compensation, Seam tracking, Force

## 1 Introduction

Welding is a major application area in industrial robotics and the use of robots to automate welding processes is the normal choice, for example in the automotive industry. To compete and complement existing flexible robotic solutions a welding process should

allow for high flexibility with respect to low volume production, product design and material to be welded. Friction Stir Welding (FSW) provides unique properties compared with other joining methods and introducing robotised FSW provides new opportunities in design and materials to be joined.

Friction Stir Welding was invented at TWI (The Welding Institute, Cambridge), UK, in 1991 and the first patent was filed in 1992 (Thomas et al., 1991). The FSW process, which is one of the latest innovations in the area of welding, has several advantages compared to traditional fusion welding techniques. Firstly, it enables welding of materials often considered unweldable, like the 2xxx and 7xxx aluminium series, and also enable joining of material such as magnesium (Lockyer and Russel, 2000) and copper (Andersson et al., 2000), which are all material characterized by a low melting temperature. Furthermore, joining of dissimilar material, such as aluminium to copper (Karlsson et al., 2000) or aluminium to steel (Jiang and Kovacevic, 2004) has been performed in laboratory set-ups. Secondly, problems often associated with welding of aluminium, such as shrinkage, porosity and distortions are eliminated to a great extent by the FSW process (Chao et al., 2003). This is mainly due to the following facts:

- The welding process takes place in solid state at around 80-90 % of the melting temperature of the material.
- The filler material (wire) used in traditional methods is absent.

Several alloys have been studied extensively, providing a better understanding of the process. A study by Peel for example, examines the AA-5083 alloy. Besides a profound microstructure analysis the hardness profile is measured and shows a typical W-profile, with the heat affected zone having the lowest yield strength. The X-ray residual stress analysis shows that the weld is under tension in both longitudinal and transversal direction and the longitudinal stresses display a direct dependence on the rotational speed (Peel et al., 2003). Today, FSW is mainly used in aircraft, marine and railway industries, and is considered a valuable technique for butt and lap joint welding of aluminium alloys with a range in plate thickness from 0.5 to 75 mm, and with a welding speed up to 100 mm/s.

The drawbacks that have been associated with FSW, mainly the high forces and torques needed to generate heat, did originally require heavy duty machinery. Thus, these requirements limit the use of the FSW process to straight or circumferential welding which obviously is less attractive in automotive industry where flexible production solutions to joining are sought for. In general, to be competitive with other joining processes, it should be flexible with respect to selection of material, geometrical variations including fixture issues, and allow flexibility in product design.

Many industrial welding applications are carried out by robots. The precision of modern robots provides an excellent repeatability and a weld quality that is comparable or better than manual welding. The major drawback of FSW concerning its robotisation, compared to classic fusion welding processes, is the contact force: the robot is in contact with the material during welding, applying a constant down force. The forces are very much depending on material and thickness but forces in the range of several tens of kN are common for FSW. This implies that the robot has to be much stronger and stiffer than

with other welding processes. Only ten years ago, the first robot that could handle 500 kg was launched by ABB. Along with the development and use of industrial robots in heavy duty applications, other robot manufacturers have followed the trend with high payload robots, mainly indented for materials handling. However, even if the main robot manufacturers offer robots in the 500-1000 kg payload range, the market niche is relatively small for such robots and the price is high compared to the mainstream spot welding robots. Other applications such as milling, grinding and drilling with robots are typical examples where stiffness and payload come into play and robot designs based on parallel kinematics principle intended for such processes might be an interesting option here. This evolution in robot design is of course beneficial for robotic FSW which has similar requirements.

This paper presents the state-of-the-art in robotic FSW and outlines important steps for its implementation in industry and specifically automotive industry. This study is part of an investigation of FSW of butt joints, and reaction forces and deviation of the TCP on the robot. As part of this endeavour, a demonstrator for robotic FSW is set up to study and develop the robotisation of the process. The experimental setup is described with specific emphasis on issues concerning robot path and related robot performances during FSW. The study presented here of using robot and in particular the precision during heavy-duty in-contact operations and relating it to the FSW process is a novelty in this domain and experimental results clearly show the possible use of robots for flexible FSW. The work presented is a step towards a more robust robotic FSW system that can weld high-strength materials in non-planar geometries in flexible production.

## **1.1 State of the art**

The robot system used in this paper is the ESAB Rosio FSW robot, see Figure 1. This is a modified industrial robot with serial kinematic design. This type of robot design is the most common industrial robot, it is widely adopted in the automotive industry and has been tested in the area of FSW by several research groups in the past (Smith et al., 2003, Soron, 2007, Voellner et al., 2006). Alternative systems have been demonstrated, using parallel kinematic robots (Strombeck et al., 2000). Such robot systems have a much better stiffness but lack the large workspace that serial kinematics robots offer.

Most of the research in the area of robotic FSW confirms the need of a force controlled robot to allow a successful welding operation. This is mainly due to mechanical deflections in robot joints. Force control for robotic FSW can be divided in two types: direct and indirect force control. Direct force control is based on force sensor measurements which are sent to a closed loop force controller around the position control loop. This additional controller overwrites the position values in the force controlled-direction(s) and makes it possible to set the force for the FSW process to a desired value. Indirect force control is based on a torque-deflection model as demonstrated by (Smith, 2000). The force at the tool centre point (TCP) is calculated from the delivered torques in each of the robots servo motors.



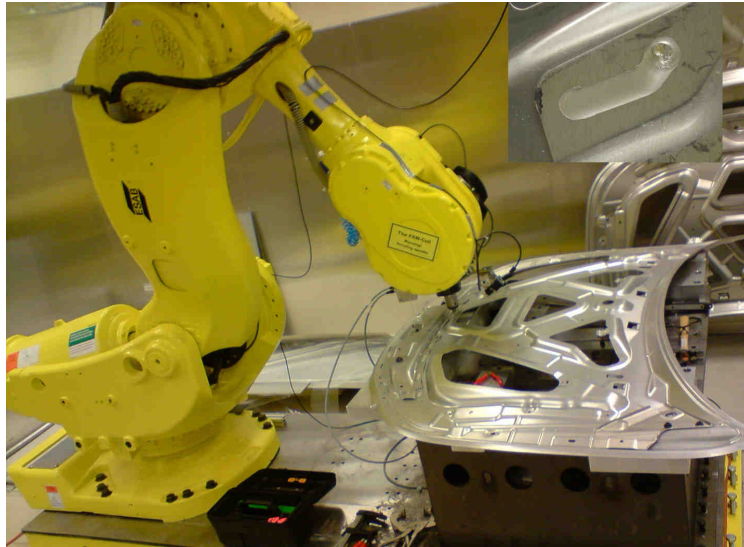


Figure 1. The ESAB Rosio FSW robot used in the experimental work. An example of an overlap weld is shown in the right top of the figure.

A force study in FSW (Cook et al., 2004) on a rigid FSW machine indicates that, in position control, a stepwise increase of the welding depth does not cause an increased axial force. Instead the axial force will reach the same steady-state value and increased production of flash on the sides of the weld is observed. This result can be interpreted as following: If the set force value (in force controlled mode) is equal to the measured value from the position controlled welding operation, similar welding results should be obtained. Another conclusion in the study is the significant reduction of axial force (again in position controlled mode) when the spindle speed is increased. This is a result of the increased heat input, which causes the material to soften more. This important conclusion suggests that the deflections in the robot can be significantly reduced by welding at higher RPM and a lower set force. However, the friction coefficient between tool and material is a limiting factor for the rotational speed; there will not be a proper material flow once a certain rotational speed is reached, causing welding defects. Within a certain parameter range, the reaction forces can be reduced through proper setting of the process parameters including tool design to make it possible to apply robots for FSW.

In the work on three-dimensional FSW (Zaeh and Voellner, 2010), design rules were given to obtain good welding quality on highly curved surfaces. A good weld was only obtained if the force in the curves was reduced and if the trailing edge (i.e. the backside) of the tool remained in contact with the material. This resulted in a tilt angle of over  $18^\circ$ . The diameter of the tools was limited by the bending radius of the work piece. Furthermore, the tool deviations in welding direction were reported up to 5 mm.

In the PhD-thesis by Soron, a first attempt was made to compensate for path deviations in a limited space. Based on force measurements during welding and deviation measurements after welding, a linear approximation was made to predict the tool deviation from the side forces. The model was then used for online path compensation (Soron, 2007).

The study presented here further evaluates different methods to measure and compensate for path deviations that are usable, not only for a limited area, but for the whole robot workspace.

## 1.2 Forces on the FSW tool

Unlike other robotised welding methods like gas metal arc welding and laser welding, FSW is an in-contact welding operation. This means that the welding process requires a certain force, in combination with the tool rotation, from the tool on the material to obtain a good welding quality. The high forces associated with this welding process affect the robot behaviour: the robot will deflect due to a lack of stiffness. The relevant forces during robotic FSW are (see Figure 2):

- *Down force*: To achieve successful robotic FSW operations, a force controlled mode of the direction, perpendicular to the plates, is required. This guarantees that the welding tool stays in contact with the work piece with a constant contact force. The down force is one of the main process parameters and affects the friction between the tool and the plates. This friction is the main contributor to the heat generation in the process.
- *Traverse force*: This force is a result of the materials resistance to the tool movement along the joint line. This force will be influenced by the welding parameters and the type of welded material (i.e. the temperature dependant material hardness).
- *Side force*: This force is perpendicular to the traverse force. It is caused by the asymmetric character of the welding process. The force is directed towards the advancing side of the weld. These forces are applied to the welding tool, causing the robot to deflect from the joint line. The resulting deviation is subjected to a further study as described in this paper.
- *Torque*: The torque is a result of the friction between the tool and the work piece and corresponds to the heat input into the system. Higher contact forces and a larger contact area result in a higher torque. A sufficiently powerful motor is required to guarantee a stable rotation of the tool i.e. without high speed fluctuations.

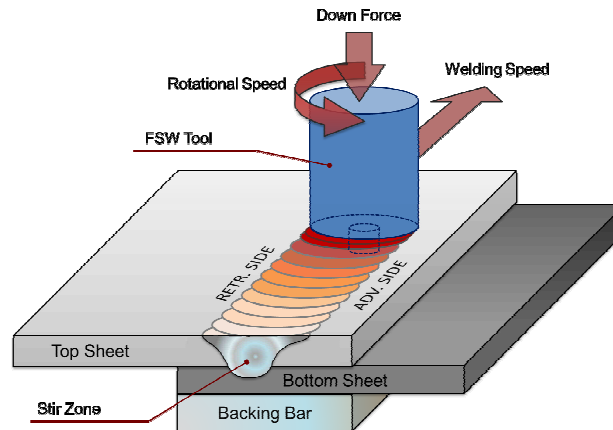


Figure 2. Forces applied on the welding tool in FSW.

For a successful introduction of robotic FSW in industry it is important to understand the forces generated in the process and how this affects the robot path accuracy. In addition, the heat input generated by the down force, spindle speed and welding speed together with the tool design, must be selected in a proper way. Too high heat input and down force together with too low welding speed will simply cause the tool to melt down into the material. On the other hand, a high heat input will produce a softer material during the FSW process, which is beneficial for the robot. To introduce robotic FSW in industry it is important to understand the process parameters and how they interact with the capability of the robot equipment.

## 2 Experimental Set-up

During welding of the harder aluminium series (2xxx and 7xxx), it was observed that the robot deviates from its programmed path. Due to the high process forces, every robot joint will slightly deflect in links, servo motors and gears, resulting in a non-negligible TCP deviation. There is no model available today that unambiguously predicts the properties of the process and the weld from the process parameters. However, several successful attempts have been made to estimate the forces, temperature, residual stresses etc. Moreover, temperature measurements and finite element models of FSW usually show an asymmetry across the weld; the advancing side is warmer than the retreating side of the weld (Gagner and Ahadi, 2009), see Figure 2. No investigations have been found that predict the side forces from this temperature asymmetry, as it is not of interest on stiff machines. However, the difference in temperature will result in softer material on the advancing side and could be the explanation for the forces towards the advancing side of the weld, causing weaker machines like robots to deflect. A different approach to pre-

dict side forces is by modelling the material flow. Different models are discussed and compared in literature (Sorensen and Stahl, 2007). The first model is the area model, assuming that the force on the pin can be calculated from a spatially varying pressure that acts on the cross-sectional area of the pin. The second model is the extrusion model; where the material flow can be seen as an extrusion of material from the front to the back of the tool, through two small zones at the side of the tool. As the tool rotates and the material sticks to the tool, more material will be extruded through the retreating side than through the advancing side. This causes a different extrusion pressure and accordingly an asymmetry in the side forces on both sides of the tool (Arbegast, 2008).

In initial tests, several butt-welded FSW samples were microscopically investigated to measure the maximum deviation from the welding joint. The distance between the joint line and the edge of the tool in the start and stop locations was measured on images taken from the weld samples. However, unpredictable vibrations in these start and stop locations resulted in highly scattered results. The limited precision of this method resulted in a new approach where the deviation was measured during welding.

It should be noted that the sensor arrangement described below was used to measure and understand the path deviation during welding for the experiments described in this paper. The need and use of a tracking sensor is dependent on many parameters including material, joint type and geometry. However, the approach here is to study the FSW process characteristics from an industrial perspective and the implications of using a robot for increased flexibility. It should also be noted that the force sensor measurements are logged in all directions but only the measured downforce is used for force control. The actual movements along the joint line are still position controlled as defined in the robot program.

A data acquisition system was developed in LabVIEW, logging data from both a laser distance sensor and a camera simultaneously. Both methods were evaluated and compared. For each welding operation, an internal log file was saved in the robot system with force sensor data and robot position data at a sample rate of 3 Hz. A limitation of the used system is the absence of a 6th robot axis. This axis was removed on the robot used for the tests because the rotation axis for the welding tool is the same as the 6th axis, which makes the last robot axis redundant. Furthermore, the stability of the robot increased with a more compact design. The welding operation should not be affected by the absence of this 6th axis but sensors fixed on the 5th axis cannot be aligned with the programmed path. Therefore the measurement system with camera and laser presented here and developed for the experiments were only usable for weld joints adapted for this set-up and aligned manually with the travel direction.

## **2.1 Vision based method**

The device for image acquisition is a monochrome camera, type Procilica EC650, with a resolution of 640×480 pixels and a maximum frame rate of 90 fps. This camera was connected through a FireWire interface to the data acquisition system in LabVIEW. The camera was first calibrated for intrinsic parameters, to compensate for lens imperfections that cause distortions at the edges of the image. These parameters have to be calibrated

just once. In addition, the camera extrinsic parameters have to be defined. They provide the relation between the camera and a world coordinate system of the robot. Extrinsic parameters have to be redefined, every time the camera position or the welding tool is repositioned. Both calibrations were easily done using the Image Processing Toolbox and Camera Calibration toolbox from the mathematical software MATLAB. Figure 3 shows the used extrinsic parameter calibration pattern.

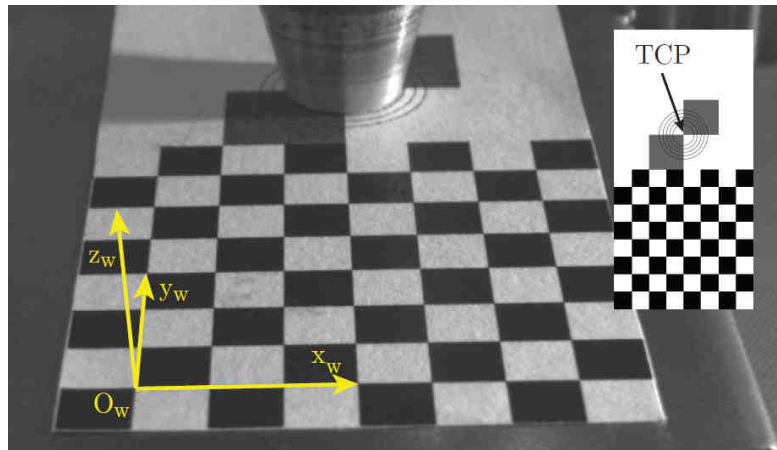


Figure 3. Calibration image of the camera for extrinsic parameters

Once the black and white image was transformed to the world coordinate system of the robot, an image processing algorithm in MATLAB was applied to detect the welding line. The difference between the known location of the tool centre point (TCP, indicated as a red dot in Figure 4) and the detected joint line (indicated as a yellow line in the same figure) provided a numerical value, corresponding to the absolute distance between the tool centre point and the joint line. This value was sent to the data acquisition system in LabVIEW.

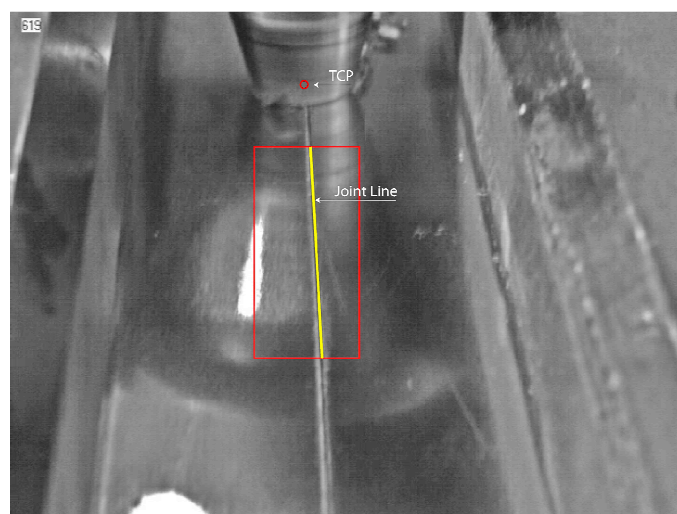


Figure 4. Camera image during welding after applying the line detection algorithm

## 2.2 Laser based method

The two laser distance sensors, type Micro-Epsilon optoNCDT 1302-200, send an analogue current signal to a data converter, which sends the data via USB to the measurement system. The sensors have a measurement range of 20 to 200 mm and a maximum sampling rate of 750 Hz. The sensing method used a smooth reference plane, standing on the welding table at about 150 mm away from the welding joint.

Figure 5 describes the sensor arrangement during the welding experiments. In principle, the FSW process is relatively easy to operate together with sensors, but for this robot a rotating axis for the sensor arrangement has to be integrated so the sensors can be aligned with the weld for further work with curved weld joints.

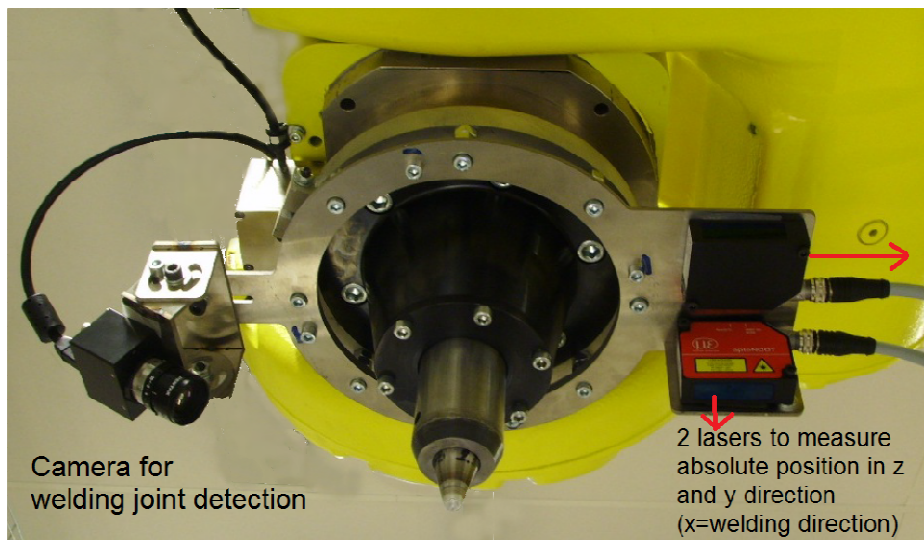


Figure 5. Sensor arrangement used during the experiments.

## 3 Experimental Results

### 3.1 Compensation needs

This section demonstrates the need for path corrections in robotic friction stir welding. In principle, such path compensation can be made by using tracking sensors or predictive analysis and estimation, which will be discussed later. Here, the description relates to the study of the reaction forces and deflection on the robot.

In order to see the effect of a misaligned tool trajectory, two plates of 3 mm thick AA-7020 aluminium were butt-welded with a concave FSW tool, having a shoulder diameter of 10 mm and a 2.3 mm long threaded pin with a 3 mm diameter. The joint line between the two plates was aligned to be parallel with the robot weld path and these weld paths had a programmed offset (P.O.) varying from -3 mm to +3 mm away from the joint line. During welding, the robot deflects causing an offset from the tool path. This deflection offset (D.O.) is around 0.8 mm for the AA-7075 material with similar hardness and setup, as shown in Figure 8. The D.O. is fairly constant within 0.3 mm in a limited work space on the work table. Four weld samples were made for each programmed path which is shown by the measured tolerance width in Figure 6. For each of the weld samples, tensile tests were performed to see the effect of misalignment on the strength of the weld. Figure 6 demonstrates the importance of a well-positioned welding line. The true offset (T.O.) from the centre line is the sum of P.O. and D.O. This means that when the tool is programmed with P.O. at 0.8 mm to the retreating side of the joint line, the joint deflections will cause the tool to deviate with D.O. at 0.8 mm to the advancing side. Thus, T.O. will end up in 0 mm and in the middle of the joint line, providing the strongest joint. For a P.O. greater than 1.4 mm to the advancing side, the T.O. will be greater than  $1.4 + 0.8 = 2.2$  mm. In that case, the pin misses the joint line completely and no FSW joint is created.

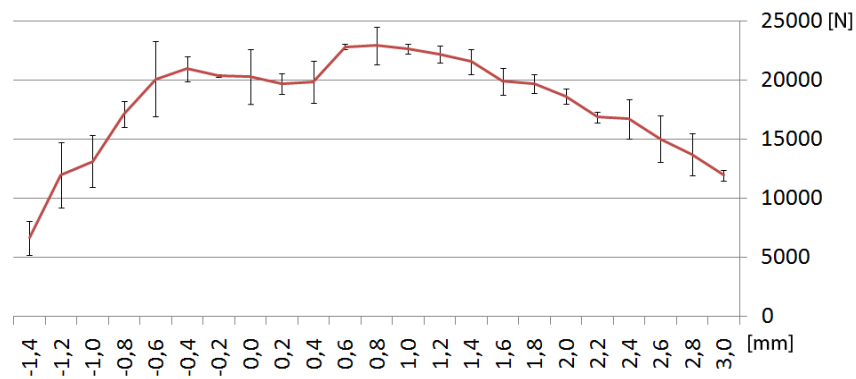


Figure 6. Tensile strength of AA-7020 during off-seam FSW. The x-axis indicates the programmed offset (P.O.) from the joint line.

Micrographic investigation, see Figure 7, demonstrated the lack of penetration when the tool was not aligned properly. Crack formation in the bottom will occur for these applications. Although tensile strength is still acceptable for relatively large path deviations (up to 1 mm), the effect on fatigue strength was expected to be much more important as cracks will initiate from the unwelded area in the bottom. The observations are in line with a study by (H.Takahara et al., 2007) where they conclude based on an experimental study that the allowed tolerance width is half the diameter of the tool.



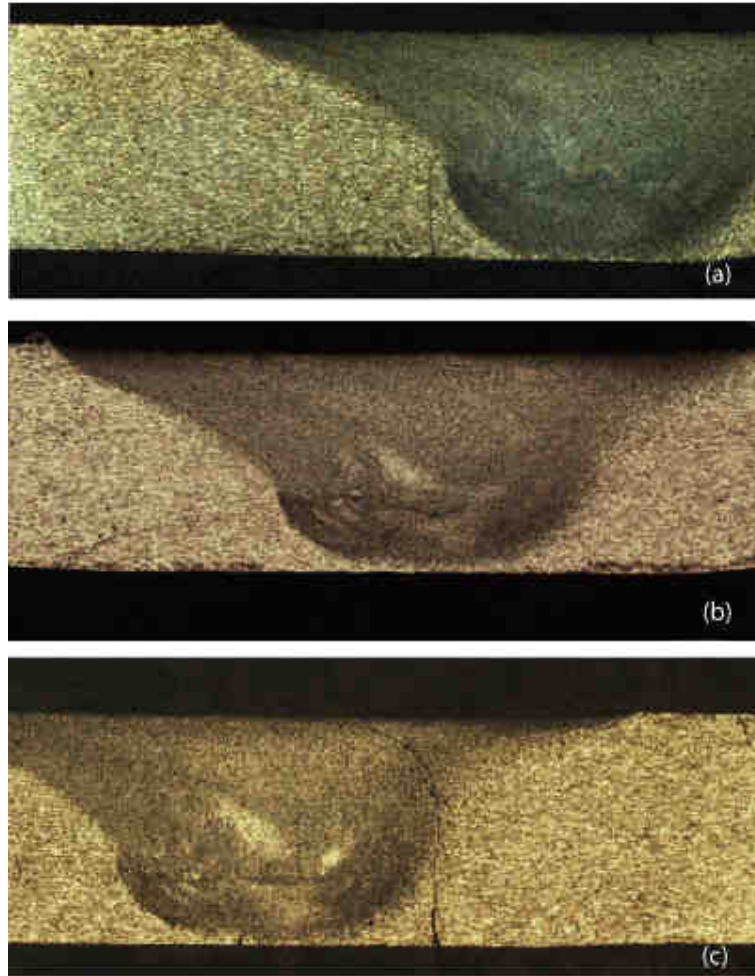


Figure 7. Effect of tool deviations on the weld quality. (a) corresponds to +2.6 mm, (b) corresponds to +0.6 mm, and (c) corresponds to -1.4 mm alignment as shown in Figure 6.

### 3.2 Microscopic Deviation Measurements

To investigate which parameters and other factors are influencing the tool deviations, a group of different aluminium alloys were welded with several operating parameters. Then the deviation was measured by cross section microscopic analysis in order to investigate which influence the asymmetry in forces and accordingly the path deviations have on the weld quality and robot operation. No clear relationship could be found between a specific parameter and the deviations. However, lower welding speeds generate in general higher heat input which requires lower forces on the robot and generates lower deviations from the path defined in the robot program. On the other hand, too low speed might generate heat that causes the base material to soften or even melt and the robot will push the tool through the plate. The parameter settings for the different materials tested are presented in Table 1.



Table 1. Parameter set-up for microscopic deviation measurements.

Material type	Brinell hardness [HB]	Welding speed [rpm]	Rot. Speed [mm/s]
AA5754	47	1000-1500	5-15
AA6063-T6	73	2500	8-10
AA2024-T3	120	700-1200	2-15
AA7075-T6	150	800-1250	5-12

To investigate the direction-dependency, tests in different welding directions were performed. After the samples were welded, the deviations from the joint line were measured on calibrated microscopic images from the start and stop positions. The average of the start and stop deviation is plotted in Figure 8 for different welding directions.

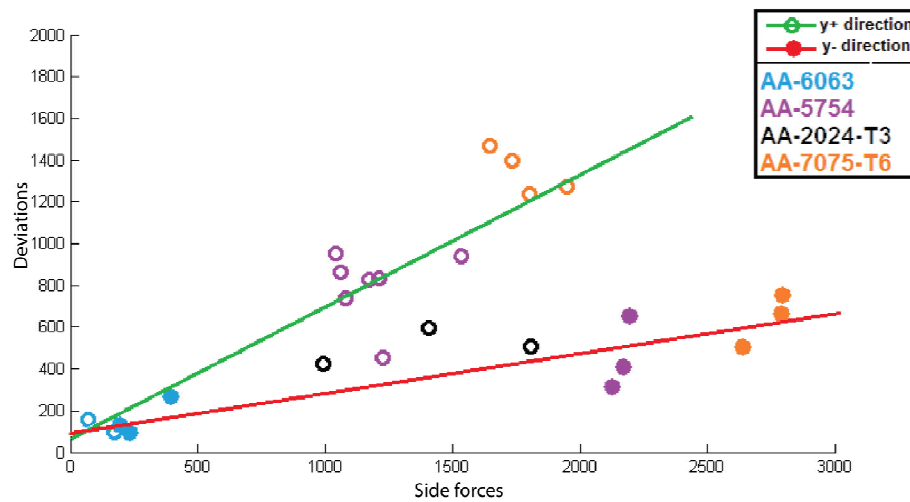


Figure 8. Path deviation as a function of the side forces. Deviations (y-axis) are in  $\mu\text{m}$  and Side forces (x-axis) are in [N].

When splitting up the measurements in different directions, a clear direction-dependency is demonstrated. Welding in “y-“ direction resulted in deviations of up to 0.8 mm, while welding the same material with the same parameters and in “y+” direction resulted in up to 1.5 mm deviation. These high direction-dependent deviations can be explained by the effect the process forces have during different movements in space based on the robot kinematics and the way the robot is designed. Also, these types of heavy duty robots are constructed primarily for lifting heavy objects. For the FSW process, however, the robot pushes in the opposite direction. Moreover, in general 3D robotic FSW welding the approach is to weld in any position and it is important to know the performance level of the robot system for such tasks. A study to develop a model to predict the deflection has been initiated. Preliminary findings indicate that the path deviation can be predicted

within the tolerance required for the process so that compensation to the path can be made, if needed, see discussion below.

### 3.3 Comparison of the vision and laser based method

Unlike the microscope measurements, vision and laser sensors can be used as an automated path compensation method during welding similar to seam tracking for arc welding. The control strategy is represented in the block diagram in Figure 9. For FSW the travel speed is relatively low and the correction of the path as an offset can be used using the functionality provided by the ABB IRC5 controller. The controlled value is sent to a register inside the robot system via a Profibus network and the ABB robot control system IRC5 facilitates for path offsetting through the “xyCorr-function”.

Both measuring methods have their advantages and disadvantages.

The laser system:

- Requires a reference plane
- Produces high precision measurement
- Only works for straight welding lines

The camera system:

- Requires controlled light conditions
- Needs a visible joint line (no overlap joints)
- Does not require a reference plane
- Cannot be used during plunging because the position is unknown to the system

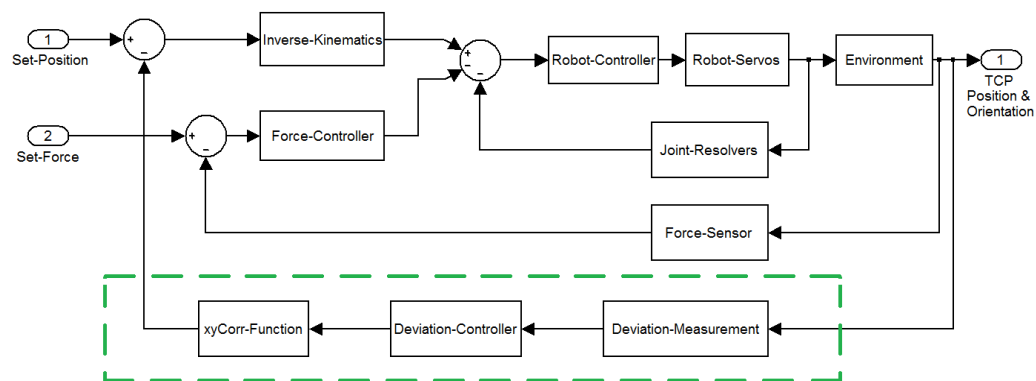


Figure 9. Control scheme for robotic FSW. The green frame indicates the additional control loop for path compensation during welding.

Both methods give a precise profile of the absolute position of the tool in cross-welding direction, as shown in Figure 10. Note that the welding starts at frame 340 in Figure 10 and the measurement before reflects an approach path of the robot which are measured differently by the two sensors. In principle, the FSW process is a “clean” process with

respect to the use of a sensor close to the weld joint and applying and selecting a sensor for measuring the path or other parameters is based on the specific case. However, for a repetitive FSW joint with predictive result, path compensation can be made in the program of the robot itself by offsetting the poses in the robot path. During all the presented deviation tests, the process forces are measured with the embedded force sensor. In a stable welding process, the side force arises when the forward movement starts and remains constant along the whole welding path. This justifies the implementation of a compensation method that only compensates the deviations once at the start of the welding operation, rather than continuously modifying the path during welding.

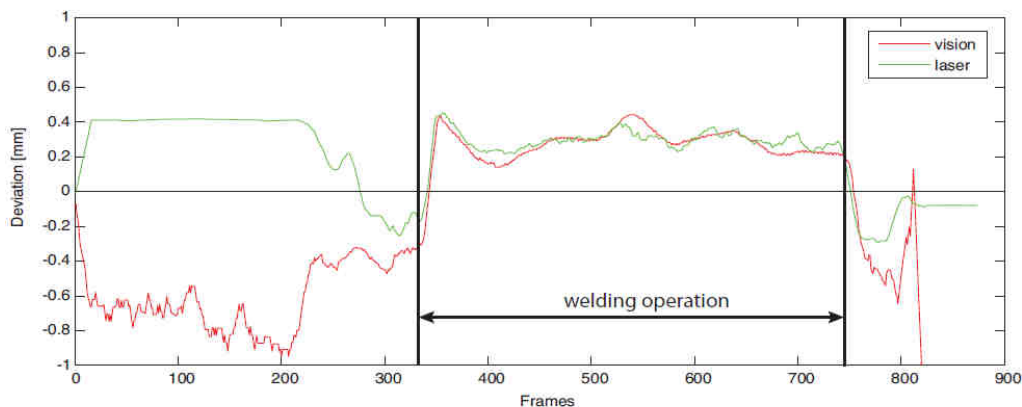


Figure 10. Profile of the absolute tool deviation from the centreline of the weld measured by vision and laser sensors. The actual weld starts at frame 340 and before that the robot performs an approach path.

## 4 Discussion and conclusions

Robotic FSW provides unique opportunities and challenges in automotive manufacturing for joining metals. This study clearly shows the capability of using a robot for FSW, but also the limitations with respect to the strength of the metal which results in substantial reaction forces on the robot.

In general, the weld strength was in the same order as the strength of the base material, and the process is executed repeatedly in a robust way with the same quality, provided proper clamping of the plates.

The deflection of the robot depends to a great extent on the strength of the plates to be welded. For the lower strength aluminium alloys such as the 6000 series this is a minor

problem as the deviation of the TCP is within 0.2 mm, but for the high strength alloys the path deviation must be compensated for either by online tracking sensors or measuring the resulting path and changing the defined path in the robot program accordingly. Another approach is to control the FSW process to minimize the forces. One possibility is to preheat the plates to lower the forces in the process. Initial tests have started to investigate this possibility with a clear indication that preheating lowers the forces significantly to make robotic FSW possible in steel material.

Due to the absence of a 6th robot axis, the sensors cannot be aligned with the programmed robot path. This is a major limitation for the measurement system for online tracking on work pieces located arbitrary in the work space. However, this could be solved by adding an external axis to the system for the purpose of aligning the sensor in the welding direction, using the data signal of the original 6th axis. In this way, the robot would be able to measure the misalignment and use the tracking data to compensate its path during welding operation.

The system performs well in the experimental set-up and produces welds that are repeatable and consistent. Therefore, the issue of using sensors for controlling or compensating the path in production is related to the actual need as in other applications such as Gas Metal Arc Welding. For series production the robot path can be compensated for the deflection if other parameters such as clamping and fixture are fixed and robust which provide stable and repeatable conditions.

This paper evaluates different methods to measure and compensate for path deviations in robotic FSW. The use of the sensors in this study allows a good measurement and understanding of the process and the robot behaviour. However, it is not always necessary to use these sensors in a production environment. The study presented here will contribute to the development of a model to predict the tool deviations in the whole workspace, based on force sensor measurements. Initial work on locating the cause for the deflections indicates that the main source can be attributed to the joints of the robot. Preliminary analysis and tests indicate that the deviation of the tool can be predicted within the permissible tolerance of the FSW process as shown in this paper. In future work, the forces in the xy-directions will be used to predict the deflection of the robot. This will alter the control scheme in Figure 9 so that the information from the force sensor will be used both for force feed-back control (downforce) and the indicated xyCorr-Function (predicted by the side forces measured by the force sensor). As the force sensor is already used for controlling the downforce, this approach will not add to the cost to the system. Initial results indicate that the deviations with this model can be decreased to an offset within the tolerances for defect-free welding. One must always be aware that a model-based compensation method will only be successful when the positioning of the welding part is always the same. If the position can vary from weld to weld, a sensor based method is required, just like the seam-tracking systems, known from other welding methods.

To conclude, this study shows the importance of understanding the reacting forces and related parameters in FSW and how proper operating settings can support a successful implementation of robotized FSW in manufacturing industry.

## 5 References

- Andersson, C. G., Andrews, R. E., Dance, B. G. I., Russel, M. J., Olden, E. J. & Sanderson, R. M. 2000. A comparison of Copper fabrication by the electron beam and friction stir processes. *2nd International Friction Stir Welding Symposium*. Gothenburg, Sweden.
- Arbegas, W. J. 2008. A flow-partitioned deformation zone model for defect formation during friction stir welding. *Scripta Materialia*, 58, 372-376.
- Chao, Y. J., Qi, X. & Tang, W. 2003. Heat transfer in friction stir welding - experimental and numerical studies. *Manufacturing Science and Engineering*, 125, 138-145.
- Cook, G. E., Crawford, R., Clark, D. E. & Strauss, A. M. 2004. Robotic friction stir welding. *The Industrial Robot*, 31, 55-63.
- Gagner, J. & Ahadi, A. 2009. Finite element simulation of an AA2024-T3 friction stir weld. *International Review of Mechanical Engineering (IREME)*, 3, 427-435.
- H.Takahara, Y.Motoyama, M.Tsujikawa, S.Oki, S.W.Chung & K.Higashi 2007. Allowance of Deviation and Gap in Butt Joint on Friction Stir Welding. *Advanced Materials Research*, 15-17, 375-380.
- Jiang, W. H. & Kovacevic, R. 2004. Feasibility study of friction stir welding of 6061-T6 aluminium alloy with AISI 1018 steel. *Proceedings of the Institution of Mechanical Engineers*.
- Karlsson, L., Larsson, H., Bergqvist, E. L. & Stoltz, S. 2000. Friction stir welding of dissimilar al-alloys. *2nd International Friction Stir Welding Symposium*. Gothenburg, Sweden.
- Lockyer, S. A. & Russel, M. J. 2000. Mechanical properties of friction stir welds in Magnesium alloys. *International conference on Magnesium alloys and their applications*. Munich, Germany.
- Peel, M., Steuwer, A., Preuss, M. & Withers, P. J. 2003. Microstructure, mechanical properties and residual stresses as a function of welding speed in aluminium AA5083 friction stir welds. *Acta Materialia*, 51, 4791-4801.
- Smith, C. 2000. Friction stir welding using a standard industrial robot. *2nd International Friction Stir Welding Symposium*. Gothenburg, Sweden.
- Smith, C., Hinrichs, J. & Crusan, W. 2003. Robotic stir welding: The state-of-the-art. *4th International Friction Stir Welding Symposium*. Salt Lake City, UT.
- Sorensen, C. & Stahl, A. 2007. Experimental Measurements of Load Distributions on Friction Stir Weld Pin Tools. *Metallurgical and Materials Transactions B*, 38, 451-459.
- Soron, M. 2007. *Robot System for Flexible 3D Friction Stir Welding*. PhD, Orebro University.

Strombeck, A. V., Schilling, C. & Santos, J. F. D. 2000. Robotic friction stir welding - tool technology and applications. *2nd International Friction Stir Welding Symposium*. Gothenburg, Sweden.

Thomas, W. M., Nicholas, E. D., Needham, J. C., Church, M. G., Templesmith, P. & Dawes, C. J. 1991. *Friction Stir Butt Welding*. International Patent Application no. PCT/GB92/02203 and GB Patent Application no. 9125978.9. Oct. 1995.

Voellner, G., Zäh, M. F., Kellenberger, O., Lohwasser, D. & Silvanus, J. 2006. 3-dimensional friction stir welding using a modified high payload robot. *6th International Friction Stir Welding Symposium*. Saint Sauveur, Canada.

Zaeh, M. & Voellner, G. 2010. Three-dimensional friction stir welding using a high payload industrial robot. *Production Engineering*, 4, 127-133.

## **Paper E**

# **Influence of Side-Tilt Angle on Process Forces and Lap Joint Strength in Robotic Friction Stir Welding**

**E**

**De Backer, Jeroen**

**Soron, Mikael**

**Cederqvist, Lars**

*9<sup>th</sup> International Friction Stir Welding Symposium*  
Huntsville, AL, USA, 15<sup>th</sup> to 17<sup>th</sup> of May 2012

## Abstract

The friction stir welding (FSW) process implies high process forces, unlike the classical fusion welding processes. This affects the selection and design of the machine to perform the process. Material flow and tool rotation will induce a difference in temperature and forces between advancing side and retreating side of the weld. This asymmetry will cause a certain force to act on the tool, perpendicular to the welding direction and tool axis, usually denoted as lateral force or side force. Side forces are generally much smaller than the axial force and are often irrelevant for most FSW research studies. However, when the welding operation is performed in a less rigid and powerful machine such as an industrial robot, the side forces will cause deflections in the robot joints, resulting in tool path deviations, both linear and angular. These deviations can affect the weld quality e.g. by crack formation at the root of the weld in case of butt joints. Furthermore in FSW lap joints, the failure location of tensile/fatigue specimens is almost exclusively in the advancing side of the weld.

It is common to add a tilt angle to the FSW tool, in order to get more pressure on the material behind the tool tip. In an attempt to reduce the asymmetrical effects induced by the welding process, an extra welding parameter is introduced: the roll angle. This is the angle in the plane perpendicular to the welding direction. The study of this angle is a novelty in the field of FSW, mainly because it requires 6 degrees of freedom, which conventional FSW machines normally do not have. All welding tests in this study are overlap joints of AA-7075-T6 with 2 mm sheet thickness performed by an ESAB Rosio™ FSW robot. The robot is equipped with a force sensor, enabling force measurements, not only along the tool axis but also in welding direction and lateral direction. The robot is operating in force controlled mode to manage the deviations in vertical direction of the tool, caused by the high process forces. By tilting the tool towards the advancing side, more pressure will be applied on that side, providing more frictional heat on one side. The effect of this roll angle on the process forces and robot deflections has been studied. A laser-based deviation measurement system is demonstrated and related to the measurements from the embedded force sensor. Furthermore, microstructure analysis and tensile tests are performed to investigate the influence of the roll angle on the weld quality. An optimal roll angle is suggested to increase weld quality.



# 1 Introduction

Twenty years after the invention of Friction Stir Welding (FSW) at The Welding Institute in Cambridge, UK (Thomas et al., 1991), an impressive collection of applications, process variants and FSW machines have been demonstrated. Along with the development of heavy-duty robots, a whole new range of applications became possible. Robots lack the stiffness of a conventional FSW machine (Soron, 2007) but have the advantage of being very flexible, easy to automate and implement in a production line, and above all, robots allow welding of three-dimensional (3D) joints. Several research groups have studied the possibility of joining materials by FSW using an industrial robot (Soron and Kalaykov, 2006, Smith, 2000, Von Strombeck et al., 2000).

The harder and thicker the material gets, the higher risk for welding defects, caused by the compliant robot. In previous research, it is demonstrated how joint deflections in a serial kinematics robot can cause deviation of the welding tool (De Backer et al., 2012). In butt-joints, these deviations cause root defects, initiating crack-formation in the root of the weld. A sensor-based strategy was presented to compensate for path deviations within the process window. Along with those findings, it was observed that the welding tool is exposed to both a linear and angular deviation relative the nominal position and orientation. This causes the tool to deviate in the plane perpendicular to the welding direction, i.e. towards the retreating side. The effect of this tilt angle is not well-documented in literature and the effect on weld quality is rather unknown. One reason is that this deviation is negligible in conventional rigid FSW-machines. However, the side-tilt angle is interesting for several reasons:

- Its influence on the side-forces, acting on the tool
- Its relation to formation of wormhole defects
- Necessity to compensate for angular deviations of the robot

Because of the asymmetry in the FSW process, the tool will encounter a side-force. This paper investigates if the addition of a side-tilt angle as a process parameter can reduce the asymmetry in the process and decrease the process force.

One article (Oki et al., 2007) investigated the effect of side-tilt angle on the properties of 3mm thick butt welds in AA-5083 and aimed to examine the side-tilt angle “tolerance” in 3D FSW seams, i.e. how much the tool can be tilted in cross-welding direction without deteriorating the weld quality. The tool is tilted from  $-10^\circ$  (towards advancing side) to  $+10^\circ$  (towards retreating side) and the effect on both tensile strength and strain is measured. The paper demonstrated that a roll angle of  $2^\circ$  does not affect the weld quality for butt joints. A joint efficiency of 85% is reached for roll angles up to  $8^\circ$ .

Tool geometry should always to be adapted to the type of application to guarantee a good weld. Inappropriate tool geometry for lap joints typically causes hooking effects, which can reduce fatigue and tensile strength significantly. Buffa reported high-quality lap welds using a tool probe with a cylindrical shape close to the shoulder and a conical

shape at the end. The cylindrical part allows obtaining large nugget areas because of the large area sheet interface while conical part induces a vertical helicoidal material flow (Buffa et al., 2009). In (Cederqvist and Reynolds, 2001) the effect of parameter variations on the strength of lap joints was studied.

## 2 Experimental Setup

All welding tests are performed at the Production Technology Centre in Trollhättan, Sweden. The lab is equipped with an ESAB Rosio™ friction stir welding robot, see Figure 1. The robot is a modified ABB IRB-7600 robot, with embedded force control using an ATI omega 190 force sensor. The robot design is further described in (Soron, 2007). The forces during welding are logged in the robot system at a sample rate of 3 Hz. In the present configuration, the tool can rotate at a speed up to 4500 RPM with torques up to 30Nm. For this study, a FSW tool is used with both clock- and counter-clockwise threads on the pin. This CounterStir™ tool is designed to create an upwards and downwards material flow, minimizing the stress in the material at the interface of the two plates and reducing the hooking effect (Burford, 2007). The used tool has a pin diameter of 4 mm and shoulder diameter of 10 mm.

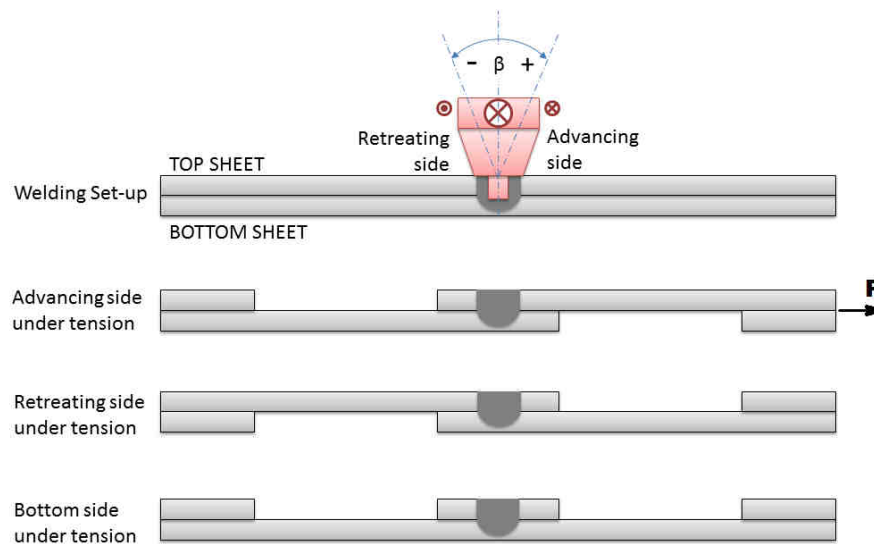


Figure 1: FSW robot at the Production Technology Centre (left) and the experimental set-up (right)

The material used in all tests is rolled aluminium alloy AA-7075-T6 with a minimal ultimate tensile strength in transversal direction of  $\sigma_{UTS,MIN} = 540$  MPa. Two plates of

250x250mm with 2mm thickness were lap-joined together with a 230 mm long weld with different side-tilt angles. After welding, the plate was watercut into nine samples of 21mm width plus one smaller for microstructure investigation. The nine samples were tested in a tensile test machine. Three of the samples were tested with advancing side under tension (A.U.T.), three with retreating side under tension (R.U.T.) and three with the bottom side under tension (B.U.T.). See Figure 2 for the different test situations. Two of the three samples were tested 3 weeks after welding and the third sample 7 weeks after welding. All tensile test results are represented as the maximal applied force before breaking,  $F_{\max}$  [N]. The choice to represent tensile strength as function of the maximal force [N] instead of stress [MPa] is based on the unconformity in literature for definition of the contact area in FSW lap joints.

The side-tilt angle ( $\beta$ ) was varied between  $-3.2^\circ$  (into the retreating side) and  $+4^\circ$  (into the advancing side) as demonstrated in Figure 2.



**Figure 2: Set-up for welding (top) and tensile testing (below) of welds with side-tilt angle  $\beta$**

### 3 Experimental results

Before the actual tests, a set of welds were performed with different parameters and the microstructure was analysed. From this analysis, the following parameters were selected:

AA7075-T6 - 2mm Parameter set-up		
Rotational Speed during plunge	6000	rpm
Down-force during plunge	1200	N
Welding Speed	8	mm/s
Rotational Speed during welding	1200	rpm
Down-force during welding	8000	N
Tilt-angle $\alpha$ (travel direction)	$2^\circ$	

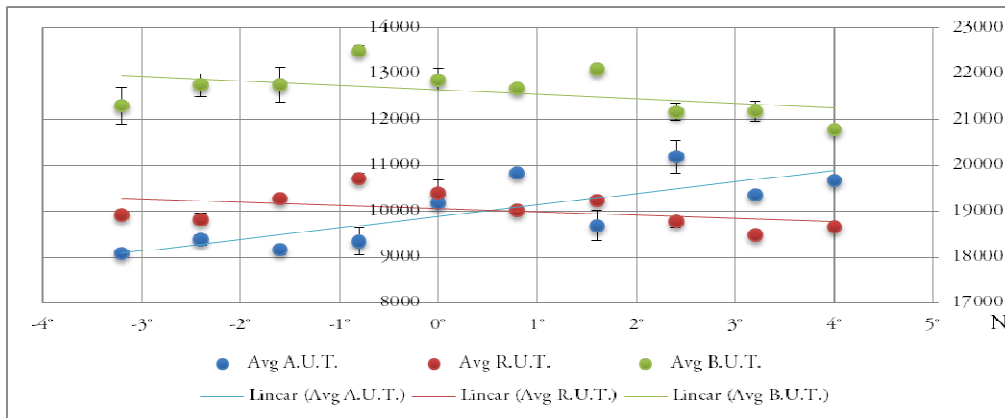
The effect of the side-tilt angle on the joint strength is shown in Figure 3. Each dot represents the average strength of 3 samples, together with the standard deviation. The standard deviation for all samples is small, indicating a good repeatability of the tests. There was no noticeable effect of the time between different tests on the joint strength. The specified base material strength of hardened 7075-T6 is 540 MPa. To allow comparison of the joint strength with the base material, this is recalculated to a corresponding strength of 22680 N for the coupon dimension. Tensile tests were also performed on coupons of base material. The material supplier specifies a tensile strength of 230 MPa for AA-7075 in unhardened state (equivalent to 9660 N for the used specimen dimension).

The strength of the joint with B.U.T. slightly decreases as the side-tilt angle increased. The maximal measured strength in this configuration was 22547N at an angle of  $\beta = -0.8^\circ$ . This implies a joint efficiency of 99.4%, compared to the supplier-specified material strength.

The strength of the joints with A.U.T. and R.U.T. are significantly lower than B.U.T.




The samples with A.U.T. clearly indicate stronger welds when the tool is tilted towards the advancing side. For A.U.T. tests the maximal measured strength was 11647N at an angle of  $\beta = +2.4^\circ$ . This corresponds to a joint efficiency of 51%. Samples with R.U.T. however, did not show a noticeable influence of the side-tilt angle on the strength. The maximal measured strength was 10758N at an angle of  $\beta = -0.8^\circ$ . This corresponds to a joint efficiency of 47%. The joints are stronger than the unhardened material.

The thickness of the top sheet will reduce when the tool is side-tilted. For the largest angle,  $\beta = 4^\circ$  into advancing side, this means that the plate thickness reduces with  $5 \cdot \tan(4^\circ) = 0.35$  mm. This is indicated with a red arrow in Figure 4c.



**Figure 3: Maximal tensile strength of the material [N] for different side-tilt angles [°] in three different testing configurations with a first-order linear approximation for each configuration**

The microstructure study is shown in Figure 4. The analysis only shows wormhole-defects when the tool is tilted more than  $3.2^\circ$  into the retreating side. The shown images contain some stains from incorrect etching. This was however not influencing the observation of defects and samples were for this reason not repolished.

$+3.2^\circ$ No defects observed	 a
$0^\circ$ No defects observed	 b
$-3.2^\circ$ Initiation of defect is observed on the advancing side.	 c

**Figure 4: Microstructure analysis for different side-tilt angles**

During welding, the process forces are logged. Afterwards, these forces are analysed and the mean value of the side forces is calculated for each weld in steady-state condition (i.e. without plunge or retraction). The side forces are not significantly affected by the change in side-tilt angle as shown in Figure 5.

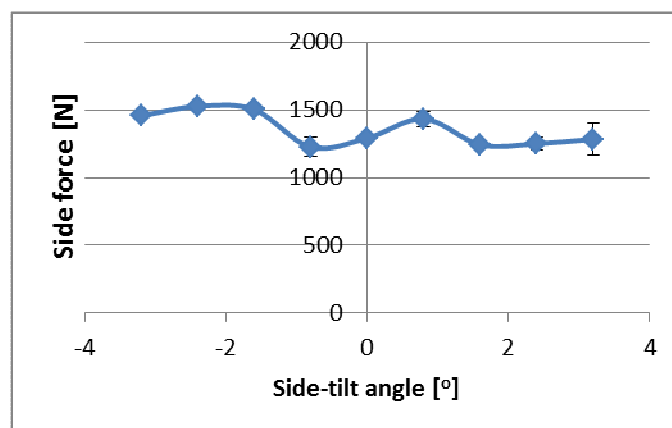


**Figure 5: Influence of the side-tilt angle on the side force**

## 4 Conclusions

If the tool is tilted more towards the retreating side of the weld, a wormhole defect initiates on the advancing side from  $3.2^\circ$ , this is most likely due to the reduced pressure on the retreating side of the tool (at the trailing edge).

When the tool is tilted towards the advancing side, the weld gets stronger in A.U.T. tests, even though the thickness of the plate is reduced. The weld is thus significantly stronger, despite 0.35 mm plate thinning.

The strength of the hardened material is not reduced from the tensile tests on the bottom sheet. Despite the defect at  $-3.2^\circ$ , the material remains equally strong, compared to the hardened base material.

The hypothesis that the side-tilt angle reduced the asymmetric effects and thus the side forces on the tool is not valid for this experiment. The forces could not be significantly reduced.

## 5 Discussion and future work

The effect of a side-tilt angle on the weld quality is limited for small tilt angles but for the A.U.T. setup, an improvement of 10%  $\sigma_{UTS}$  was reached for  $2.4^\circ$  side-tilt angle, compared to zero tilt angle. Even though the linear approximation for A.U.T.-experiments suggests an improved weld for increased side-tilt angle, the quality will obviously not linearly increase for bigger tilt angles due to plate thinning.

In future experiments, the angle can be increased further to see if this makes a difference.

As the serial kinematics robot deflects, due to the process forces, the programmed side-tilt angle will not be the same as the actual angle. Initial studies indicate that the angular tool deviation is up to 1 degree. This deflection is not constant and depends on the location and which direction the robot is moving in.

Furthermore, it should be studied if a weld with wormhole defect at  $0^\circ$  side-tilt angle could be improved by adding a side tilt angle towards the advancing side.

Only one tool geometry is investigated; the CounterStir tool. The results from this paper should be compared to different tool geometries.

## 6 Acknowledgements

The authors would like to thank Dr. Dwight Burford at Wichita State University for support with the selection of appropriate tool geometries. Special thanks to Aleris Aluminum Duffel BVBA – Belgium for supplying the required material for all the tests. Furthermore, we like to acknowledge the financial support to the StiRoLight research project from the Swedish Governmental Agency for Innovation Systems, Vinnova.

## 7 References

- BUFFA, G., CAMPANILE, G., FRATINI, L. & PRISCO, A. 2009. Friction stir welding of lap joints: Influence of process parameters on the metallurgical and mechanical properties. *Materials Science and Engineering: A*, 519, 19-26.
- BURFORD, D. A. 2007. *Friction stir welding tool having a counterflow pin configuration*. US patent application 11/786,961.
- CEDERQVIST, L. & REYNOLDS, A. P. 2001. Factors Affecting the Properties of Friction Stir Welded Aluminum Lap Joints. *The Welding Journal Research Supplement*, 80, 281-287.
- DE BACKER, J., CHRISTIANSSON, A.-K., OQUEKA, J. & BOLMSJÖ, G. 2012. Investigation of Path Compensation Methods for Robotic Friction Stir Welding. *Industrial Robot - An International Journal* [Accepted for publication].
- OKI, S., TAKAHARA, H., OKAWA, Y., TSUJIKAWA, M., MARUTANI, Y. & HIGASHI, K. 2007. Influence of Continuous Transversal Inclination of Tool on FSW Joints. *Materials Science Forum*, 539-543, 3850-3855.
- SMITH, C. 2000. Friction Stir Welding using a Standard Industrial Robot. *2nd International Friction Stir Welding Symposium*. Gothenburg, Sweden: TWI.
- SORON, M. 2007. *Robot System for Flexible 3D Friction Stir Welding*. PhD, Örebro University.
- SORON, M. & KALAYKOV, I. 2006. A Robot Prototype for Friction Stir Welding. *IEEE Conference on Robotics, Automation and Mechatronics, 2006*
- THOMAS, W. M., NICHOLAS, E. D., NEEDHAM, J. C., MURCH, M. G., TEMPLE-SMITH, P. & DAWES, C. J. 1991. *Friction stir butt welding*.
- VON STROMBECK, A., SCHILLING, C. & DOS SANTOS, J. F. Robotic friction stir welding - tool technology and applications. *2nd International Friction Stir Welding Symposium, 2000 Gothenburg, Sweden. TWI*.





## **Paper F**

### **Three-Dimensional Friction Stir Welding of Inconel 718 using the ESAB Rosio FSW-Robot**

**F**

De Backer, Jeroen

Soron, Mikael

*Trends in Welding Research Conference*  
Chicago, IL, USA, 4<sup>th</sup> to 6<sup>th</sup> of June 2012

## Abstract

Robotic Friction Stir Welding (FSW) facilitates for increased welding flexibility, and allows for studies of forces in three dimensions without having the high cost of a stiff 5-axes FSW machine. Recent developments in tool materials and welding equipment motivate this study on FSW of high-strength alloys by a robot in a three dimensional workspace. New concepts of aircraft engines suggest higher temperatures to increase engine efficiency, requiring more durable materials such as the nickel-based alloy 718. The ESAB Rosio™ FSW robot, used in this study, can deliver up to 15 kN downforce and 90 Nm torque. This is sufficient for welding high-strength alloys of limited thickness. This study focuses on the process forces during friction stir welding of Inconel 718 with thickness up to 3mm in butt-joint configuration. A newly developed threaded Poly-Crystalline Boron Nitride (PCBN) tool with convex shoulder is used in a local argon-shielded atmosphere. Initial tests are performed in a stiff FSW machine in position controlled mode. The measured process forces in position control are later on used as parameters on the force-controlled robot. Different backing bar materials are investigated with the aim to decrease the risk of root defects. Tool steel and regular inconel backing bars are proven to be too soft for this purpose and alternatives are suggested. The optimal welding parameters are tuned to combine a good weld quality with the process forces that can be obtained by the robot. Preheating is used to further decrease the need of high process forces.

**Keywords:** Friction Stir Welding, robot, nickel alloy, Inconel 718, force control, preheating, backing bar

## 1 Introduction

Friction Stir Welding (FSW) was originally developed for joining lightweight materials with low melting point such as aluminum and magnesium alloys. During the twenty years after the process was invented and patented [1], many different alloys have been tested such as copper [2], steel and nickel alloys [3]. FSW makes it possible to create high quality defect-free welds with limited distortion and allows welding of dissimilar materials. These factors caused great interest from the aerospace industry. Besides, FSW is a solid state joining process, which is sometimes a requirement for joining of critical components in aero engines.

All previous investigations of ferrous and nickel-based alloys are carried out on the classical FSW machines, performing linear welds. By using a robot to perform the welding

operation, it is possible to join three-dimensional shapes. The limitations of the robot system are investigated and FSW of superalloys is tested to be possible with a serial kinematics robot. This type of robot has been adopted by several research groups in the past [4] [5] [6]. The big drawback associated with these robots is their compliance and the limited force capability. Higher forces and increased stability can be reached with parallel kinematics robots [7].

For this paper, the nickel alloy 718, distributed under the brand name Inconel 718, was selected for a feasibility study on robotic FSW of superalloys. Several additional challenges are associated with robotic FSW of superalloys, compared to FSW of aluminum such as the high process forces, tool material and backing bar material. The tool cannot be manufactured out of hardened steel. Several solutions have been presented, initially using only tungsten [9] and later using tungsten-rhenium and the ceramic material Polycrystalline Boron Nitride (PCBN) [10]. Recently, Miyazawa reported good initial results with iridium-based FSW-tools [11]. SLV in Germany conducted promising tests with tantalum-based tools. The weld quality was comparable to the welds with PCBN tools [12]. It is expected that the tools for ferrous and nickel alloys will become cheaper, less brittle and more wear-resistant.

## 2 Experimental Setup

An initial feasibility study was carried out at the ESAB facilities in Laxå, Sweden, using an ESAB SuperStir™ FSW machine. The system used for robotic welding tests is an ESAB Rosio™ FSW robot, shown in Figure 1. The robotic tests were performed at the Production Technology Centre in Trollhättan, Sweden. The system is based on an ABB IRB-7600 robot. The maximal specified payload for the robot is 500 kN. The motor, driving the welding spindle delivers 45 Nm, and a rotational speed up to 4000 rpm. The performance of the robot system is further discussed in [4]. The motor is connected to the spindle through an angular gear with ratio 3:2. This reduces the spindle torque to 30 Nm and increases the rotational speed to 6000 rpm. This gearing configuration was chosen for high-speed welding ( $>2$  m/min) in aluminum alloys.

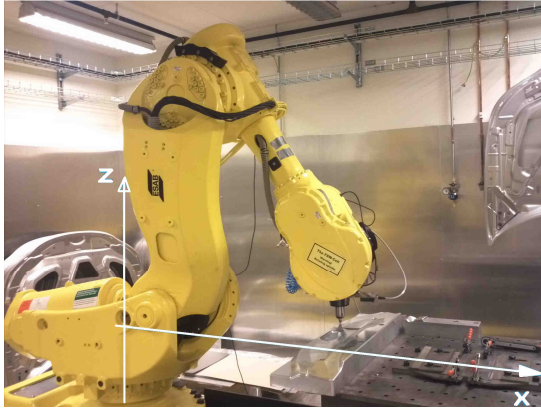


Figure 1: FSW robot at the Production Technology Centre



Figure 2: PCBN tool with convex shoulder

For FSW of superalloys, a high downforce is necessary. The force that the robot can deliver is much smaller than on a conventional FSW machine. The tool force is generated by five collaborating servo motors in the robot. Each of the motors delivers a certain torque, and the further the tool is away from a motor, the lower the force this motor can deliver. In order to find out if the robot is capable of delivering the forces required for FSW of superalloys, the maximal force is mapped by pushing the robot tool against the welding table and stepwise increasing the force until one of the motors reaches its torque limits. The maximal deliverable tool force is logged, together with which axis has reached the maximal torque.

The joints are performed in butt joint configuration on the nickel alloy 718, without heat treatment. Earlier reports have demonstrated the feasibility for both the Inconel 718 alloy and Inconel 600 alloy [8]. For these tests, a PCBN welding tool, manufactured by MegaStir<sup>®</sup>, is used with convex scrolled geometry designed for 3 mm thickness as shown in Figure 2. The first part of the investigation focused on the process forces during position-controlled welding and on tuning of the process parameters to allow implementation on robots. Three materials were evaluated as backing bar with yield strength at room temperature ranging from 520 to 1000 MPa in room temperature. An extra oxidation process was used to prevent the welded material from sticking to the backing bar. For the FSW tests, argon shielding gas was used in a local area just around the tool; the backside of the weld was not protected with gas.

Three test series were performed on the SuperStir<sup>™</sup> machine to find the optimal parameters, backing bar material and preheating conditions. The first series were butt joints of 3 mm sheets. The second were butt joints of 2 mm material and the third series, both 2 and 3 mm was used with preheating.

To study the effect of preheating on the process forces, a set of samples were preheated to about 400°C in an electric furnace and then clamped in the fixture, leaving a remaining temperature of around 175°C during plunging, which further decreased to 125°C at the end of the welding process. The temperature of the process was measured with a thermocouple, inserted in the tool, measuring the temperature under the shoulder at about 5mm from the centerline of the tool.

## 3 Experimental Results

### 3.1 Influence of backing bar material

The three backing bar materials were evaluated.. The first material was a typical stainless steel backing. As the temperatures under the welded plates reach up to 1000°C, the steel softens too much. This causes the backing bar to deform under the joint line, and extrude into the gap between the two butted plates. This gave a root defect as demonstrated in the micrograph of a cross-section in Figure 3. Even with a downforce of 80 kN, the material did not join in the bottom of the sheets with the two steel backing materials.

With a backing material hardened to 1000 MPa, the root defects in the welded plates could be avoided. This material was used as backing bar for more than 10 welds and no backing bar deformation could be visually observed.

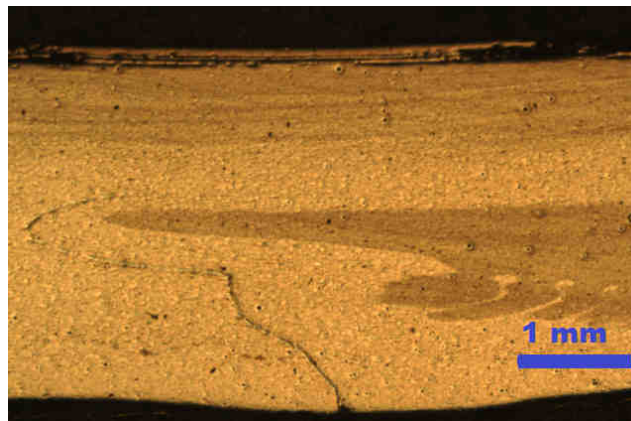


Figure 3: Micrograph of 3mm thick butt weld showing a root defect due to backing bar deformation.

### 3.2 Process forces

The first test series of the 3 mm sheets were in position controlled mode. The forces measured were up to 80 kN at rotational speeds of 300 rpm. As the downforce increased, the tool penetrated deeper into the material. Root defects could however not be eliminated with increased pressure because these were caused by deformation of the backing bar, rather than the lack of penetration.

The next series of welding test were performed in 2 mm thick sheets with the same tool. To obtain a good weld quality in these thinner plates, the required downforce was significantly lower than in the 3 mm sheets. The process forces decreased to about 20 kN.

The third series with 2 and 3 mm thick preheated plates provided the best results. With a preheating temperature of 150°C, a good weld was obtained with only 12 kN downforce of the machine. The parameters for the test with preheating are shown in Table 1. The first three samples are performed in position controlled mode. This means that the depth of the tool is set as parameter and the resulting force is measured. The 4<sup>th</sup> sample was

welded in force controlled mode: after plunging, the real depth of the tool is not controlled but instead a constant downforce is applied by the tool on the material. For stability reasons, force controlled mode is also required for robotic welding. It is of great importance that the applied force is enough to maintain the required depth during welding.

### 3.3 Influence of rotational speed

In an attempt to generate more heat with reduced downforce, the rotational speed was raised stepwise from 300 rpm. From around 900 rpm, the quality of the weld decreased and from 1200 rpm, glowing material started to fly away from the tool. No acceptable weld was obtained above 900 rpm. This limitation can be explained by the friction coefficient between the PCBN and the welded alloy. From a certain speed, the lack of friction will cause the tool to spin without dragging the material around and the necessary stirring effect is lost. One test was carried out without protecting shielding gas and no acceptable weld was obtained. This weld is shown in Figure 5.



Figure 4: High quality FSW joints were obtained on the ESAB SuperStir™ machine



Figure 5: The weld without shielding gas showed severe oxidation during welding

In one of the samples, shielding gas was used but the formation of flash around the tool caused interruptions in the gas flow. This also resulted in color variations from oxidation. The unprotected root side on all samples showed similar color changes due to the oxidation.

Table 1: Influence of material thickness and rotational speed on the process forces.

Experiment nr.	thickness [mm]	Welding Speed cm/min	Rotational speed [RPM]	Force [kN]	Preheating temperature [°C]
1	2	3	300	20	25
2	3	3	300	35 to 40	125
3	3	3	300	45 to 50	170
4	2	3	300:900 $\Delta$ 100	12	150

### 3.4 Implementation on the robot

Once a good set of parameters was selected, a test with the robot system could be performed. As the maximal deliverable down force of the robot depends on the location in the robot's workspace, the maximal force was mapped as function of the distance from the robot base at a height of 0.8 m. This corresponds to the x-axis in Figure 1. The resulting maximal force is shown in Figure 6. Due to geometrical restrictions the robot can only reach points that are further than 1.5 m away from the base (red line in Figure 6). In that location the robot was able to push down with 15 kN. The further away from the tool, the lower the maximal force was. The minimal force that could be delivered on the table was 8 kN. This is still 3 kN more than the specified maximal force by the robot manufacturer (green line in Figure 6).

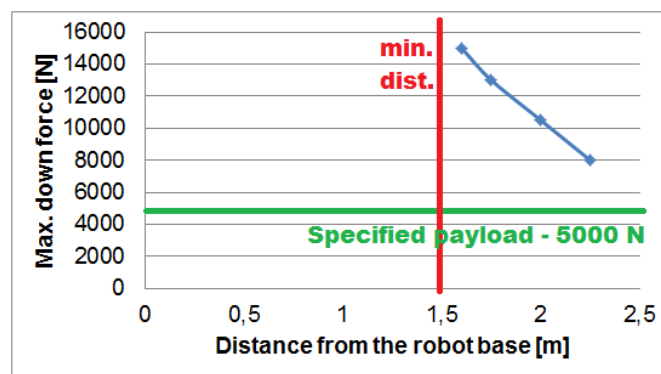


Figure 6: Maximal deliverable force by the robot on different points of the welding table.

The first welding trial on the robot system did not pass the plunging stage. As the tool penetrated into the material, the motor exceeded the stall torque and generated an emergency stop in the robot system. The tool was stuck in the material and had to be removed, causing the brittle PCBN to break. A new gear with a 3:1 ratio was implemented between the motor and the spindle. This increased the maximal spindle torque to 135 Nm and decreased the maximal rotational speed of the spindle to 1333 rpm. With the used welding parameters, a torque of about 100 Nm can be reached, which meets the requirements for FSW of the used super alloy.

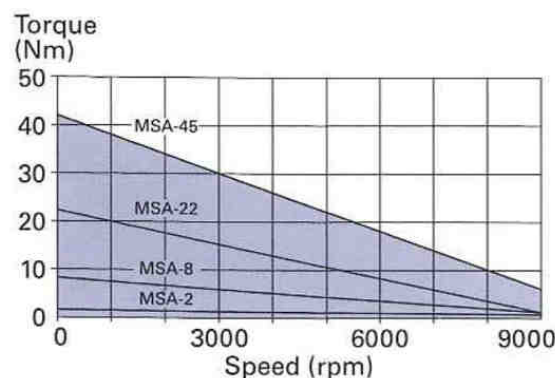


Figure 7: Performance curve of the spindle motor (Mavilor MSA-45)

A new welding trial successfully plunged the tool into a 2 mm sheet of the 718 alloy to the required depth and could maintain a downforce of 12 kN. The material was not preheated and therefore the penetration depth decreased as the tool moved forward, causing a bad looking weld.

## 4 Conclusions

The backing bar material must be sufficiently hard at high temperatures to withstand the high pressure from the tool. For welding of superalloys, a stainless steel backing does not meet the requirements in terms of hardness at elevated temperatures and will deform just under welded joint.

The limited friction between the PCBN tool and the 718 alloy did not allow welding at rotational speeds above 900 rpm.

The required loads to obtain a good weld quality could be significantly reduced by preheating the material. With a preheating temperature of 150°C, a weld of good quality was obtained with a force of 12 kN for the 2 mm material, which is within the robot's force capabilities.

It is demonstrated that the robot can deliver the required spindle torque and downforce for a successful welding operation. Further adaptations of the system (i.e. implementation of preheating) is required to obtain a good weld.

## 5 Discussion and future work

Performing FSW of superalloys on a serial kinematics robot is really pushing the system to its limits. Using this robot system for ferrous or nickel alloys requires the system to exceed the specified load limits. The use of it for mass production will most likely decrease the live length of the system significantly. The aim here, however, is to benefit from the flexibility of the robot system to FSW prototypes of expensive components. The possibility to test 3D joints of superalloys on a robot system allows end-users to experiment with the new technology at a relatively low cost.



By placing the part strategically in the robot's workspace, the maximal downforce can increase significantly.

To obtain a good quality weld, a certain heat input is required. It was not possible to increase the heat input by increasing the rotational speed, due to friction limitations. Higher rpm welds will only be possible using tools with a higher friction coefficient. For future experiments, higher preheating temperatures will be used, up to 400°C. This would enable a further decrease of the loads on the robot.

Even though the performed welding test with the robot was short, the whole welding head heated up fast. A good cooling system is mandatory to prevent overheating of gears and sensors.

## 6 Acknowledgments

The authors acknowledge the financial support from the Swedish Governmental Agency for Innovation Systems, Vinnova, within the StiRoLight research project. The authors also want to thank Volvo Aero Corporation for supplying the material required for these investigations and especially Mr. Fremäng at Volvo Aero and Mr. Säll at ESAB for their technical support.

## 7 References

- [1] W. M. Thomas, E. D. Nicholas, J. C. Needham, M. G. Murch, P. Temple-Smith, and C. J. Dawes, "Friction stir butt welding," 1991.
- [2] L. Cederqvist, O. Garpinger, T. Hägglund, and A. Robertsson, "Cascade control of the friction stir welding process to seal canisters for spent nuclear fuel," *Control Engineering Practice*, vol. 20, pp. 35-48, 2012.
- [3] C. D. Sorensen and T. W. Nelson, "Friction Stir Welding of Ferrous and Nickel Alloys," in *Friction Stir Welding and Processing*, R. S. Mishra and M. W. Mahoney, Eds., ed: ASM International, Materials Park, OH, USA, 2007, pp. 111-121.

- [4] M. Soron, "Robot System for Flexible 3D Friction Stir Welding," PhD, Department of Technology, Örebro University, 2007.
- [5] C. Smith, "Friction Stir Welding using a Standard Industrial Robot," presented at the 2nd International Friction Stir Welding Symposium, Gothenburg, Sweden, 2000.
- [6] G. Voellner, M. F. Zäh, O. Kellenberger, D. Lohwasser, and J. Silvanus, "3-Dimensional Friction Stir Welding using a modified high payload robot," 6th International Friction Stir Welding Symposium, Saint Sauveur, Canada, 10-13 October 2006 2006.
- [7] A. Von Strombeck, C. Schilling, and J. F. Dos Santos, "Robotic friction stir welding - tool technology and applications," in 2nd International Friction Stir Welding Symposium, Gothenburg, Sweden, 2000.
- [8] Y. S. Sato, P. Arkom, H. Kokawa, T. W. Nelson, and R. J. Steel, "Effect of microstructure on properties of friction stir welded Inconel Alloy 600," *Materials Science and Engineering: A*, vol. 477, pp. 250-258, 2008.
- [9] T. J. Lienert, W. L. Stellwag, B. B. Grimmer, and R. W. Warke, "Friction stir welding studies on mild steel," *Welding Journal*, vol. 82, 2003.
- [10] M. Mahoney, T. Nelson, C. Sorensen, and S. Packer, "Friction Stir Welding of Ferrous Alloys: Current Status," *Materials Science Forum*, vol. 638 - 642, p. 6, 2010.
- [11] T. Miyazawa, Y. Iwamoto, T. Maruko, and H. Fujii, "Development of Ir based tool for friction stir welding of high temperature materials," *Science and Technology of Welding & Joining*, vol. 16, pp. 188-192, 2011.
- [12] R. Boywitt, "Entwicklung und Erprobung von neuen Werkzeugmaterialien für das Rührreischweißen von Stahl," in *Große Schweißtechnische Tagung 2011*, Hamburg, 2011, pp. 166-170.

